

DEVELOPMENT OF GLUCOSE AND PH SENSITIVE
HYDROGELS FOR MICROFABRICATED
BIOMEDICAL SENSOR ARRAYS

by
Genyao Lin

A dissertation submitted to the faculty of
The University of Utah
in partial fulfillment of the requirements for the degree of

Doctor of Philosophy

Department of Materials Science and Engineering

The University of Utah

May 2010

Copyright © Genyao Lin 2010

All Rights Reserved

STATEMENT OF DISSERTATION APPROVAL

The dissertation of Genyao Lin
has been approved by the following supervisory committee members:

<u>Jules J. Magda</u>	, Chair	<u>3/30/2010</u> Date Approved
<u>Grant D. Smith</u>	, Member	<u>3/30/2010</u> Date Approved
<u>Agnes Ostafin</u>	, Member	<u>3/30/2010</u> Date Approved
<u>Mataz Alcoutlabi</u>	, Member	<u>4/2/2010</u> Date Approved
<u>Patrick F. Kiser</u>	, Member	<u>3/30/2010</u> Date Approved

and by Anil V. Virkar, Chair of
the Department of Materials Science and Engineering

and by Charles A. Wight, Dean of The Graduate School.

ABSTRACT

This dissertation is concerned with the development of glucose-sensitive hydrogels and pH-sensitive hydrogels for biomedical sensor applications. The research is motivated by the limitations of current glucose sensors and an urgent societal need, which has not yet been met, for a continuous glucose monitoring sensor suitable for implantation and long-term use in diabetic patients. The sensing approach is the confinement of thin smart hydrogels between the diaphragm of a piezoresistive pressure sensor and a rigid porous membrane through which analyte diffusion occurs. Such a sensor is termed a “chemomechanical sensor.” First, a macrosized chemomechanical sensor is used to screen various totally synthetic phenylboronic acid (PBA) containing glucose-sensitive hydrogels (GSHs) on the basis of 1) magnitude of osmotic swelling pressure response to glucose concentration change, 2) selectivity for glucose relative to fructose, and 3) response kinetics. All testing was performed *in vitro*, and a polyampholytic GSH is found to be the best choice. Next, polyampholytic GSHs are synthesized without use of potentially toxic acrylamide monomer and tested in the macrosized glucose sensor. Finally a UV-curing process is developed for *in-situ* synthesis of GSHs on integrated sensing chips containing custom-designed piezoresistive pressure sensors. Preliminary *in vitro* results for a microchip glucose sensor with pressure transducer diaphragms measuring 1 mm by 1 mm are presented. The results of this thesis will aid the long-term development of a smart hydrogels based sensor array suitable for subcutaneous implantation that is

able to simultaneously measure glucose and pH values in real-time on a long-term basis for diabetic patients.

To my wife Huahua Xue

TABLE OF CONTENTS

ABSTRACT	iii
LIST OF TABLES	viii
ACKNOWLEDGMENTS	ix
Chapter	
1. INTRODUCTION	1
1.1 Motivation	1
1.2 Background	3
1.3 Thesis Overview	43
1.4 References	44
2. FREE SWELLING AND CONFINED SMART HYDROGELS FOR APPLICATIONS IN CHEMOMECHANICAL SENSORS FOR PHYSIOLOGICAL MONITORING	55
2.1 Abstract	56
2.2 Introduction	56
2.3 Experimental methods	57
2.4 Results	59
2.5 Discussion	62
2.6 Conclusions	64
2.7 Acknowledgement	64
2.8 References	64
3. OSMOTIC SWELLING PRESSURE RESPONSE OF SMART HYDROGELS SUITABLE FOR CHRONICALLY IMPLANTABLE GLUCOSE SENSORS	66
3.1 Abstract	67
3.2 Introduction	67
3.3 Experimental methods	68

3.4 Results and discussion.....	69
3.5 Conclusions and perspectives.....	70
3.6 Acknowledgement.....	70
3.7 References.....	70
4. OPTIMIZATION OF GLUCOSE SENSITIVE HYDROGELS FOR SENSOR APPLICATIONS.....	72
4.1 Introduction.....	72
4.2 Synthesis of 2-(Methacrylamido)phenylboronic acid (2-MPBA) and glucose-sensitive hydrogels (GSHs).....	75
4.3 Investigation of polyampholytic glucose-sensitive hydrogels based on AAM, DMAPAA and 3-APB.....	81
4.4 Novel glucose sensitive hydrogels containing HEMA, DMAPAA and 3-APB....	101
4.5 Conclusions.....	107
4.6 References.....	108
5. IN SITU SYNTHESIS OF PH AND GLUCOSE SENSITIVE HYDROGELS WITHIN MICROFABRICATED SENSOR ARRAYS.....	110
5.1 Introduction.....	110
5.2 Microfabricated sensor array construction and ionic strength tests for pH sensitive hydrogels.....	111
5.3 In situ synthesis using redox initiator systems.....	119
5.4 Photopolymerization of pH sensitive hydrogels.....	123
5.5 Photopolymerization of glucose sensitive hydrogel.....	127
5.6 Conclusions.....	136
5.7 References.....	137
6. CONCLUSIONS AND FUTURE DIRECTIONS.....	139
6.1 Conclusions.....	139
6.2 Future directions.....	141
6.3 References.....	145

LIST OF TABLES

Table	Page
1.1. Ionic strength response times and response magnitudes of sensor with various membrane configurations	63
4.1. Materials chemical structures	74
4.2. Comparison of ¹ H NMR results for synthesized 2-(Methacrylamido) phenylboronic acid with published data [3], numbers in the parenthesis indicate the area of that specific peak after integration	78
4.3. Experimental attempts to synthesize glucose-sensitive hydrogels (GSHs) containing 2-(Methacrylamido) phenylboronic acid (2-MPBA).....	80
4.4. Various GSHs of higher acrylamide content subjected to various glucose deswelling tests, where “no” indicates no two-step deswelling was observed and “yes” indicates two-step deswelling was observed in 0.15 M PBS at pH 7.4.....	94
4.5. Various GSHs of lower acrylamide content subjected to various glucose deswelling tests, where “no” indicates no two-step deswelling was observed and “yes” indicates two-step deswelling was observed	97
4.6. Glucose-sensitive hydrogels and phase separation during synthesis. The amount of DMSO used in this table was 10 vol% and equal moles of NaOH and 3-APB were used in each synthesis	100

ACKNOWLEDGMENTS

First and foremost, I would like to express my sincere gratitude to my advisor, Dr. Jules J. Magda, for his support, guidance, and the opportunity to work with him in the last four years. I also deeply appreciate his friendship, advices and enormous support to help advance my career. Special thanks go to Dr. Seok Chang for his assistance in polymer synthesis. I would like to acknowledge my committee members Dr. Grant D. Smith, Dr. Mataz Alcoutlabi, Dr. Agnes Ostafin, and Dr. Patrick F. Kiser, for their suggestions and input. I am also grateful to Dr. Jindrich Kopecek, Dr. Feng Liu, and Dr. Stacy M. Bamberg for their teaching and advices.

Many thanks go to my friends and coworkers Madhu Kandadai, Hong Hao, Seunghei Cho, Mike Orthner, Mahender Avula, Prashant Tathireddy, Hongtao Wang, Liyong Wang, and Suhui Li. I would also like to thank my department and the University of Utah for providing me a wonderful place to live and study.

Most importantly I would like to thank my family, my parents Qizhu Lin and Fenlan Zhou and my wife Huahua Xue, for their support, love and motivation.

CHAPTER 1

INTRODUCTION

1.1 Motivation

Diabetes mellitus is a worldwide disease that currently accounts for 5% of the world's population, and is one of the leading causes of death and disability [1,2]. The risks and complications associated with diabetes mellitus include ketoacidosis, heart disease, kidney failure, amputation, and blindness. Since no cure has been discovered for diabetes to date, the main route to reduce its complications is tight monitoring of patient's blood glucose level, and then therapeutic interventions if necessary. Tight and strict blood glucose concentration control aimed at maintaining normal glycemic levels has been well documented as the most effective way to dramatically alleviate or prevent complications and substantially reduce the overall cost of medical care [3,4]. Indeed, thanks to the huge number of diabetic patients, glucose has become the most commonly tested analyte and 85% of the entire sensor market corresponds to glucose biosensors [1].

The current standard glucose sensing technique is the fingerstick approach, in which the diabetic patient intermittently removes a drop of blood from the fingertip and tests its glucose concentration using an electrochemical sensor located outside the body. The fingerstick is painful and eventually causes fingertip scarring, hence patient compliance is poor. Furthermore, fingerstick approach obviously cannot be used to

monitor blood sugar during sleep. For these reasons, the fingerstick method is not suitable for tight control of blood sugar levels as needed to avoid the complications of diabetes. For this purpose, a continuous glucose monitoring method is clearly superior and highly desirable. In recognition of this need, currently there are several minimally invasive, subcutaneously (sub-Q) implantable continuous electrochemical glucose monitoring systems commercially available. These include the Freestyle Navigator [5] and MiniMed Paradigm [6]. Although these enzyme based systems show high specificity to glucose detection, they suffer from several major limitations such as the use of glucose-restrictive membranes [7], dependence on the blood oxygen level as well as glucose diffusivity [8,9], and large signal drifts over time and thus frequent calibrations required involving the fingerstick method [2,10,11]. Due to the various limitations of enzyme based electrochemical glucose sensors, they have been approved only for professional use with a lifetime in the body of three days [12,13]. Hence development of alternative enzyme-free glucose sensors is an area of intensive investigation.

Much attention has been paid to the development of glucose-sensitive hydrogels (GSHs) containing the glucose-binding moiety phenylboronic acid (PBA) for enzyme-free glucose sensors. A GSH is a crosslinked polymer network that can reversibly change its volume or other properties in response to changes in environmental glucose concentration [14]. By coupling a GSH of micron-scale thickness to a method of detecting the hydrogel change, such as optical or pressure measurements, one can obtain a sensor suitable for glucose detection for diabetic patients [15-18]. Meanwhile, ketoacidosis can be reflected by a change in pH, thus pH is also an important biomarker

for diabetes [19].

The goal of this thesis is to develop stimuli-responsive hydrogels for a novel implantable biomedical sensor array for simultaneous and continuous monitoring of both glucose and pH. We believe that such a sensor array will provide better diabetes management. The underlying principle of this smart hydrogels based sensor array device is the change of osmotic swelling pressure of confined hydrogels in response to variations in environmental glucose concentration and pH value.

1.2 Background

1.2.1 Management of diabetes

Diabetic mellitus, usually referred to simply as diabetes, is a disease in which the patients are unable to maintain the normal blood glucose concentration due to lack of insulin, or ineffective insulin, a hormone produced by beta-cells in the islets of Langerhans of the pancreas. According to the World Health Organization (WHO), the number of diabetics will increase from 177 million in 2000 to 300 million by 2025; and it is also projected that 9% of all deaths worldwide will be attributable to diabetes [20].

Generally, diabetes can be classified into three types, namely type 1, type 2 and gestational diabetes [21]. To date no practical cure is available for diabetes. In type 1 diabetes, T-cells caused autoimmune attack against beta-cells and then the destruction of beta-cells is the main disease mechanism [22]; type 1 diabetes is the condition in which the body fails to produce insulin [21]. Type 2 diabetes results from insulin resistance or reduced insulin sensitivity, and its exact disease mechanism still remains obscure [22]. Insulin has extensive effects on the metabolism such as glucose metabolism. It causes the cells in the fat tissue, liver, and muscle to convert the glucose in the blood into glycogen

and store it in the liver and muscle; when appropriate insulin control fails, diabetes ensues [23]. The normal blood glucose concentration in the body is in the range of 80-120 mg/dl. There are two types of abnormal blood glucose concentrations associated with diabetes: hypoglycemia (lower than normal glucose level) and hyperglycemia (higher than normal glucose level). Complications associated with diabetes include, but are not limited to, ketoacidosis, heart disease, kidney failure, amputation, and blindness. Until the discovery of the cure for diabetes, the most effective way to diabetes management is development of a self-regulated insulin delivery system mimicking the function of artificial pancreas, with continuous glucose sensor as the cornerstone component.

With respect to diabetes, pH is also an important biomarker related to diabetic ketoacidosis (DKA). Diabetic ketoacidosis (DKA) is among one of the many complications associated with diabetes, with the characteristic of low blood pH. DKA is the most serious side effects of type 1 and type 2 diabetes and is associated with significant mortality and morbidity [24]. DKA occurs when excessive ketones are accumulated in the blood. Ketones are a product of oxidation of fatty acid to produce alternate energy for the body when the carbohydrate oxidation process is severely limited due to insulin deficiency or insulin resistance, which substantially blocks the entry of glucose into the cells for energy production via glycolysis. Blood pH is a measure of the severity of DKA, lower pH indicates more severe DKA. For mild DKA the pH range is 7.3-7.35, 7.2-7.3 for moderate DKA and less than 7.2 for severe DKA [19]. Accurate and continuous monitoring of blood pH should reduce or prevent the complications even before severe DKA kicks in.

Tight and strict blood glucose concentration control aiming at normal glycemic levels, via insulin delivery, has been well documented as the most effective way to dramatically alleviate or prevent the complications and substantially reduce the overall cost of medical care [3,4]. Not surprisingly, due to the large number of diabetic patients, glucose sensors account for 85% of the entire biosensor market [1]. Such a tremendously large market along with the limitations of current glucose sensors has motivated intensive research towards the development of continuous glucose sensors with high stability, accuracy and suitability for long-term use. An ideal continuous glucose sensor would be one that offers reliable real-time continuous measuring of blood glucose concentration variations 24 h/day for extended periods with high selectivity, excellent biocompatibility and fast response rate under harsh physiological conditions [1].

1.2.2 Stimuli-responsive hydrogels

Hydrogels are three-dimensional, cross-linked networks of hydrophilic polymer chains that are able to absorb a large amount of water but do not dissolve in water [25]. Hydrogels are biocompatible because of their high water content along with the low interfacial tension at the hydrogel-body fluid interface [26]. In addition, hydrogels are quite versatile materials and can be tailor-made corresponding to specific requirements by manipulating the synthetic chemistry and processing protocols. A ‘stimuli-responsive’ or ‘smart’ hydrogel is a cross-linked polymer network that reversibly swells and absorbs water in response to external stimuli variations such as change in temperature, pH, and concentration of some analyte such as glucose [14,18]. In the past several decades, great attention has been paid to the development of stimuli-responsive hydrogels due to its potential applications in drug delivery, biological coatings, implantable biomedical

sensors and autonomous drug delivery devices [27,28]. In this thesis, attention is paid exclusively to two specific stimuli-responsive hydrogels, namely glucose-sensitive hydrogels and pH-sensitive hydrogels. Meanwhile, their suitability for biomedical sensors is evaluated and presented.

1.2.2.1 Theory-thermodynamics

Hydrogel swelling equilibrium is obtained when the total change in free energy (ΔF_{tot}) reaches a minimum value or, equivalently, the chemical potential of each mobile species becomes the same in the coexisting phases [29]. For a nonionic hydrogel, the total change in free energy contains two contributions: a negative contribution from the mixing of polymer segments with water (ΔF_{mix}), and a positive contribution from the entropy penalty associated with polymer network stretching (ΔF_{el}). For a polyelectrolyte hydrogel, there is an additional contribution from the mixing of water with the counterions within the hydrogel (ΔF_{ion}). Supposing that these terms are independent [29-31], we can write

$$\Delta F_{tot} = \Delta F_{mix} + \Delta F_{el} + \Delta F_{ion} \quad (1.1)$$

The swelling pressure Π of hydrogel is obtained by differentiating ΔF_{tot} with respect to moles of water V_1 [29-31], i.e.,

$$\Pi = -(\partial \Delta F_{tot} / \partial n_1) / V_1 = (\mu_{1,0} - \mu_1) / V_1 = \Pi_{ion} + \Pi_{mix} + \Pi_{el} \quad (1.2)$$

where V_1 is the molar volume of water, n_1 is the number of moles of water, μ_1 denotes the chemical potential of water in the hydrogel at ambient pressure, and $\mu_{1,0}$ represents the chemical potential of water in the reference solution that surrounds the hydrogel.

Π_{ion} , Π_{mix} , and Π_{el} are the osmotic pressures due to, respectively, the ionic, mixing and elastic contributions of hydrogel swelling pressure Π .

Generally speaking, there is a difference in mobile ion concentrations inside and outside a polyelectrolyte gel. This difference is caused by the requirement of electroneutrality to maintain the gel as a whole electrically neutral [29]. The difference in mobile ion concentrations causes a difference in ionic osmotic pressure between the gel and its surrounding solution. A complete effect of ions would include the contributions due to mixing of ions with solvent molecules and interactions between ions, solvent molecules and polymer chains [32]. In general, only the first contribution is considered to calculate Π_{ion} , meanwhile, it should be noticed that only the mobile ions in the gels contribute to the hydrogel swelling pressure, Π_{ion} can be estimated from the Donnan equilibrium theory [31]

$$\Pi_{ion} = RT(c_{gel} - c_{sol}) \quad (1.3)$$

where c_{gel} and c_{sol} are the concentrations of ions within the gel and its surrounding solution.

Π_{mix} is the osmotic pressure due to the mixing of polymer chains with solvent molecules and can be expressed by the Flory-Huggins equation [29]

$$\Pi_{mix} = -\frac{RT}{V_1} \left[\ln(1 - \varphi) + \left(1 - \frac{1}{P}\right) \varphi + \chi \varphi^2 \right] \quad (1.4)$$

where R is gas constant, T is absolute temperature, V_1 is the molar volume of solvent, φ is the volume fraction of polymer in gel, P is the degree of polymerization, and χ is the polymer-solvent interaction parameter or Flory-Huggins interaction parameter. For a

cross-linked polymer network such as hydrogel $P = \infty$. Since the polymers involved in this thesis are hydrogels which are crosslinked, Eq. (1.4) can be rewritten as

$$\Pi_{mix} = -\frac{RT}{v_1} [\ln(1 - \varphi) + \varphi + \chi\varphi^2] \quad (1.5)$$

Π_{el} is the elastic pressure originated from the polymer network stretching. For polymer networks consisting of flexible chains, Π_{el} can be derived from the rubber elasticity theory [29]

$$\Pi_{el} = -ARTv\varphi^{1/3} = -G \quad (1.6)$$

where A is a prefactor which is dependent on the functionality of the junctions, v is the concentration of the polymer elastic chains, and G is the shear modulus of the gel. Shear modulus G is defined as the ratio of shear stress to the shear strain.

Hydrogels can be used in unconfined or free swelling state and confined state, as illustrated in Fig. 1.1. Fig. 1.1 (a) represents the hydrogel in the free swelling or unconfined state. In this case, hydrogel will change its volume upon environmental analyte concentration change. In contrast, in Fig. 1.1 (b), the hydrogel is in an isochoric condition or confined state and the hydrogel will exert a change of swelling pressure to its surrounding surfaces, instead of a change in its volume, upon environmental analyte concentration variation. In this thesis work, the construction of Fig. 1.1 (b) was primarily employed to investigate the swelling properties of stimuli-responsive hydrogels upon external analyte concentration change.

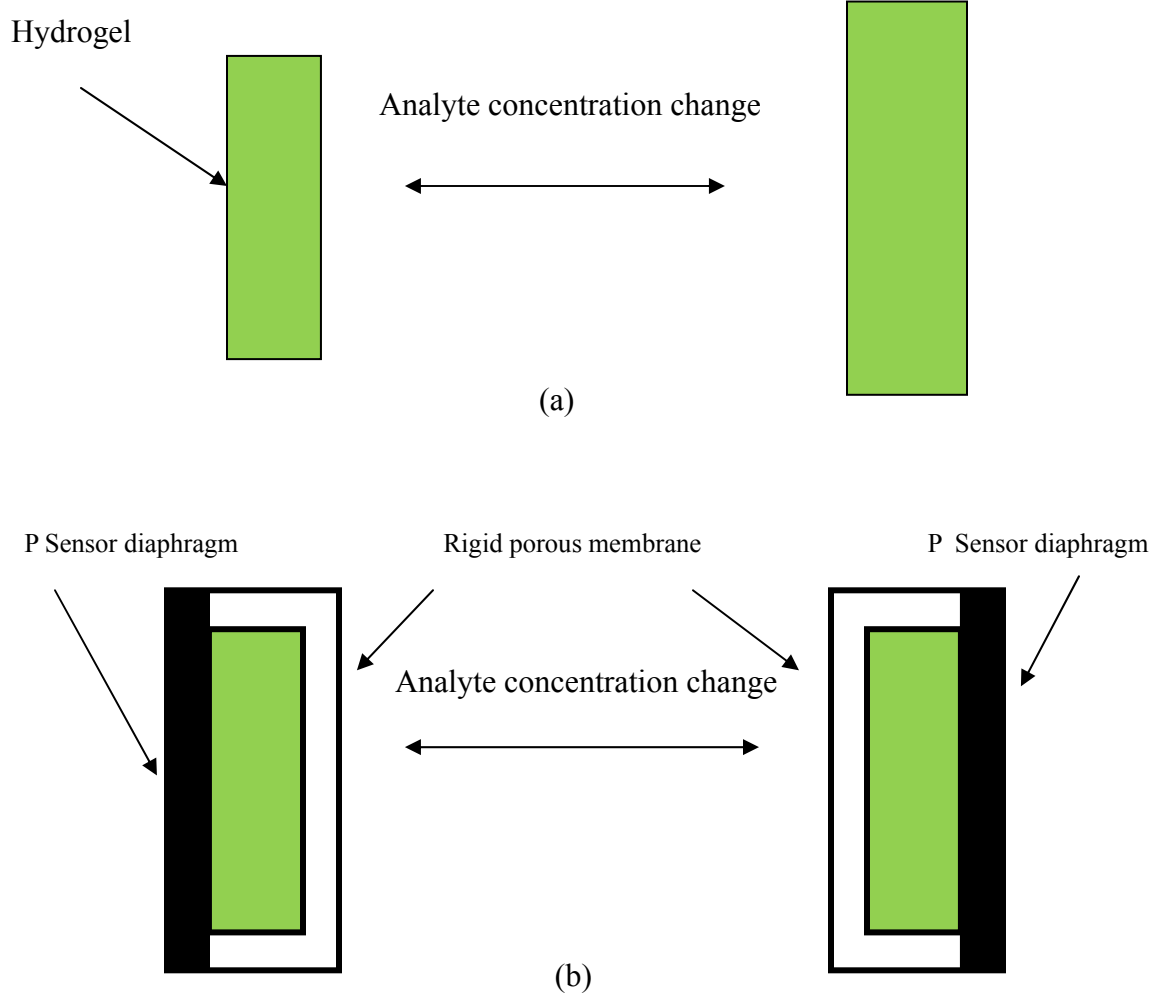


Fig. 1.1. Stimuli-responsive hydrogels in unconfined (a) and confined state (b).

According to the definition of hydrogel swelling and Eq. (1.2), hydrogel swelling pressure Π must equal to zero at equilibrium for the unconfined or free swelling hydrogel. For the confined hydrogel, however, Π can be increased above zero at equilibrium by compressing the hydrogel inside the cavity, which is essentially isochoric, of a chemomechanical sensor, thereby increasing the thermodynamic pressure of the hydrogel so that it exceeds that in the surrounding solution by an amount P . This principle is the same as used in reverse osmosis or in the membrane osmometry, and thus the standard thermodynamic equation for a membrane osmometer [33] may be applied here:

$$P = \Pi = (\mu_{1,0} - \mu_1)/V_1 \quad (1.7)$$

It should be noted that hydrogel in the confined state still obey the swelling equilibrium definition, namely the chemical potential of each mobile species, water in this case, is the same in the coexisting phases at equilibrium. At first glance, Eq. (1.7) may suggest chemical potential of water inside and outside the gel is not the same because P is not zero. In Eq. (1.7), $\mu_{1,0}$ and μ_1 are both calculated at the same ambient pressure so they are different in this regard, however, the hydrostatic pressure difference P between the hydrogel and the surrounding solution can just compensate this difference in water chemical potential.

With respect to hydrogels for sensor and actuator applications, hydrogels in the confined state are more widely used than free swelling hydrogel, because uninfluenced free swelling hydrogels can hardly be used to generate signal [34]. For a confined hydrogel inside a chemomechanical sensor subjected to osmotic swelling pressure tests, we must have $\Delta P = \Delta \Pi$, where Π is manipulated by varying the environmental ionic

strength, pH or glucose concentration, etc., and ΔP can be captured by a pressure transducer data acquisition system.

1.2.2.2 Theory-kinetics

The rates of hydrogel swelling and deswelling kinetics can be influenced by a number of processes, which include diffusion, stimulus rate and polymer network relaxation [14]. The swelling process of a stimuli-responsive hydrogels upon stimuli administration includes two steps. First of all, a stimulus must permeate the hydrogel itself; for example, a pH sensitive hydrogel will not respond immediately to external pH change until an ion exchange process has shifted the pH value within the hydrogel. As soon as the stimulus has altered the hydrogel, mass transfer proceeds allowing the solvent to move into or out of the hydrogel, which results in swelling or shrinking of the hydrogel.

Unfortunately, the response time for hydrogel swelling or shrinking is notoriously long. In most cases, this is because the kinetics are governed by polymer network relaxation through the solvent, because the collective diffusion coefficient that dictates this process is much smaller than translational diffusion coefficient of small analytes [35]. This lengthy response time can be alleviated by using constant volume approach or confined method, and because of this isochoric condition, kinetics of hydrogel response time should be limited by the diffusion of analyte to the hydrogel, rather than by the diffusion of polymer network through the solvent. Furthermore, since the osmotic pressure is independent of the hydrogels thickness [35], the response rate of hydrogel could be substantially increased by downsizing the thickness, as the diffusion time is proportional to the square of hydrogel dimension [36].

1.2.2.3 pH sensitive hydrogels

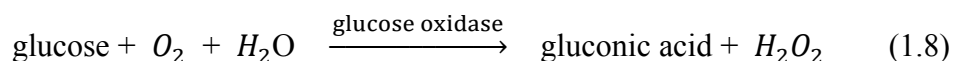
Polyelectrolyte hydrogels are pH responsive because they possess pendant acidic and/or basic groups, which can be ionized. A polyampholytic hydrogel contains both acidic and basic groups in the backbone chains. For example, hydrogels containing basic groups will swell under acidic conditions because the basic groups are protonated and shrink under basic conditions due to the deprotonation of the basic groups. This swelling behavior can be expected from Eq. 1.2 and 1.3, protonation suggests increased ion concentration within hydrogel (c_{gel}) due to electroneutrality constraints. This increase in c_{gel} results in an increase in osmotic swelling pressure which causes swelling. The deprotonation process is the reverse of protonation. pH-sensitive hydrogels have been widely used for controlled drug delivery [37], and other applications include use in biosensors and permeation switches [8,34]. In this work, dimethylaminoethyl methacrylate (DMA) containing tertiary amine group was used as the functional monomer to obtain pH sensitive hydrogels [8]. This pH-sensitive hydrogel containing tertiary amine groups is expected to swell under acidic conditions and deswells under basic conditions.

1.2.2.4 Glucose-sensitive hydrogels

Glucose-sensitive hydrogels are potentially relevant to the development of self-regulated insulin delivery system that can be used to construct an artificial pancreas to control the blood glucose concentration for diabetic patients [38]. To date three principal classes of glucose sensitive hydrogels have been investigated and they are described as follows.

1.2.2.4.1 Enzyme-loaded pH responsive hydrogels

Currently, glucose oxidase (GOx) is the most widely studied enzyme for glucose sensors applications as it is widely used in commercial fingerstick glucose sensors. The underlying working principle is based on the following reaction [39]:



Combining glucose oxidase (GOx) with pH-responsive hydrogels to sense glucose value is the approach that many investigators have employed to develop insulin delivery system [38]. In this sensing approach, GOx is immobilized inside pH-sensitive hydrogels, glucose can be catalyzed by glucose oxidase to produce gluconic acid, thus reducing the pH in the pH-sensitive hydrogels and causing swelling. Insulin is released when the permeability of the pH-sensitive hydrogel increases due to swelling which in turn is a function of glucose concentration. Kost et al. [38] investigated the swelling and permeability properties of glucose-sensitive membranes, which are essentially thin pH-responsive hydrogels containing GOx. GOx was introduced into this pH-responsive hydrogel as one component of the pregel mixture prior to hydrogel synthesis. This study demonstrated that glucose-sensitive membranes containing ionizable groups and GOx are responsive to glucose concentrations near the physiological pH range and might be promising for controlled delivery of insulin.

Ishihara et al. [41] investigated insulin release from pH-sensitive hydrogel capsules containing both glucose oxidase and insulin. This study revealed that insulin release was enhanced in the presence of glucose, but was inhibited in the absence of glucose.

1.2.2.4.2 Hydrogels containing concanavalin A

Concanavalin A (Con A) is a lectin protein that possesses carbohydrate-binding properties. This unique binding property can be explored to fabricate glucose-sensitive systems such as glucose-sensitive hydrogels. Con A contains four glucose binding sites and it has been widely investigated for glucose sensing [38].

The development of Con A based glucose-sensitive hydrogels for insulin delivery systems were pioneered by Brownlee et al. [42] and Kim et al. [43,44]. Their sensing principle was to synthesize a stable, biologically active insulin derivative grafted with oligosaccharides, which are complementary to the binding sites of Con A, and the obtained insulin derivative is able to form a complex with Con A. This insulin derivative could be released from its complex with Con A in the presence of free glucose due to the competitive and complementary binding mechanism [38]. It turns out that the binding constant to Con A for free glucose is larger than that of grafted insulin derivative.

Hydrogels based on this mechanism swell with increasing glucose concentration due to the breaking of the crosslinks between grafted oligosaccharide and Con A with increasing glucose concentration. This swelling occurs because the decrease in crosslinks decreases the shear modulus (see Eq. 1.6), which consequently results in an increase in osmotic swelling pressure and causes swelling (see Eq. 1.2). This sensing mechanism is reminiscent of the antigen-responsive hydrogels reported by Miyata et al. [45]. In this study, antigen and corresponding antibody were grafted to the hydrogel network, so reversible crosslinks in the network were induced by the interaction between grafted antigen and grafted antibody. In the presence of free antigen, the crosslinks were dissociated due to competitive binding and the hydrogel swelled. Once again, free antigen

shows higher affinity to antibody than grafted antigen.

Combination of synthetic polymers containing saccharide residues with Con A can be used to fabricate glucose-sensitive hydrogels. Nakamae et al. [46] investigated a polymer with pendant glucose groups, poly(2-glucosyloxyethyl methacrylate) (PGEMA). The addition of Con A to the aqueous PGEMA solution resulted in flocculation, because the complex formation between pendant glucose groups of PGEMA with Con A gelled the polymer. This turbid PGEMA-Con A solution became transparent upon the addition of free glucose. This occurred because of the dissociation of the PGEMA-Con A complexes induced by glucose. This phenomenon could also be accomplished by free mannose, but not free galactose. This indicates different monosaccharides show different affinity to Con A. These results suggest that PGEMA-Con A complex is sensitive to monosaccharides, and as such is considered a promising candidate for the development of novel glucose sensor or glucose-sensitive insulin delivery system [38].

1.2.2.4.3 Hydrogels containing phenylboronic acid (PBA)

As opposed to the preceding studies that utilized proteins, such as glucose oxidase and concanavalin A, to obtain glucose sensitive hydrogels (GSHs); GSHs that are totally synthetic and involve no biological components can be obtained using phenylboronic acid (PBA). PBA and its derivatives can react with polyols, such as fructose and glucose, to form reversible complexes in aqueous solution. This complex between polyol and boronic acid, however, can be dissociated by a competing polyol which is capable of forming a more stable complex [38]. To date the most widely studied phenylboronic acid for glucose sensitive hydrogels synthesis is 3-acrylamidophenylboronic acid (3-APB) [9,49,51,53], as illustrated in Fig. 1.2.

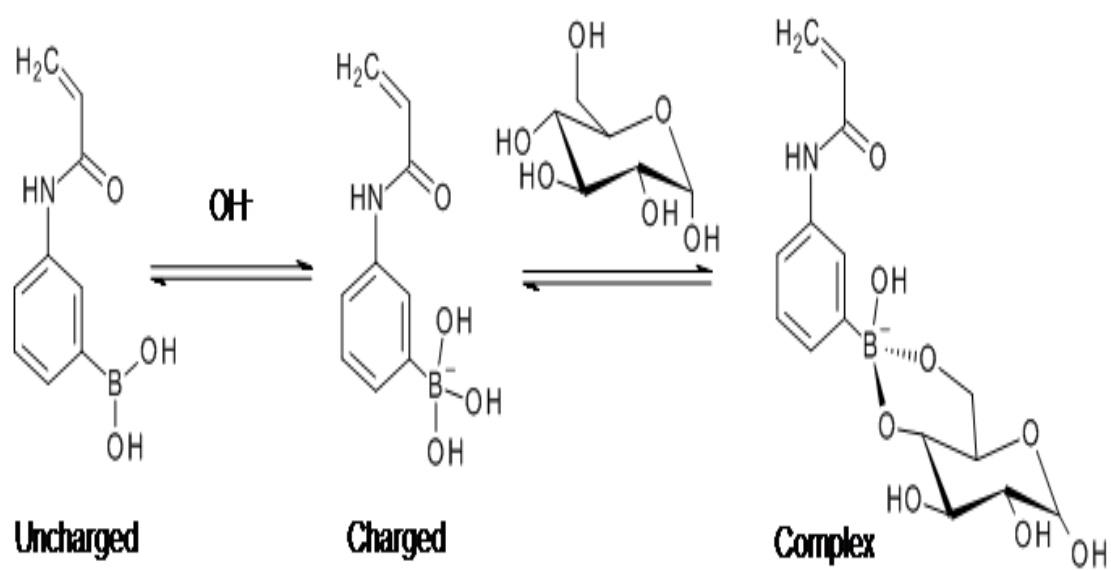


Fig. 1.2. 3-acrylamidophenylboronic acid (3-APB) and its reversible binding with glucose.

In hydrogels containing 3-APB as sketched in Fig. 1.2, the majority of the boronic acid moieties are in the deswelling or uncharged form at physiological pH 7.4, as the pK_a of 3-APB is about 8.6 [47]. The overall reaction is shifted to the right in the presence of glucose, and this results in a greater fraction of boronic acid moieties in the charged form. Hydrogels will thus swell with increasing glucose concentration due to increased osmotic contribution from counterions within the hydrogels. An increase in fixed charges along the hydrogel polymer chain due to increasing glucose concentration (Fig. 1.2) results in an increase in counterions within the hydrogel, which causes increasing osmotic swelling pressure and hydrogel swelling, as seen in Eq. 1.2 and 1.6. Unfortunately, 3-APB will also combine with other molecules containing cis-diols, and in fact the binding constant of PBA for fructose is 40 times higher than for glucose [48].

One can design a phenylboronic acid based hydrogel that shrinks with increasing glucose concentration to essentially eliminate fructose interferences [15-17, 49-53]. This mechanism, however, requires the majority of 3-APB to be in the charged form at physiological pH 7.4. In this sensing principle, glucose contains two sets of cis-diols and thus can bind to two boronic acids simultaneously to form reversible crosslinks, as illustrated in Fig. 1.3. Increasing glucose concentration indicates increasing glucose crosslink density which in turn results in increasing shear modulus (Eq. 1.6), which results in a decrease in osmotic swelling pressure and causes shrinking (Eq. 1.2 and 1.6). Fructose, however, only has one set of cis-diol and thus cannot mediate the formation of such crosslinks. Therefore, phenylboronic acid containing glucose-sensitive hydrogels that shrink with increasing glucose concentration exhibiting high selectivity towards glucose over fructose.

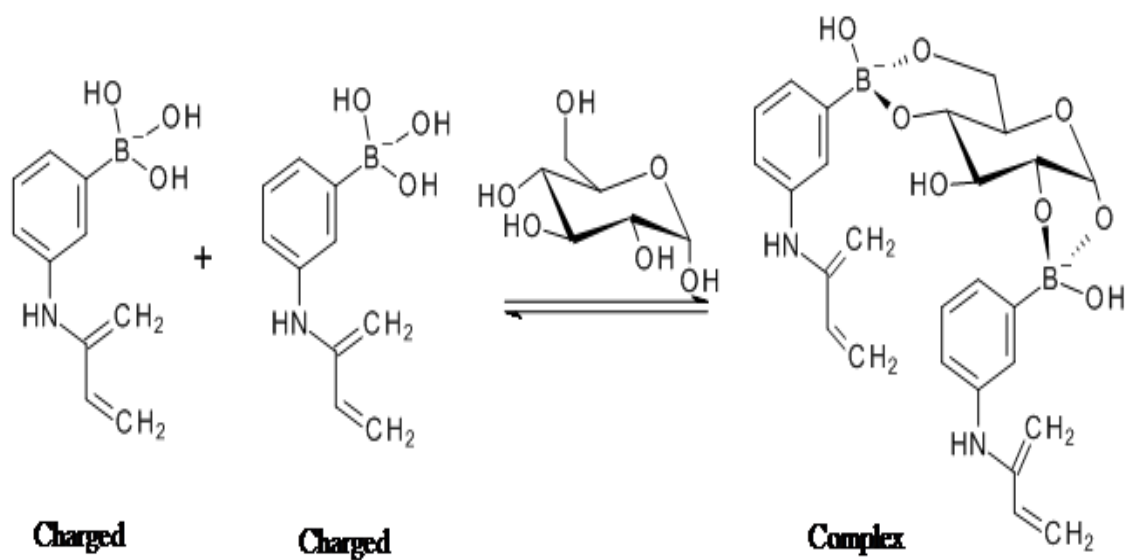


Fig. 1.3. Glucose induced reversible crosslink formation with 3-Acrylamido-phenylboronic acid (3-APB).

In order to generate the charged form of boronic acid at physiological pH 7.4, two methods have been proposed. The first approach is to introduce electron withdrawing groups such as fluorine to the phenylboronic acid to lower the pK_a value of 3-APB, preferably lower than 7.4 [54]. The second method is to design a boronic acid in which chemical bonds such as B-N and B-O bond can be formed to stabilize the charged forms of boronic acid. This can be accomplished by introducing amine groups adjacent to the 3-APB to form B-N bond [53]. In this case, the pK_a of 3-APB can be lowered to about 7.1, and the majority of the 3-APB is in the charged form as shown in Fig. 1.2. Alternatively, 2-Acrylamidophenylboronic acid (2-APB) can be used rather than 3-APB, because 2-APB forms an intramolecular B-O bond that stabilizes the charged form of boronic acid at pH 7.4 [16,50].

1.2.2.4.4. Summary of glucose sensitive hydrogels

While enzyme based glucose-sensitive hydrogels exhibit high sensitivity and specificity to glucose, they also suffer from several major disadvantages. First of all, the reaction continuously consumes glucose, the targeted analyte, and produces hydrogen peroxide. Therefore, this consumptive process will affect the measured glucose value and they can only be used to obtain a transport glucose sensor but cannot be used to make an equilibrium glucose sensor [9]. For an equilibrium sensor that is in the diffusion-limited regime, the sensor sensitivity is determined by the initial and final analyte concentrations, but is independent of analyte diffusivity. However, the response time is affected by analyte diffusivity. In contrast, for a transport sensor, sensor sensitivity and response time are always affected by analyte diffusivity; also, it consumes the analyte of interest. Meanwhile, two major problems associated with the use of glucose oxidase (GOx) have

been identified: the oxygen deficit for the reaction and the decay of the GOx activity with time due to hydrogen peroxide induced degradation [39]. The oxygen deficit reflects the fact that the oxygen molar concentration in the interstitial fluid where the glucose sensor resides is, 1 order of magnitude lower than the glucose concentration (~5.5 mM) [1]. Unlike the sensing mechanism of enzyme based glucose-sensitive hydrogels, concanavalin A (con A) based glucose-sensitive hydrogels are based on competitive glucose binding, which is a nonconsumptive process. Therefore, con A could be used to make an equilibrium sensor and glucose sensors based on this are expected to be stable. Unfortunately, concanavalin A has been reported to be immunogenic and toxic [55]. In contrast, phenylboronic acid based glucose sensitive hydrogels involve no biological components such as proteins and are totally synthetic. Furthermore, boronic acid is generally a biocompatible material with low immunogenicity and low toxicity [56]. Accordingly, phenylboronic acid based glucose sensors can be highly stable and suitable for long-term use. For this reason, glucose sensitive hydrogels employed in this thesis are based on phenylboronic acid.

1.2.3 Review of transduction mechanisms that can be coupled to stimuli-responsive hydrogels

As defined previously, stimuli-responsive hydrogels reversibly swell or shrink with external stimuli stimulation. Other properties of stimuli-responsive hydrogel that may change with external stimulus include mass, density, refractive index, fluorescence, conductivity and modulus [27,34]. Hydrogels-based sensors can be obtained by a scheme in which analyte-induced chemical or physical changes in a hydrogel are transduced into an electrical or optical signal [26]. In this thesis, the transducer is a

piezoresistive pressure sensor array that transduces changes in hydrogel swelling pressure (see Eq. 1.2) into a change of voltage. The hydrogels employed are specifically responsive to either external pH or glucose concentration. In the following, transduction mechanisms that have been coupled to stimuli-responsive hydrogels by previous researchers to obtain sensors are reviewed.

1.2.3.1 Sensors utilizing free swelling hydrogels

Sensors employing free swelling hydrogels must be able to note the changes in one or more hydrogel properties. At least three sensing principles to date have been identified: optical, conductimetric, and oscillator resonant frequency sensing principles [34].

Various optical properties have been explored to obtain hydrogels based pH sensors. Odeh et al. [57] utilized the change in optical transmission to obtain pH sensor where the shrinking hydrogels are opaque indicated by a low optical transmission coefficient, whereas swelling hydrogels are transparent accompanied by a high optical transmission coefficient. Hydrogel swelling or shrinking is also correlated with the change in the refractive index of the hydrogel, and this change in refractive index has been exploited to attain pH sensors [58]. Furthermore, changes in optical wavelength diffraction and fluorescence intensity have also been utilized to obtain hydrogel sensors by Asher [59,60], and McCurley [61], respectively.

Conductometric sensors are devices utilizing their changes in conductivity. Sheppard et al. [62] described an electrode array coated with a pH-responsive hydrogel layer. Hydrogel swelling or shrinking with environmental pH variation induced a change

in ion mobility within the hydrogel which ultimately leads to the change in sensor resistance and conductivity.

Oscillating sensors are based on the measurement of their change in resonance frequency. For a sensor coated with a pH-responsive hydrogel layer, a change in hydrogel mass induced by environmental pH change results in the shift in sensor resonance frequency [34].

1.2.3.2 Sensors utilizing hydrogel mechanical work

Such sensors exploit the capability of hydrogels, under appropriate conditions, to deform or to strain certain sensor components resulting in a change in sensor property outputted as a detectable signal [34]. Two sensing techniques based on mechanical work of hydrogels have been suggested, one is to track the change in optical properties of the sensor and the other is to record the mechanical properties directly [34].

With respect to optical sensors, a responsive hydrogel coupled to a reflector has been investigated where changes in hydrogel volume causes the reflective diaphragm to move which leads to the changes in the intensity of light reflected back to the optical fiber [63]. Meanwhile, hydrogel based fiber Bragg grating sensors based on wavelength change have been described by Cong et al. [64]; the Bragg wavelength is dependent on hydrogel swelling because of hydrogel pushing against the fixed clamps on the Bragg gratings, which results in the change in grating spacing.

For mechanical sensors, microcantilevers and bending plate sensors have been demonstrated [34]. Microcantilevers are devices that can convert the changes in mass, stress, etc. into bending or a change in resonance frequency [34]. The microcantilever is usually accompanied by a read-out system such as an optical or piezoresistive system

[65]. Upon external stimulation, hydrogels attached to the microcantilever will bend the sensor due to hydrogel swelling or shrinking which will exert a change in stress or mass in the sensor. At least two types of bending plate sensors have been explored; one is the capacitance sensors [66-68] and the other is the piezoresistive sensors [35,69,70]. The former utilized the deflection, due to hydrogel swelling pressure change, of one capacitor plate. This deflection changes the distance between two capacitor plates, which results in a change in capacitance which in turn is reflected by a change in sensor resonant frequency. Piezoresistive sensors are based on the stress induced resistance variation and consequently electric signal change such as voltage. As piezoresistive sensors were employed in this thesis, relevant previous studies on this mechanism are reviewed in detail in a separate section below.

1.2.3.3 Previous studies of sensors that combine smart hydrogels with piezoresistive sensors (chemomechanical sensors)

In this sensing principle, a stimuli-responsive hydrogel is fixed between a piezoresistive diaphragm and a rigid porous membrane through which mass transfer occurs [35, 69, 71, 72]. Hydrogel swelling deflects the piezoresistive diaphragm and causes a change in the resistance of the piezoresistive bridge, specifically the resistance of a Wheatstone bridge. The change in resistance is reflected by the change in the output electrical signal such as voltage.

Trinh et al. [69] attached a pH-responsive hydrogel to the backside of a piezoresistive silicon diaphragm, and used a rigid porous membrane to hold the hydrogel in place. To expedite the response kinetics, the hydrogel was chosen to be smaller than the piezoresistive diaphragm and was fixed inside a hard square frame, because the

response time is proportional to the square of hydrogel dimension [36]. In another study from the same research group, Guenther et al. [72] attached a pH-responsive hydrogel thin film to the backplate of a piezoresistive diaphragm. The hydrogel thin film, however, was not held in place by a rigid porous membrane surrounding it or fixed by a hard square frame in this study. Instead, an adhesion promoter layer was introduced to hold a stimuli-responsive hydrogel thin film onto the piezoresistive diaphragm. This novel design should allow rapid response as hydrogel thin film can be easily miniaturized, provided that hydrogel has strong bond with the adhesion promoter and does not detach from the piezoresistive diaphragm.

Herber et al. [71] confined an in situ UV polymerized pH-responsive hydrogel to the front side of a silicon piezoresistive diaphragm, with the hydrogel held in place by a microporous silicon membrane. The hydrogel volume change was estimated to be less than 7% during the sensor response testing, whereas a 125% volume change was observed for the same hydrogel in free swelling state, indicative of essentially isochoric condition in the confined state.

1.2.3.4 Glucose sensors

The current standard glucose sensing technique is the finger-stick method, which is unsuitable for tight blood glucose control as has already been discussed. Briefly, patients have to prick their fingers to get a drop of blood and place the blood on a sensor strip to obtain glucose value. In the real-world sensor marketplace, the big carrot for biosensing companies or developers is a sensor that can continuously and reliably monitor blood glucose concentrations in real-time without having to prick fingers [73]. Tight and strict glucose control can be accomplished by continuous glucose monitoring (CGM) systems,

which involve either noninvasive or minimally invasive blood glucose sensing for glucose detection [9]. In the mid-1990s, two companies squandered hundreds of millions of dollars in a futile attempt to develop noninvasive continuous glucose sensors, employing noninvasive techniques such as near infrared spectroscopy (NIRS) [73]. In NIRS, the infrared beam is transmitted painlessly through the skin [73]. One of the problems with NIRS is that it receives a large background signal from water, which has the IR peaks in the same wavelength range as glucose [74]. Furthermore, the feedback signal returning to the NIRS detector is a complex of contributions from blood vessel, tissue fluid, and is also dependent on the fat levels that vary with the patients. Accordingly, after these checked unsuccessful attempts of noninvasive techniques, research attention shifted to minimally invasive glucose sensors, achieved by either extracting some bodily fluid or making the glucose measurements in situ [73].

Blood glucose concentration measurement can be achieved by either testing the whole blood directly or by testing the subcutaneous interstitial fluid (ISF), where the glucose concentration correlates well with whole blood glucose concentration at steady-state [75]. Generally, for rapid rises in blood glucose, the ISF glucose concentration lags that of the whole blood by about 5-10 min [76,77]. Thus, in case of rapid glucose variation, computer algorithms are used to correct the transient lag between subcutaneous glucose and blood glucose concentration [76]. Due to the severe blood induced biofouling and potential sensor dislodging, which may cause life-threatening embolism, most of the recent attention regarding implantable sensors has been paid to the development of subcutaneously implantable glucose sensors [1].

As of this writing the most widely studied continuous glucose sensing system is the

subcutaneously implanted enzymatic electrochemical glucose biosensor, which is the basis of several commercially available glucose sensors including MiniMed Medtronic Paradigm, Freestyle Navigator, and DexCom Seven [9]. The aforementioned electrochemical glucose sensors are based on the enzyme glucose oxidase (GOx). Admittedly, enzyme-based continuous electrochemical glucose sensors show high selectivity toward glucose and have improved, to some extent, the life quality of diabetic patients. The underlying working mechanism of the enzyme based glucose sensor is given by Eq. 1.8. The sensor sensitivity is proportional to the diffusional flux of hydrogen peroxide to the electrode surface or, equivalently, proportional to the flux of oxygen to the electrode surface [39].

Unfortunately, the electrochemical glucose sensors suffer from several limitations which continue to thwart their long-term use. First of all, for indwelling electrochemical glucose sensors that are only partially implanted and thus require a throughhole in the skin, the risks of infection always exist [73]. Also, two major problems associated with the use of GOx have been identified: oxygen deficit for the reaction and the decay of the GOx activity with time due to hydrogen peroxide induced degradation [39]. Meanwhile, electrochemical glucose sensors are transport sensors, not equilibrium sensors. This means that sensor sensitivity is dependent on glucose diffusivity to the sensors [9]. Unfortunately, the ubiquitous biofouling (proteins or cells' deposition to the surface of the sensor) will definitely alter this diffusivity over time. Furthermore, enzyme based glucose sensors are susceptible to interferences from the endogenous species such as ascorbic acid at the electrode [78]. Lastly, electrochemical CGM generally exhibits large drifts with time and have to be calibrated frequently by fingerstick method [2,10,11].

The above mentioned drawbacks of electrochemical glucose sensors have elicited a widespread search for alternate avenues for continuous glucose monitoring. Glucose sensitive hydrogels (GSHs) sensing is a very promising approach and many studies have been conducted [17,50,52,79,80], presumably because hydrogels are biocompatible since they contain a large percentage of water. To date, the majority of the GSHs developed for glucose sensors utilize the glucose binding moiety phenylboronic acid (PBA). In conjunction with the preceding analysis regarding advantages of phenylboronic acid based hydrogels (see 1.2.2.4), only phenylboronic acid containing glucose sensitive hydrogels sensing will be discussed herein.

In principle, all the aforementioned smart hydrogels transduction sensing principles could also be applied to glucose-sensitive hydrogels to obtain glucose sensors. A glucose sensor could be obtained by coupling GSHs to either an optical sensor which can detect the volume change of GSHs upon environmental stimuli alteration [9,49,50,79-81], or a mechanical sensor which can monitor the change of mechanical properties, such as pressure and resonant frequency [8,67]. Several major publications concerning the use of phenylboronic acid containing glucose-sensitive hydrogels for glucose sensors are listed as follows.

Lowe et al. [50,79] described holographic sensors based on glucose-sensitive hydrogel synthesized from 3-acrylamidophenylboronic acid (3-APB) and 2-acrylamidophenylboronic acid (2-APB). A glucose sensor consisting of a reflection hologram embedded into a thin sugar sensitive hydrogel thin film containing 3-APB was presented [79]. In this study, various mono- and disaccharides were investigated. They found the diffraction wavelength or the color of the hologram reversibly varies with

either saccharide concentration or with type of saccharide due to hydrogel swelling upon cis-diol binding with 3-APB. Unfortunately, this real-time holographic sensor exhibits no specificity for glucose. In a more recent study, Lowe et al. [50] described a similar holographic sensor intended for real-time monitoring of glucose in tear fluid. In this report, however, a novel glucose sensitive hydrogel thin film based on 2-APB was employed to construct the sensor. The results demonstrated that this holographic sensor contracts with increasing glucose concentration due to the glucose crosslinks formation between two charged 2-APB moieties and glucose (see Fig. 1.3). More importantly, this 2-APB based glucose sensor exhibits negligible interference from the metabolic byproduct, lactate, present at a high concentration in the tear fluid, and a significantly reduced pH interference. These observed characteristics made the authors believe that 2-APB based holographic glucose sensor can be used to construct ophthalmic glucose sensing technology to continuously monitor glucose concentration in real-time.

Asher et al. [52,80] reported a glucose sensing materials termed, polymerized crystalline colloidal array (PCCA), consisting of a colloidal crystal within a glucose-sensitive hydrogel based on phenylboronic acid. Herein, the change of PCCA volume due to glucose binding to form reversible crosslinks induced the change in the lattice spacing which in turn changed the wavelength and the color of the PCCA. The PCCA shrinks with increasing glucose concentration as the material involved was 5-amino-2fluorophenylboronic acid, and the introduction of fluorine to the phenylboronic lowers the pK_a and generates the charged boronic acid at pH 7.4. Glucose thus mediated reversible crosslinks between two charged PBA units (see Fig. 1.3). In addition, glucose response kinetics of these materials was improved by graft polymerization of

hydrophobic segments onto the hydrogel backbone. Sensors based on PCCA were also proposed for potential use in contact lenses for detection of glucose in tear fluid.

Tierney et al. [17] investigated an optical glucose sensor based on the incorporation of glucose sensitive hydrogel as a Fabry-Perot cavity to the end of an optical fiber. In this setup, changes in glucose concentration are reflected by the change in optical path length. The glucose sensitive hydrogel employed contains both 3-acrylamidophenylboronic acid and tertiary amines in its backbone and thus shrinks with increasing glucose concentration due to reversible glucose crosslink formation. This occurs because the interaction between the boronic acid moiety and the amino group stabilizes the charged form of boronic acid at physiological pH 7.4.

Siegel et al. [67] proposed a glucose sensor utilizing the change of hydrogel swelling pressure upon glucose addition, similar to the approach of this thesis. In this sensing principle, a microfabricated resonator was coupled to a glucose sensitive hydrogel, which is confined between a thin glass diaphragm and a rigid nanoporous membrane through which glucose diffusion occurs. With increasing glucose concentration, the hydrogel swells and deflects the movable, flexible thin glass capacitor diaphragm. This deflection changes the distance between two capacitor plates, which results in a change in capacitance which in turn is reflected by a change in sensor resonant frequency. Glucose-dependent hydrogel swelling and deswelling results in the change in capacitance of the diaphragm which corresponded to the change in resonant frequency, which can be remotely detected. The glucose sensitive hydrogel involved is based on 3-acrylamidophenylboronic acid (3-APB) and thus exhibits interferences from other simple sugars and pH.

Lastly, fluorescent glucose sensors containing boronic acid are also under intensive investigation [82,83]. As with other sensors, a signaling event that reports the binding of boronic acid with glucose is required to obtain fluorescent glucose sensors. Therefore, a fluorophore that changes fluorescence intensity upon glucose binding is required for fluorescent glucose sensors [82]. Coupling glucose recognition functional moiety boronic acid to a fluorophore, one can obtain a fluorescent glucose sensor. The underlying mechanism responsible for the change in fluorescence of fluorescent sensor is usually photoinduced electron transfer (PET) [84]. PET is one way to quench the fluorescence.

Yoon and Czarnik developed the first fluorescent sugar sensor termed anthrylboronic acids [85], as illustrated in Fig. 1.4. These chemicals exhibit significant fluorescent intensity changes upon binding with saccharide. At physiological pH 7.4, boronic acids are mostly in the neutral trigonal state. In this case, boron acts as electron acceptor in the neutral form, and PET to the boron can occur in the excited state that quenches the fluorescence [82]. However, upon binding with saccharide, the boronic acids become charged and exist in the anionic tetrahedral form due to a decreased pK_a [86]. In the anionic form, the boronic acid is no longer an electron acceptor and thus removes the fluorescence quenching mechanism, which causes an increased fluorescence [82]. The anthrylboronic acids, however, exhibit no selectivity towards glucose, as the boronic acid functional moiety can combine with cis-diols in general.

To increase the selectivity of fluorescent glucose sensors, James et al. [87] developed a novel compound containing two appropriately spaced boronic acid moieties, as illustrated in Fig. 1.5.

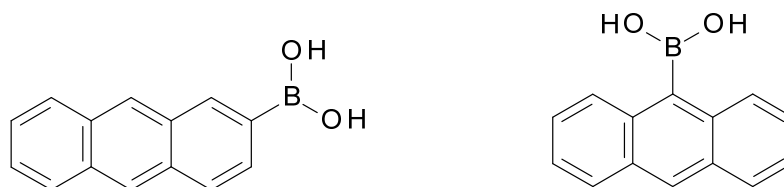


Fig. 1.4. First fluorescence photoinduced electron transfer (PET) sensors for saccharides- Anthrylboronic acids, with boronic acid moiety for glucose binding, and the anthracene moiety being responsible for the transduction of the fluorescent signal.

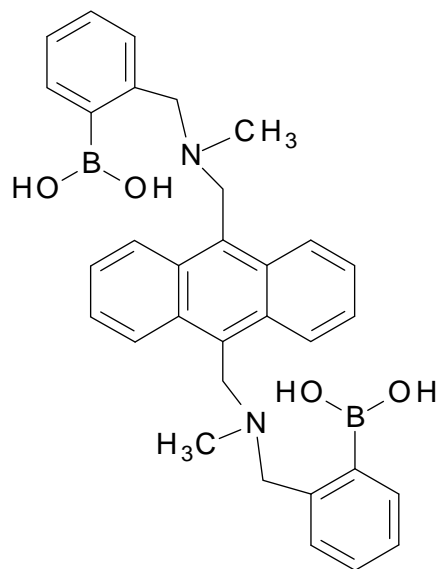


Fig. 1.5. Diboronic acid compound for fluorescent glucose sensing. Adapted from [87].

This diboronic acid (Fig. 1.5) compound exhibits high selectivity towards glucose over other monosaccharides. For instance, the binding constant of this diboronic acid compound with glucose is 12-fold higher than that with fructose [87]. This material was shown to exhibit significant fluorescence intensity change upon glucose binding. Specifically, nitrogen lone pair electrons (not shown in Fig. 1.5) act as electron donor and this quenches the fluorescence in excited state through photoinduced electron transfer (PET); upon binding with glucose, however, the B-N bond strength is strengthened because of the lowering of pK_a value of boron functionality [86]. This B-N bond strength enhancement ties up the nitrogen lone pair electrons and makes them less suitable as electron donor, which consequently results in reduced quenching and increased fluorescence. The selectivity towards glucose of this diboronic acid compound is mainly attributed to the fact that glucose can easily form a 1:1 complex (intramolecular glucose crosslink) with this diboronic acids compound, whereas other monosaccharides such as fructose cannot [87].

Recently, Gamsey et al. [88] developed a poly(2-hydroxyethyl methacrylate) hydrogel, containing a viologen appended with diboronic acids and a fluorescent anionic dye, for the use as a fluorescent hydrogel for continuous glucose sensor applications. In this study, it was observed that the fluorescent hydrogel exhibited excellent reversible dynamic response to glucose concentrations range between 2.5-20 mM. However, the fluorescent hydrogel showed no selectivity towards glucose and the binding affinity towards fructose was the highest; this happened because the distance between the two boronic acid moieties in their compound was too great for glucose to mediate reversible crosslinking formation resulting in poor selectivity. This indicates that an appropriate

distance between two boronic acid moieties is critical in achieving high selectivity to glucose. More recently, a derivative of the Fig. 1.5 diboronic acids compound was employed to obtain a fluorescent hydrogel film for in vivo glucose sensing [89]. In this mouse study, the authors demonstrated fluorescence intensity changed in response to in vivo glucose levels, and the response range was 0-1000 mg/dL of glucose concentration. This study shows the promise of fluorescent glucose sensors for in vivo glucose sensing. Interested readers on fluorescent glucose sensors are referred to the excellent reviews by Wang [82] and Pickup [83] for more detailed information.

1.2.4 Biocompatibility of implantable sensors

As the long-term goal of the research is to develop a sensor that is suitable for in vivo subcutaneous implantation, biocompatibility issues along with corresponding potential approaches to address these issues are discussed in the following.

Upon implantation of a sensor in vivo, the physiological foreign body response to the sensor immediately kicks in. Sensor in vivo utility and performance continues to be compromised by the foreign body response, despite a great deal of intense research effort [78,90,91]. Foreign body response is a physiological cascade to any foreign material that begins with adsorption of proteins to the implant surface and then the accumulation of various inflammatory cells [92, 93].

Neutrophils initially mediate the host response for the first several hours upon implantation before macrophages take over for the next several days [93,94]. Foreign body giant cells (FBGC) are formed and eternally remain at the tissue/implant interface when the implant is too big for the macrophages to get rid of it [93,94]. Subsequently, fibrous encapsulation of the implant occurs when FBGC secrete cytokines that signal

fibroblasts to deposit a dense layer of collagen on the implant to permanently sequester it from the normal tissue [92,93]. For nondegradable implants, fibrous encapsulation is referred to as the final stage of the wound healing response of the tissue to the implant [95]. The final capsule is commonly composed of several different cellular layers surrounding the implant: with macrophages as the inner layer, vascularized tissue as the outer layer, and a fibrous tissue/fibroblast as the middle layer [96].

All aspects of the foreign body response conspire to compromise the sensor's in vivo performance [97]. Sensor sensitivity loss and errant analytic data are mainly due to biofouling, a phenomenon of various proteins, cells and other biological components accumulating onto the surface, and fibrous encapsulation of the implanted biosensor [98]. The biocompatibility of the surface or the outer membrane/coating of an implantable sensor is considered by many to be the pivotal factor in determining the lifetime and performance of the sensor in vivo [99]. Thus considerable research efforts have been devoted to improving the biocompatibility of the membranes and coatings for biosensors. Attempted approaches to improve biocompatibility of implantable sensor coating can be classified into passive coatings and active coatings, as detailed below.

1.2.4.1 Surface modifications – static or passive coatings

As previously stated, surface biocompatibility of the biosensor is deemed by many to be vital in determining the in vivo performance of any implantable biosensor [99]. Various surface modification approaches have been attempted to reduce biosensor membrane biofouling. Wisniewski et al. [100] summarized these methods, which include hydrogel overlays, flow based systems, Nafion coatings, surfactants, phospholipids-based biomimicry, naturally derived materials, covalent attachment,

topology treatments and diamond-like carbons. However, none of these methods were able to completely eradicate biofouling, and no single method stands out as being the most beneficial, though some methods such as the Nafion coating was a good candidate for short-term sensor applications [99]. Hydrophilic surfaces such as hydrogels are commonly employed to minimize or retard proteins adhesion to the implantable surface, since protein adhesion triggers a series of biological responses [101]. However, the in vivo environment is harsh and dynamic; static and passive surfaces by themselves may only be capable of retarding the protein adsorption, but cannot prevent the proteins from adsorbing onto surfaces in vivo. Subsequently, the attached proteins or other biological components that mediate the inflammatory response induce platelet adhesion/activation, and eventually inflammation or thrombus formation will ensue [100]. As indicated in the review by Wisniewski et al., the development of renewable biosensor surfaces or membranes that actively mediate or direct the behavior of the tissue that come in contact with them might be the keys to the success of long-term implantable biosensors [100].

1.2.4.2 Active coatings-nitric oxide (NO) coatings and switchable coatings

Active coatings denote coatings that are capable of releasing or generating physiologically active species, say, NO, which can mediate the extent of protein and cell adsorption and other biological responses [102]. Over the past two decades, nitric oxide (NO) has received extensive research attention and effort from the biomedical research community due to its versatile physiological functions as a regulatory, protective and signaling molecule involved in the modulation of clotting, blood pressure and immune response [99]. In fact, NO is widely known as a pivotal anti-platelet, anti-inflammatory

and vasodilating molecule [103,104-106]. Also, NO has been reported to be able to promote angiogenesis [107] and inhibit bacterial growth [108,109]. Furthermore, NO has a lifetime of less than one second in whole blood owing to its reaction with heme-containing components such as oxyhemoglobin [110]. The endothelium, a thin layer of endothelial cells that line in the interior surface of blood vessels, continuously release NO at an estimated flux in the range of 0.5×10^{-10} to 4.0×10^{-10} molcm⁻²min⁻¹[111]. The short lifetime of NO indicates that a NO-releasing sensor is unlikely to cause any systemic effects because the released NO will be immediately consumed locally [102].

Indeed, several studies employing NO releasing/generating coatings for implantable sensors have been conducted both in vitro and in vivo. The results show the promise of this approach in enhancing biocompatibility. Wilson et al. utilized polyurethane membranes doped with a NO donor as the outer coating for an electrochemical glucose sensor in vivo [112]. They found that the release of NO significantly decreased the inflammatory response during the first 24 h; improved sensitivity with better signal linearity for the NO releasing glucose sensor compared with the control sensor. This was supported by in vivo characterization. Furthermore, the in vivo run-in or break-in period, that is, the time from implantation to stable baseline response, for NO releasing sensor was substantially decreased to minutes as opposed to hours for the control sensor. Though the in vivo study showed no further improvement for the NO releasing sensor after 24 h, this was because the NO donor they employed only has a release time of about 16 h [112]. Schoenfisch et al. [113] employed NO releasing xerogels as the electrochemical glucose biosensor membrane and reduced

bacterial adhesion was reported *in vitro*. In another similar study conducted by Oh et al. [114] about 70-80% less bacteria surface coverage was observed for NO releasing xerogel microarrays compared with the control microarray *in vitro*, indicative of reduction in biofilm formation and implant infection. In addition, cellular adhesion was reduced by more than 40% in the NO-releasing microarray. To tackle the limited release time of NO from the coating containing NO donors, Wu et al. [115] recently evaluated the biocompatibility of intravascular electrochemical oxygen sensors coated with NO-generating coatings with lifetimes of up to 20h *in vivo*. Small metallic copper particles were incorporated within the outer membrane of the oxygen sensor and the NO generation was achieved *in situ* via catalytic decomposition of the endogenous S-nitrosothiols by copper ions originating from copper corrosion. This study suggests that the coatings containing copper particles significantly reduce the occurrence of surface thrombosis and result in more accurate analytical data, most likely because of the NO generated at the sensor/blood interface [115].

On the other hand, switchable or stimuli-responsive coatings for biomedical devices have also been suggested as a better avenue to control over the interaction between biomedical device surfaces and surrounding biological elements [116-118]. A notable example is poly(N-isopropylacrylamide) (PNIPAm), which has a lower critical solution temperature (LCST) of about 32 °C in water. The most well-recognized application of PNIPAm is in the field of cell sheet engineering [119-122], a concept based on the observation that surface coatings of PNIPAm are capable of fostering cell sheet formation at physiological temperature of 37°C and releasing the intact cell sheet at temperatures below the LCST. Furthermore, thermo-reversible adsorption/desorption of

proteins, mammalian cells and bacterial cells on PNIPAm has been reported [123-125]. Therefore, PNIPAm's could be used as self-cleaning implantable sensor coatings to enhance biocompatibility [126].

1.2.4.3 Summary

As discussed above, either NO releasing/generating coatings or PNIPAm based self-cleaning hydrogels seem to be excellent candidates for the development of a long-term implantable biosensor. Unfortunately, neither NO releasing/generating coatings nor PNIPAm based self-cleaning hydrogel are perfectly biocompatible compared with vascular endothelium. The vascular endothelium is an absolutely non-thrombogenic surface because a variety of biological molecules, including NO, work synergistically to maintain its homeostasis and perfect biocompatibility [99]. Coatings that exploit the synergistic effects from several factors might be more biocompatible, for instance, coatings utilize the benefits of both NO and PNIPAm might be more biocompatible than coatings that exploit NO or PNIPAm alone.

1.2.5 Proposed hydrogel-based piezoresistive pressure sensor arrays

1.2.5.1 Method

Chemomechanical sensors proposed in this thesis specifically refer to stimuli-responsive hydrogels based piezoresistive pressure sensors. For the hydrogel in the confined state, osmotic swelling pressure change due to environmental stimuli concentration variations results in the deflection of the diaphragm which in turn leads to the change in resistance and consequently the change in sensor output signal, voltage. The working mechanism of chemomechanical sensors is shown in Fig. 1.6.

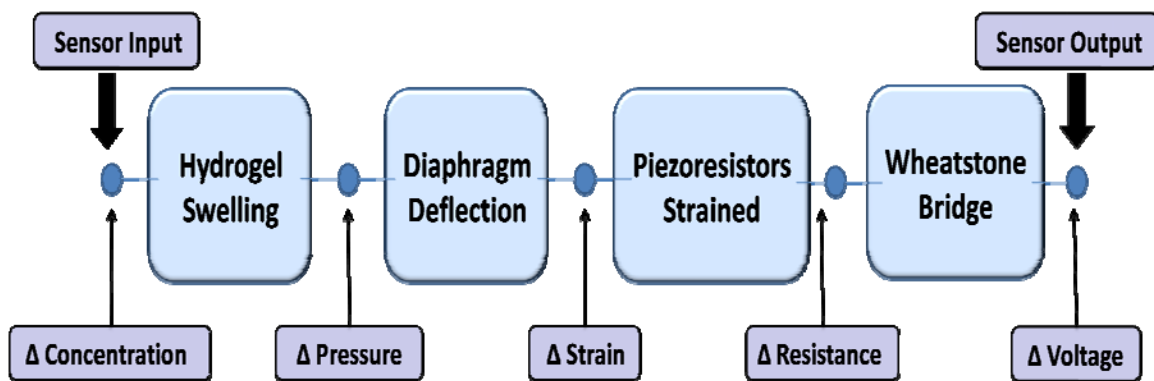


Fig. 1.6. Schematic illustration of hydrogel based chemomechanical sensors. Environmental stimuli cause hydrogel swelling resulting in elevated pressure within the sensor cavity. Elevated pressure induces diaphragm deflection which leads to elevated stress to be developed within the piezoresistors. Use of a Wheatstone bridge is intended to maximize the DC voltage output signal. Adapted from [127].

Based on the foregoing discussion, stimuli-responsive hydrogel based sensors are proposed, with the underlying principle of osmotic swelling pressure response of confined smart hydrogels in contact with the piezoresistive sensors (see Fig. 1.1). This sensing mechanism is perhaps the simplest among the many approaches reviewed above

More significantly, the incorporation of both pH sensitive hydrogels and glucose sensitive hydrogels into the sensor array would enable the sensor array to simultaneously monitor both pH and glucose value. Also, a preliminary macroscale version of such a chemomechanical sensor was used to obtain most of the data in this thesis. Its working mechanism is schematically shown below in Fig. 1.7 [8,70].

In this sensing approach, a smart hydrogel film (B) is confined between a rigid porous membrane (D) and the diaphragm of a piezoresistive pressure transducer (A). A change of environmental analyte concentration, as sensed through the pores of the membrane (D) where analyte transportation occurs, is detected by measuring the change in pressure exerted by the hydrogel on the pressure transducer diaphragm (A).

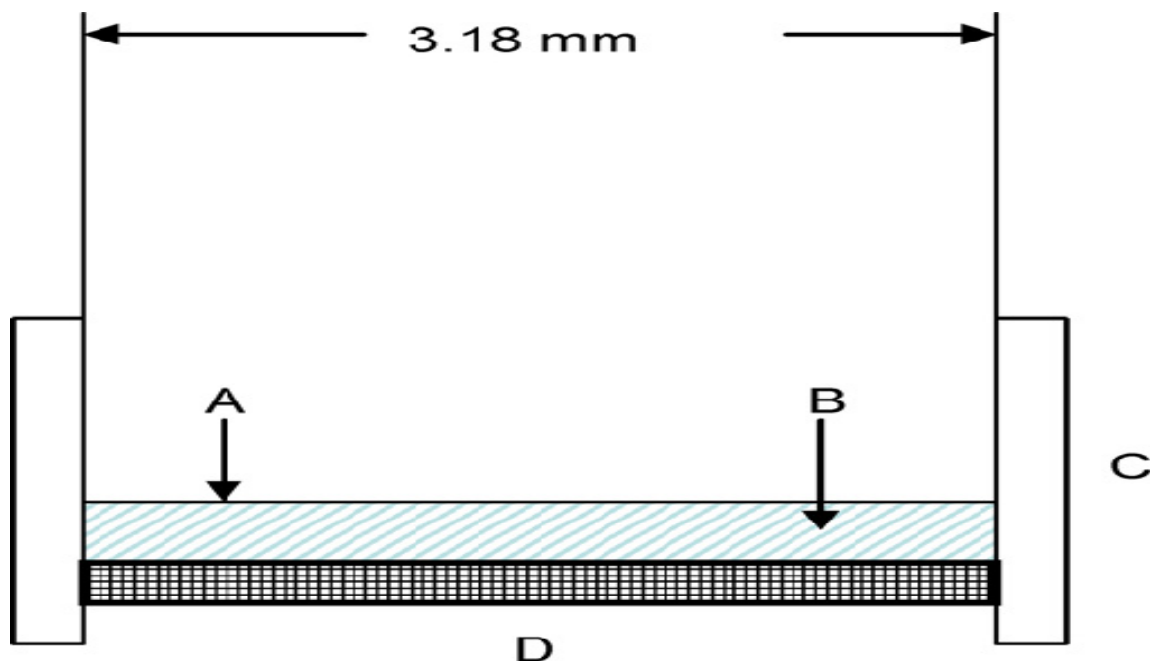


Fig. 1.7. Preliminary version of the chemomechanical sensor used in this study. A piezoresistive pressure transducer with a cylindrical sensing area (A) is completely covered with a disc-shaped hydrogel film (B) of approximate thickness $400\ \mu\text{m}$. The hydrogel is held in place by a cap (C) that has a top surface which is a replaceable wire mesh/porous membrane (D) [8,70].

1.2.5.2 Advantages and disadvantages of proposed

chemomechanical glucose sensors

Use of piezoresistive pressure sensors possesses several advantages: low cost measurement electronics, low power requirement, highly linear output, configurability over large pressure ranges, and easy bulk manufacture with low cost [127]. With regard to chronically-implantable glucose sensors, glucose-responsive hydrogels based chemomechanical sensors holds many advantages over electrochemical sensors that employ the enzyme glucose oxidase; these advantages for chemomechanical sensors are listed below:

1. Versatility- smart hydrogels can be tailor-made to exhibit selective response to almost any analyte.
2. Selectivity- the selectivity of the chemomechanical sensor stems from the incorporated hydrogel binding with the analyte, not from the porous membrane employed. Thus optimal pore size could be used to minimize biofouling.
3. Equilibrium Sensing- a glucose-responsive based chemomechanical glucose sensor can work as an equilibrium sensor, indicating sensor sensitivity is independent of analyte diffusivity. In contrast, electrochemical glucose sensors using the enzyme glucose oxidase continuously consume oxygen and glucose and are transport sensors, with calibration constants depending on analyte diffusivity.
4. Oxygen Independence- the binding between glucose-responsive hydrogels and glucose is independent of oxygen level in the body, whereas electrochemical sensors employing glucose oxidase require oxygen to function and this usually leads to the problem of “oxygen deficit” when blood oxygen level is low relative to glucose.

5. Simple sensing mechanism- perhaps the simplest sensing technique is to confine a stimuli-responsive hydrogel between a rigid porous membrane and the diaphragm of a miniature pressure transducer.
6. Sensor Array- one can easily combine hydrogels for sensing pH, glucose on a single microfabricated sensor chip to simultaneously monitor glucose and pH.

As compared to the proposed chemomechanical glucose sensors, fluorescent glucose sensing also appears to be a very promising approach. Fluorescent glucose sensors contain several advantages such as they can be extremely sensitive, measurements can cause little or no damage to the host, and they can also be equilibrium sensors if boronic acid moieties are employed [83]. The challenges associated with fluorescent glucose sensors are the intrinsic limitations of photostability and the loss of recognition capability [128]; also, leaching problems upon prolonged use have also been reported [129]. These challenges may pose significant problems for the development of fluorescent glucose-sensors for long-term use. With regard to the disadvantages of our proposed sensor array, these include baseline drift and slow response. The retarded response may be mitigated by designing a thinner hydrogel or a hydrogel with an interconnected microporous network.

1.2.5.3 Goals and thesis novelty

The short term goal of our research is to demonstrate the proof-of-concept in vitro that integration of smart hydrogels with microfabricated piezoessitive sensors can be used to obtain both pH sensors and glucose sensors, showing potential application for measuring pH and glucose in vivo for diabetic patients. The long-term goal of the research is to develop a sensor array suitable for subcutaneous implantation and can

simultaneously measure pH, and glucose values for diabetic patients.

We believe the proposed stimuli-responsive hydrogels based sensor array could simultaneously monitoring glucose and pH in the interstitial fluid and thus provide more accurate monitoring and offer better diabetes management in the future. Due to the stability of the totally synthetic hydrogel, the proposed sensor is expected to be quite stable and suitable for long-term use in the future.

This thesis contains several novel topics that have not been explored previously. These include the first measurement of osmotic swelling pressure change of the shrinking glucose sensitive hydrogel (Chapter 3), the first observation of a retarded deswelling process for shrinking glucose sensitive hydrogels (Chapter 4), and the first comparison between swelling pressure response of UV cured and thermally cured polyampholytic glucose-sensitive hydrogels (Chapter 5).

1.3 Thesis overview

This thesis consists of six chapters. Chapter 1 contains the background and review of relevant previous studies. Chapter 2 and chapter 3, both of which have been published, are preliminary in vitro studies on the application of pH-sensitive hydrogels and glucose-responsive hydrogels for sensor applications, respectively. In these two chapters, results were obtained with a macrosized sensor using an off-the-shelf pressure transducer (Fig. 1.7).

Chapter 4, which is basically an extension of chapter 3, investigates the swelling pressure response of different chemical compositions of glucose-sensitive hydrogels that were synthesized, again using the macrosized sensor. Comparison is made between the various glucose-sensitive hydrogels. Meanwhile, novel glucose sensitive hydrogels based

on hydroxyethylmethacrylate (HEMA) are presented. In chapter 5, focus is shifted to the synthesis of both pH-sensitive hydrogels and glucose-sensitive hydrogel via photopolymerization, as opposed to redox initiator induced polymerization employed in the previous chapters. Photopolymerization is more suitable for in situ synthesis of smart hydrogels in the microfabricated sensor array. Proof-of-concept was first demonstrated in the macrosized sensor, and comparison is made between the hydrogels synthesized by either photopolymerization or polymerization induced by redox initiator. Furthermore, pH-sensitive hydrogels and glucose-sensitive hydrogels were synthesized in situ in the microfabricated sensor and some preliminary results are presented.

In chapter 6, conclusions of this thesis are presented and future directions are proposed.

1.4 References

1. J. Wang, Electrochemical Glucose Biosensors, *Chem. Rev.* 108 (2008) 814-825.
2. A. Heller, and B. Feldman, Electrochemical glucose sensors and their applications in diabetes management, *Chem. Rev.* 108 (2008) 2482-2505.
3. The Diabetes Control and Complications Trial Research Group, The effect of intensive treatment of diabetes on the development and progression of long-term complications in insulin-dependent diabetes mellitus, *New Engl. J. Med.* 329(1993) 977-986.
4. UK Prospective Diabetes Study Group, Intensive blood-glucose control with sulfonylureas or insulin compared with conventional treatment and risk of complications in patients with type 2 diabetes, *Lancet* 352 (1998) 837-853.
5. D.M. Wilson, R.W. Beck, W.V. Tamborlane, The accuracy of the FreeStyle navigator continuous glucose monitoring system in children with type 1 diabetes, *Diabetes Care* 30 (2007) 59-64.
6. J.J. Mastrototaro, The minimed continuous glucose system, *Diabetes Technology & Therapeutics* 2 (2000) 13-18.

7. R. Gifford, J.J. Kehoe, S.L. Barnes, B.A. Kornilayev, M.A. Alterman, G.S. Wilson, Protein interactions with subcutaneously implanted biosensors, *Biomaterials* 27 (2006) 2587-2598.
8. G. Lin, S. Chang, H. Hao, P. Tathireddy, M. Orthner, J. Magda, F. Solzbacher, Osmotic swelling pressure response of smart hydrogels suitable for chronically implantable glucose sensors, *Sensors and Actuators B: Chemical* 144 (2010) 332-336.
9. X. Huang, S. Li, J.S. Schultz, Q. Wang, Q. Lin, A MEMS affinity glucose sensor using a biocompatible glucose-responsive polymer, *Sensors and Actuators B: Chemical* 140 (2009) 603-609.
10. B. Feldman, R. Brazg, S. Schwartz, R. Weinstein, A continuous glucose sensor based on wired enzyme technology- results from a 3-day trial in patients with type 1 diabetes, *Diabetes Technology & Therapeutics* 5 (2003) 769-779.
11. N. Sachedina, J.C. Pickup, Performance assessment of the Medtronic-minimed continuous monitoring and its use for measurement of glycaemic control in type 1 diabetic subjects, *Diabetic Medicine* 20 (2003) 1012-1015.
12. G.S. Wilson, Y. Hu, Enzyme-based biosensors for in vivo measurements, *Chem. Rev.* 100 (2000) 2693-2704.
13. W. Kerner, Implantable glucose sensors: Present status and future developments, *Exp. Clin. Endocrinol. Diabetes* 109 (2001) S341-S346.
14. S.H. Gehrke, Synthesis, equilibrium swelling, kinetics, permeability and applications of environmentally responsive gels, *Adv. Polym. Sci.* 110 (1993) 81-144.
15. V.L. Alexeev, A.C. Sharma, A.V. Goponenko, S. Das, I.K. Lednev, C.S. Wilcox, D.N. Finegold, S.A. Asher, High ionic strength glucose-sensing photonic crystal, *Anal. Chem.* 75 (2003) 2316-2323.
16. X. Yang, M.-C. Lee, F. Sartain, X. Pan, C.R. Lowe, Designed boronate ligands for glucose-selective holographic sensors, *Chem. Eur. J.* 12 (2006) 8491-8497.
17. S. Tierney, S. Volden, B.T. Stokke, Glucose sensors based on a responsive gel incorporated as a Fabry-Perot Cavity on a fiber-optic readout platform, *Biosensors and Bioelectronics* 24 (2009) 2034-2039.
18. I.Y. Galaev, B. Mattiasson, Smart polymers and what they can do in biotechnology and medicine, *Trends Biotechnol.* 17(1999) 335-340.
19. N. H. White, Management of diabetic ketoacidosis, *Reviews in Endocrine & Metabolic Disorders* 4 (2003) 343-353.

20. V.R. Kondepati, H.M. Heise, Recent progress in analytical instrumentation for glycemic control in diabetic and critically ill patients, *Anal Bioanal Chem.* 388 (2007) 545-563.
21. http://en.wikipedia.org/wiki/Diabetes_mellitus
22. K.I. Rother, Diabetes Treatment — Bridging the Divide. *N Engl. J. Med.* 356 (2007) 1499–1501.
23. <http://en.wikipedia.org/wiki/Insulin>
24. A.E. Kitabchi, J.N. Fisher, M.B. Murphy, M.J. Rumbak, Diabetes ketoacidosis and hyperglycemic hyperosmolar nonketotic state, *Joslin's diabetes mellitus textbook*. 13th ed. Philadelphia: Lea and Febiger, (1994) 738-770.
25. A.S. Hoffman, Hydrogels for biomedical application, *Adv. Drug Delivery Rev.* 54 (2002) 3-12.
26. I. Tokarev, S. Minko, Stimuli-responsive hydrogel thin films, *Soft Matter* 5 (2009) 511-524.
27. G.R. Hendrickson, L. A. Lyon, Bioresponsive hydrogels for sensing applications, *Soft Matter* 5 (2009) 29-35.
28. N.A. Peppas, J.Z. Hilt, A. Khademhosseini, R. Langer, Hydrogels in biology and medicine: from molecular principles to biotechnology, *Adv. Mater.* 18 (2006) 1345–1360.
29. P.J. Flory, *Principles of Polymer Chemistry*, Cornell University Press: Ithaca, NY, (1953).
30. K. Dusek, W. Prins, Structure and elasticity of non-crystalline polymer networks, *Adv. Polymer Sci.* 6 (1969) 1-102.
31. F. Horkay, I. Tasaki, P.J. Basser, Osmotic swelling of polyacrylate hydrogels in physiological salt solutions, *Biomacromolecules* 1 (2000) 84-90.
32. M.M. Prange, H.H. Hooper, J.M. Prausnitz, Thermodynamics of aqueous systems containing hydrophilic polymers or gels, *AIChE Journal* 35 (1989) 803-813.
33. J.M. Prausnitz, R.N. Lichtenthaler, E.G.D. Azevedo, *Molecular thermodynamics of fluid-phase equilibrium*, 3rd ed., Prentice Hall, Upper Saddle River, New Jersey, (1999).
34. A. Richter, G. Paschew, S. Klatt, J. Lienig, K.F. Arndt, H.J.P. Adler, Review on hydrogel-based pH sensors and microsensors, *Sensors* 8 (2008) 561-581.

35. I.S. Han, M.-H. Han, J. Kim, S. Lew, Y.J. Lee, F. Horkay, J.J. Magda, Constant-volume hydrogel osmometer: A new device concept for miniature biosensors, *Biomacromolecules* 3 (2002) 1271-1275.
36. T. Tanaka, D. Fillmore, Kinetics of swelling of gels, *Journal of Chemical Physics* 70 (1979) 1214-1218.
37. Y. Qiu, K. Park, Environment-sensitive hydrogels for drug delivery, *Advanced Drug Delivery Reviews* 53 (2001) 321-339.
38. T. Miyata, T. Uragami, K. Nakamae, Biomolecule-sensitive hydrogels, *Advanced Drug Delivery Reviews* 54 (2002) 79-98.
39. D.Y. Jung, J.J. Magda, I.S. Han, Catalase effects on glucose-sensitive hydrogels, *Macromolecules* 33 (2000) 3332-3336.
40. J. Kost, T.A. Horbett, B.D. Ratner, M. Singh, Glucose-sensitive membranes containing glucose oxidase: Activity, swelling, and permeability studies, *Journal of Biomedical Materials Research* 19(1985) 1117-1133.
41. K. Ishihara, K. Matsui, Glucose-responsive insulin release from polymer capsule, *J. Polym. Sci. Polym. Lett. Ed.* 24 (1986) 413-417.
42. M. Brownlee, A. Cerami, A glucose-controlled insulin delivery system: semisynthetic insulin bound to lectin, *Science* 206 (1979) 1190-1191.
43. L.A. Seminoff, G.B. Olsen, S.W. Kim, A self-regulating insulin delivery system. I. Characterization of a synthetic glycosylated insulin derivative, *Int. J. Pharm.* 54 (1989) 241-249.
44. S.W. Kim, C.M. Pai, K. Makino, L.A. Seminoff, D.L. Holmberg, J.M. Gleeson, D.E. Wilson, E.J. Mack, Self-regulated glycosylated insulin delivery, *J. Controlled Release* 11 (1990) 193-201.
45. T. Miyata, N. Asami, T. Uragami, A reversibly antigen-responsive hydrogel, *Nature* 399 (1999) 766-769.
46. K. Nakamae, T. Miyata, A. Jikihara, A.S. Hoffman, Formation of poly(glucosyloxyethyl methacrylate)-concanavalin A complex and its glucose-sensitivity, *J. Biomater. Sci. Polym. Ed.* 6 (1994) 79-90.
47. O. Hidenori, U. Eiichiro, K. Hiroyuki, O. Teruo, K. Kazunori, Anomalous binding profile of phenylboronic acid with N-acetylneuraminic acid (Neu5Ac) in aqueous solution with varying pH, *J. Am. Chem. Soc.* 125 (2003) 3493-3502.
48. Y. Gu, Ph.D. Thesis, University of Minnesota, 2003.

49. S. Tierney, B.M.H. Falch, D.R. Hjelme, B.T. Stoeke, Determination of glucose levels using a functionalized hydrogel-optical fiber biosensor: Toward continuous monitoring of blood glucose in vivo, *Anal. Chem.* 81 (2009) 3630-3636.
50. X. YANG, X. Pan, J. Blyth, C.R. Lowe, Towards the real-time monitoring of glucose in tear fluid: Holographic glucose sensors with reduced interference from lactate and pH, *Biosensors and Bioelectronics* 23 (2008) 899-905.
51. S.K. Mujumdar Ph.D. Thesis, University of Minnesota, 2008.
52. M.B. Moshe, V.L. Alexeev, S.A. Asher, Fast response crystalline colloidal array photonic crystal glucose sensors, *Anal. Chem.* 78 (2006) 5149-5157.
53. D. Shiino, A. Kubo, Y. Murata, Y. Koyama, K. Kataoka, A. Kikuchi, Y. Sakurai, T. Okano, Amine effect on phenylboronic acid complex with glucose under physiological pH in aqueous solution, *J. Biomater. Sci. Polymer Ed.* 7 (1996) 697-705.
54. M.B. Moshe, V.L. Alexeev, S.A. Asher, Fast response crystalline colloidal array photonic crystal glucose sensors, *Anal. Chem.* 78 (2006) 5149-5157.
55. T. Kataoka, F.O. Hashi, Y. Sakurai, Immunogenicity and amplifier cell production by tumor vaccines enhanced by ConcanavalinA, *Gann* 73 (1982) 193-205.
56. W. Yang, X. Gao, B. Wang, Boronic acid compounds as potential pharmaceutical agents, *Medicinal Research Reviews* 23 (2003) 346-368.
57. Z.M. Shakhsher, I. Odeh, S. Jabr, W.R. Seitz, An optical chemical sensor based on swellable dicarboxylate functionalized polymer microspheres for pH copper and calcium determination, *Microchim. Acta* 144 (2004) 147-153.
58. J. Dübendorfer, R.E. Kunz, G. Jobst, I. Moser, G. Urban, Integrated optical pH sensor using replicated chirped grating coupler sensor chips, *Sens. Actuat. B*, 50 (1998) 210-219.
59. J.H. Holtz, S.A. Asher, Polymerized colloidal crystal hydrogel films as intelligent chemical sensing materials, *Nature* 389 (1997) 829-832.
60. K. Lee, A.S. Asher, Photonic crystal chemical sensors: pH and ionic strength, *J. Am. Chem. Soc.* 122 (2000) 9534-9537.
61. M.F. McCurley, An optical biosensor using a fluorescent, swelling sensing element, *Biosens. Bioelectronics* 9 (1994) 527-533.
62. N.F. Sheppard, M.J. Lesho, P. McNally, S. Francomacaro, Microfabricated conductimetric pH sensor, *Sens. Actuat. B* 28 (1995) 95-102.

63. W.R. Seitz, New directions in fiber optic chemical sensors: sensors based on polymer swelling, *J. Mol. Structure* 292 (1993) 105-114.
64. J. Cong, X. Zhang, K. Chen, J. Xu, Fiber optic Bragg grating sensor based on hydrogels for measuring salinity, *Sens. Actuat. B* 87 (2002) 487 – 490.
65. L.G. Carrascosa, M. Moreno, M. Alvarez, L.M. Lechuga, Nanomechanical biosensors: a new sensing tool, *Trends in Analytical Chemistry* 25 (2006) 196-206.
66. M. Lei, A. Baldi, E. Nuxoll, R.A. Siegel, B. Ziaie, Hydrogel-based microsensors for wireless chemical monitoring, *Biomed Microdevices* 11 (2009) 529-538.
67. M. Lei, A. Baldi, E. Nuxoll, R.A. Siegel, B. Ziaie, A hydrogel-based implantable micromachined transponder for wireless glucose measurement, *Diabetes Technology and Therapeutics* 8 (2006) 112-122.
68. Z.A. Strong, A.W. Wang, C.F. McConaghy, Hydrogel-actuated capacitive transducer for wireless biosensors, *Biomedical Microdevices* 4 (2002) 97-103.
69. Q.T. Trinh, G. Gerlach, I. Sorber, K.F. Arndt, Hydrogel-based piezoresistive pH sensors: design, simulation and output characteristics, *Sensors and Actuators B* 117 (2006) 17-26.
70. G. Lin, S. Chang, C.-H. Kuo, J. Magda, F. Solzbacher, Free swelling and confined smart hydrogels for applications in chemomechanical sensors for physiological monitoring, *Sensors and Actuators B: Chemical* 136 (2009) 186-195.
71. S. Herber, J. Eijkel, W. Olthuis, P. Bergveld, A.V. Berg, Study of chemically induced pressure generation of hydrogels under isochoric conditions using microfabricated device, *Journal of Chemical Physics* 121 (2004) 2746-2751.
72. M. Guenther, D. Kuckling, C. Corten, G. Gerlach, J. Sorber, G. Suchaneck, K.F. Arndt, Chemical sensors based on multiresponsive block copolymer hydrogels, *Sensors and Actuators B* 126 (2007) 97-106.
73. R.F. Service, Can sensors make a home in the body? *Science* 297 (2002) 962-963.
74. M.A. Arnold, Non-invasive glucose monitoring, *Current Opinion Biotech.* 7 (1996) 46-49.
75. G. Reach, G.S. Wilson, Can continuous glucose monitoring be used for the treatment of diabetes?, *Analytical Chemistry* 64 (1992) 381-386.
76. D.W. Schmidtke, A.C. Freeland, A. Heller, R.T. Bonnecaza, Measurement and modeling of the transient difference between blood and subcutaneous glucose concentrations in the rat after injection of insulin, *Proc. Natl. Acad. Sci. USA* 95

77. T. Danne, K. Lange, O. Kordonouri, Real-time glucose sensors in children and adolescents with type-1 diabetes, *Hormone Research* 70 (2008) 193-202.
78. G.S. Wilson, Y. Hu, Enzyme-based Biosensors for in vivo Measurements, *Chem. Rev.* 100 (2000) 2693-2704.
79. M.C. Lee, S. Kabilan, A. Hussain, X. Yang, J. Bylth, and C.R. Lowe, Glucose-sensitive holographic sensors for monitoring bacterial growth, *Anal. Chem.* 76 (2004) 5748-5755.
80. J.H. Holtz, J.S.W. Holtz, C.H. Munro, and S.A. Asher, Intelligent polymerized crystalline colloidal arrays: Novel chemical sensor materials, *Anal. Chem.* 70 (1998) 780-791.
81. G.J. Worsley, G.A. Tourniaire, K.E.S. Medlock, F.K. Sartain, H.E. Harmer, M. Thatcher, A.M. Horgan, J. Pritchard, Continuous blood glucose monitoring with a thin-film optical sensor, *Clinical Chemistry* 53 (2007) 1820-1826.
82. H. Fang, G. Kaur, B. Wang, Progress in boronic acid-based fluorescent glucose sensors, *Journal of Fluorescence* 14 (2004) 481-489.
83. J.C. Pickup, F. Hussain, N.D. Evans, O.J. Rolinski, D.J.S. Birch, Fluorescence-based glucose sensors, *Biosensors and Bioelectronics* 20 (2005) 2555-2565.
84. D. Silva, A.P. Fox, D.B. Moody, T.S. Weir, S.M. Weir, The development of molecular fluorescent switches, *Trends Biotechnol.* 19 (2001) 29-34.
85. J. Yoon, A.W. Czarnik, Fluorescent chemosensors of carbohydrates. A means of chemically communicating the binding of polyols in water based on chelation-enhanced quenching, *J. Am. Chem. Soc.* 114 (1992) 5874-5875.
86. G. Springsteen, B. Wang, A detailed examination of boronic acid-diol complexation, *Tetrahedron* 58 (2002) 5291-5300.
87. T.D. James, K.R.A. Sandanayake, R. Iguchi, S. Shinkai, Novel saccharide-photoinduced electron transfer sensors based on the interaction of boronic acid and amine, *J. Am. Chem. Soc.* 117 (1995) 8982-8987.
88. S. Gamsey, J.T. Suri, R.A. Wessling, B. Singaram, Continuous glucose detection using boronic acid-substituted viologen in fluorescent hydrogels: linker effects and extension to fiber optics, *Langmuir* 22 (2006) 9067-9074.
89. H. Shibata, Y. Tsuda, T. Kawanishi, N. Yamamoto, T. Okitsu, S. Takeuchi, Implantable fluorescent hydrogel for continuous blood glucose monitoring, *Transducers* (2009) 1453-1456.

90. M.C. Frost, M.E. Meyerhoff, Implantable chemical sensors for realtime clinical monitoring: progress and challenges, *Curr Opin Chem Biol.* 6 (2002) 633–641.
91. G.S. Wilson, R. Gifford, Biosensors for real-time in vivo measurements, *Biosensors and Bioelectronics* 20 (2005) 2388–2403.
92. B.D. Ratner, Reducing capsular thickness and enhancing angiogenesis around implant drug release systems, *J Controlled Release* 78 (2002) 211–8.
93. B.D. Ratner, S.J. Bryant, Biomaterials: where we have been and where we are going, *Annu Rev Biomed Eng* 6 (2004) 41–75.
94. Z. Xia, J.T. Triffitt, A review on macrophage responses to biomaterials, *Biomed Mater* 1 (2006) R1–R9.
95. B. Ratner, A. Hoffman, F. Schoen, J. Lemons, *Biomaterials science: an introduction to materials for medicine*, Academic Press, San Diego, CA (1996).
96. J.H. Brauker, V.E. Carr-Brendel, L.A. Martinson, J. Crudele, W.D. Johnston, R.C. Johnston, Neovascularization of synthetic membranes directed by membrane microarchitecture, *J of Biomed Mater Res* 29 (1995) 1517-1524.
97. E.M. Hetrick, H.L. Prichard, B. klitzman, M.H. Schoenfisch, Reduced foreign body response at nitric oxide-releasing subcutaneous implants, *Biomaterials* 28 (2007) 4571-4580.
98. N. Wisniewski, F. Moussy, W.M. Reichert, Characterization of implantable biosensor membrane biofouling, *Fresenius J Anal Chem.* 366 (2000) 611-621.
99. Y. Wu, and M.E. Meyerhoff, Nitric oxide-releasing/generating polymers for the development of implantable chemical sensors with enhanced biocompatibility, *Talanta* 75 (2008) 642-650.
100. N. Wisniewski, M. Reicher, Methods for reducing biosensor membrane biofouling, *Colloids and Surfaces B: Biointerfaces* 18 (2000) 197-219.
101. J.M. Anderson, Mechanisms of inflammation and infection with implanted devices, *Cardiovasc. Pathol.* 2 (1993) 33-41.
102. M. Frost, M.E. Meyerhoff, Sensors: tackling biocompatibility, *Analytical Chem.* 78 (2006) 7371-7377.
103. L.J. Ignarro, G.M. Buga, K.S. Wood, R.E. Byrns, G. Chaudhuri, Endothelium-derived relaxing factor produced and released from artery and vein is nitric oxide, *Proc. Natl. Acad. Sci. U.S.A.* 84 (1987) 9265-9269.

104. J.G. Diodati, A.A. Quyyumi, N. Hussain, L.K. Keefer, Complexes of nitric oxide with nucleophiles as agents for the controlled biological release of nitric oxide: antiplatelet effect, *Thromb. Haemost.* 70 (1993) 654-658.
105. C.M. Maragos, D. Morley, D.A. Wink, T.M. Dunams, J.E. Saavedra, A. Hoffman, A.A. Bove, L. Isaac, J.A. Hrabie, L.K. Keefer, Complexes of $\cdot\text{NO}$ with nucleophiles as agents for the controlled biological release of nitric oxide. Vasorelaxant effects, *J. Med. Chem.* 34 (1991) 3242-3247.
106. K. Wong, X.B. Li, Nitric oxide infusion alleviates cellular activation during preparation, leukofiltration and storage of platelets, *Transfus. Apheresis Sci.* 30 (2004) 29-39.
107. J.P. Cooke, NO and angiogenesis, *Atheroscler. Suppl.* 4 (2003) 53-60.
108. J. MacMicking, Q.W. Xie, and C. Nathan, Nitric oxide and macrophage function, *Annu. Rev. Immunol.* 15 (1997) 323-350.
109. B.J. Nablo, H.L. Prichard, B.D. Butler, B. Klitzman, M.H. Schoenfisch, Inhibition of implant-associated infections via nitric oxide release, *Biomaterials* 26 (2005) 6894-6990.
110. J.P. Wallis, Nitric oxide and blood: a review, *Transfus. Med.* 15 (2005) 1-11.
111. M.W. Vaughn, L. Kuo, J.C. Liao, Estimation of nitric oxide production and reaction rates in tissue by use of a mathematical model, *Am. J. Physiol. (Heart Circ. Physiol.)* 43 (1998) H2163-2176.
112. R. Gifford, M.M. Batchelor, Y. Lee, G. Gokulrangan, M.E. Meyerhoff, and G.S. Wilson, Mediation of in vivo glucose sensor inflammatory response via nitric oxide release, *J Biomed Mater Res* 75A (2005) 755-766.
113. M.H. Schoenfisch, A.R. Rothrock, J.H. Shin, M.A. Polizzi, M.F. Brinkley, K.P. Dobmeier, Poly(vinylpyrrolidone)-doped nitric oxide-releasing xerogels as glucose biosensor membranes, *Biosensors & Bioelectronics* 22 (2006) 306-312.
114. B.K. Oh, M.E. Robbins, B.J. Nablo, M.E. Schoenfisch, Miniaturized glucose biosensor modified with nitric oxide-releasing xerogel microarray, *Biosensors & Bioelectronics* 21 (2005) 749-757.
115. Y. Wu, A.P. Rojas, G.W. Griffith, A.M. Skrzypchak, N. Lafayette, R.H. Bartlett, M.E. Meyerhoff, Improving blood compatibility of intravascular oxygen sensors via catalytic decomposition of S-nitrosothiols to generate nitric oxide in situ, *Sensors & Actuators B* 121 (2007) 36-46.

116. A.L. Hook, H. Thissen, J.P. Hayes, N.H. Voelcker, Spatially controlled electro-stimulated DNA adsorption and desorption for biochip applications, *Biosensors & Bioelectronics* 21(11) (2006) 2137-2145.
117. Y. Wang, X. Cheng, Y. Hanein, A. Shastry, D.D. Denton, B.D. Ratner, K.F. Bohringer, Selective attachment of multiple cell types on thermally responsive polymer, *Proc. 12th International conference on solid state sensors Actuators and Microsystems*, (2003) 979-982.
118. M. Cole, N.H. Voelcker, H.W. Thissen, Switchable coatings for biomedical applications. *Proceedings of SPIE-The international Society for Optical Engineering*, 5651(Biomedical Applications of Micro-and Nanoengineering II) (2005) 19-27.
119. H.E. Canavan, X.H. Cheng, D.J. Graham, B.D. Ratner, D.C. Castner, Surface characterization of the extracellular matrix remaining after cell detachment from a thermoresponsive polymer, *Langmuir* 21(5) (2005) 1949-55.
120. M. Ebara, T. Aoyagi, K. Sakai, T. Okano, Introducing reactive carboxyl side chains retains phase transition temperature sensitivity in N-isopropylacrylamide copolymer gels, *Macromolecules* 33(22) (2000) 8312-6.
121. M. Yamato, C. Konno, M. Utsumi, A. Kikuchi, T. Okano, Thermally responsive polymer-grafted surfaces facilitate patterned cell seeding and co-culture, *Biomaterials* 23 (2002) 561-7.
122. A. Kushida, M. Yamato, C. Konno, A. Kikuchi, Y. Sakurai, T. Okano, Decrease in culture temperature releases monolayer endothelial cell sheets together with deposited fibronectin matrix from temperature-responsive culture surfaces, *J Biomed Mater Res.* 45(4) (1999) 355-62.
123. D.L. Huber, R.P. Manginell, M.A. Samara, B.I. Kim, B.C. Bunker, Programmed adsorption and release of proteins in a microfluidic device, *Science* 301(5631) (2003) 352-4.
124. D. Cunliffe, C.D. Alarcon, V. Peter, J.R. Smith. C. Alexander, Thermoresponsive surface-grafted poly(N-isopropylacrylamide) copolymers: effect of phase transitions on protein and bacterial attachment, *Langmuir* 19(7) (2003) 2888-99.
125. M.D. Kurkuri, M.R. Nussio, A. Deslandes, N.H. Voelcker, Thermosensitive copolymer coatings with enhanced wettability switching, *Langmuir* 24(8) (2008) 4238-44.
126. R.M. Gant, Y. Hou, M.A. Grunlan, G.L. Cote, Development of a self-cleaning sensor membrane for implantable biosensors, *J Biomed Mater Res A* 90 (2009) 695-701.

127. M. Orthner, Ph.D Thesis, University of Utah, 2010.
128. D.D. Cunningham, J.A. Stenken, *In vivo* glucose sensing, John Wiley & Sons, Inc., New Jersey, 2010.
129. K. Ertekin, S. Cinar, T. Aydemir, S. Alp, Glucose sensing employing fluorescent pH indicator: 4-[(p-N,N-dimethylamino)benzylidene]-2-phenyloxazole-5-one, *Dyes and Pigments* 67 (2005) 133-138.

CHAPTER 2

FREE SWELLING AND CONFINED SMART HYDROGELS FOR APPLICATIONS IN CHEMOMECHANICAL SENSORS FOR PHYSIOLOGICAL MONITORING

Reprinted by permission from Elsevier

Sensors and Actuators B: Chemical 136 (2009) 186-195



Contents lists available at ScienceDirect

Sensors and Actuators B: Chemical

journal homepage: www.elsevier.com/locate/snb

Free swelling and confined smart hydrogels for applications in chemomechanical sensors for physiological monitoring

G. Lin^a, S. Chang^a, C.-H. Kuo^a, J. Magda^{a,*}, F. Solzbacher^{a,b,c}^a Department of Materials Science & Engineering, University of Utah, Salt Lake City, Utah 84112, USA^b Department of Electrical & Computer Engineering, University of Utah, Salt Lake City, Utah 84112, USA^c Department of Bioengineering, University of Utah, Salt Lake City, Utah 84112, USA

ARTICLE INFO

Article history:

Received 18 July 2008

Received in revised form 11 October 2008

Accepted 3 November 2008

Available online 12 November 2008

Keywords:

Chemical sensor

Hydrogel

Piezoresistive sensor

Smart material

ABSTRACT

We investigate thin films of “smart” polymer hydrogels used to convert miniature pressure sensors into novel chemomechanical sensors. In this versatile sensing approach, a smart hydrogel is confined between a porous membrane and the diaphragm of a piezoresistive pressure transducer. An increase in the environmental analyte concentration, as sensed through the pores of the membrane, is detected by measuring the change in pressure exerted by the hydrogel on the pressure transducer diaphragm. We compare the response of such a sensor with the response of a free-swelling hydrogel identical to the one used within the sensor. The sensor and the free hydrogel are observed to have comparable mean response times. However, the time-dependent response curve of the sensor, unlike that of the free hydrogel, is highly asymmetric between swelling and deswelling, with a smaller time constant for deswelling. We also investigate novel methods for increasing sensor sensitivity, such as use of a two-layer membrane with a nanoporous polymer inner layer, and pre-loading of the hydrogel under pressure. In ionic strength response tests, use of an inner membrane increases sensor sensitivity without increasing mean response time, an effect that varies with membrane water fraction.

© 2008 Elsevier B.V. All rights reserved.

1. Introduction

A ‘smart’ or ‘stimuli-responsive’ hydrogel is a cross-linked polymer network that reversibly swells and absorbs water in response to some external stimulus such as change in temperature, pH, or concentration of some analyte [1,2]. Since smart hydrogels are also biocompatible, they are highly suitable for use in implantable biomedical sensors and autonomous drug delivery devices [3], particularly when the hydrogel response time is reduced by miniaturization [4]. Many sensing approaches have been proposed that employ smart hydrogels [5], but perhaps the simplest sensing scheme can be obtained by confining a smart hydrogel between a porous membrane and the diaphragm of a miniature pressure transducer. In such a scheme, a change in the environmental analyte concentration, as sensed through the pores of the membrane, changes the hydrogel osmotic swelling pressure (see definition in Section 2.5), thereby changing the mechanical pressure measured by the pressure transducer. Sensor selectivity can be enhanced by attaching moieties to the hydrogel that selectively bind the analyte of interest [6,7]. Fig. 1 shows our preliminary version of a “chemomechanical sensor” that embodies this sensing principle. The sensor consists of a piezoresistive pressure transducer with a

cylindrical stainless steel sensing area (diameter 3.18 mm) completely covered with a hydrogel film (thickness $\approx 400 \mu\text{m}$). This hydrogel is held in place with a cap having a top surface that consists of a replaceable porous membrane through which mass transfer occurs. The smart hydrogel was synthesized in our lab and is responsive to both pH and ionic strength [8,9]. In previous work with this sensor, we performed tests with a single type of porous membrane and a single value of the hydrogel loading pressure, and analyzed the results neglecting mechanical compliance [9]. In the current study, we present some of the first results for the effect of variations in membrane pore size, open area, and rigidity on chemomechanical sensor response. This is important because the optimum pore size is not known *a priori*, and a tradeoff is likely to exist in its selection. On one hand, a membrane with larger pores and high porosity will allow rapid mass transport, which should reduce sensor response time. On the other hand, such a membrane may also allow the hydrogel to partially exude through the pores, which should reduce sensor sensitivity. Hence we present the results of empirical tests of the effect of the membrane and of the initial hydrogel loading pressure on sensor performance. We also compare the time-dependent response of the sensor with the time-dependent response of a free-swelling hydrogel identical to the one in the sensor. Outside the sensor, smart hydrogel response to an external stimulus is isotropic and unconstrained. However, when the same hydrogel is placed in the sensor, the swelling response is almost completely constrained in the transverse direction by the

* Corresponding author. Tel.: +1 11 801 581 7536.

E-mail address: jj.magda@utah.edu (J. Magda).

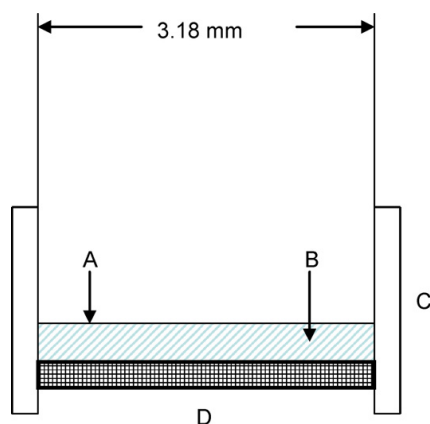


Fig. 1. Preliminary version of the chemomechanical sensor used in this study. A piezoresistive pressure transducer with a cylindrical sensing area (A) is completely covered with a disc-shaped hydrogel film (B) of approximate thickness 400 μm . The hydrogel is held in place by a cap (C) that has a top surface which is a replaceable wire mesh/porous membrane (D).

sensor sidewalls, and partially constrained in the axial direction by the porous membrane and pressure transducer diaphragm. Furthermore, the hydrogel in the sensor experiences elastic forces exerted by the porous membrane and the piezoresistive diaphragm that are not present outside the sensor. In order to assess the significance of these elastic forces, we compare the asymmetry of the time-dependent response (swelling vs. deswelling) for hydrogels inside and outside the sensor.

Although smart hydrogels have been studied for many years, their use as pressure-generating materials in chemomechanical sensors has been studied in only a few laboratories [6,9–12]. The most relevant previous studies were published by Herber et al. [11] and Trinh et al. [12]. Both of these publications include results for the time-dependent response of a chemomechanical sensor, as well as estimates of the degree of hydrogel constraint within the sensor. Trinh et al. [12] attached a pH-responsive hydrogel (40 μm thick) to the backside of a piezoresistive silicon diaphragm (20 μm thick), and used a rigid porous silicon membrane (320 μm thick, 600 μm pore size) to hold the hydrogel in place. The deflection of the piezoresistive membrane during sensor response to pH was determined via nanofocus microscan measurements. Herber et al. [11] attached a pH-responsive hydrogel (10 μm thick) to the front side of a silicon piezoresistive diaphragm, with the hydrogel held in place by a rigid microporous silicon membrane (200 μm thick, 50 μm pore size). The hydrogel volume change was estimated to be less than 7% during sensor response testing. In both of these previous studies, commercial pressure chips were used in the construction of the chemomechanical sensor, which is also true for our prototype chemomechanical sensor (Fig. 1). In the future, we plan to fabricate chemomechanical sensors with custom-designed pressure chips, and the results presented here will guide the design of the porous membranes and piezoresistive diaphragms.

2. Experimental methods

2.1. Materials

The monomers hydroxypropyl methacrylate (HPMA), *N,N*-dimethylaminoethyl methacrylate (DMA), and tetra-ethyleneglycol dimethacrylate (TEGDMA) were obtained from Polysciences, Inc. and used as received. Ammonium peroxydisulfate (APS, Sigma-Aldrich), *N,N,N',N'*-tetra-methylethylenediamine (TEMED,

Sigma-Aldrich) and Delbecco's phosphate-buffered saline solution (PBS, Sigma-Aldrich) were also used as received. Market grade wire cloth meshes (type 304 stainless steel) were obtained from Small Parts, Inc., Miramar, FL, USA. Nanoporous polyethylene terephthalate (PET) membranes made by ion bombardment and nonporous cellulosic paper membranes were donated by Andreas Koch of Oxyphen AG, Lachen, Germany.

2.2. Hydrogel synthesis

Polyelectrolyte pH-responsive hydrogels containing HPMA/DMA/TEGDMA at a nominal mole ratio of 70/30/02 were prepared by free radical cross-linking copolymerization as in Refs. [8,9]. In brief, nitrogen gas was bubbled through pregel solutions containing measured amounts of the monomers HPMA and DMA and cross-linker TEGDMA, after which the pregel solution was injected into a cavity (thickness 400 μm) between two square glass plates of surface area 64 cm^2 . Shortly thereafter, free radical polymerization was initiated at room temperature by injection of the initiator APS and the reaction accelerator TEMED. After 4 h at room temperature, the hydrogel slab was removed from the glass mold, cut into square samples (1–2.3 cm in length) and washed in PBS buffer (pH 7.4) for at least 2 days before testing. In order to accelerate the cleaning process, the hydrogels were subjected to several swelling/deswelling cycles induced by variations in bath ionic strength between 0.05 M and 0.15 M.

2.3. Sensor construction and sensor response tests

Fig. 1 contains a sketch of the chemomechanical sensor employed in this study. This is the same sensor employed in a previous investigation from this lab [9], though the porous membrane was varied in the current study as described below. The sensor consists of a piezoresistive pressure transducer (model EPB-501-5P, Entran, Inc., Fairfield, NJ, USA) with a cylindrical stainless steel sensing area (diameter 3.18 mm) completely covered with a hydrogel film of thickness $\approx 400 \mu\text{m}$. The hydrogel is held in place in the sensor by a cap with a top surface that consists of a replaceable porous membrane through which mass transfer can occur. The sensor cap porous membrane is a stainless steel wire cloth mesh (mesh size 40–200, corresponding mesh opening 381–74 μm), used with or without either an Oxyphen nanoporous membrane (pore size 0.1 μm , thickness 20 μm , porosity 15%) or a nonporous paper membrane (thickness 80 μm). The Entran pressure transducer was calibrated using a water column (pressure range 0–14 kPa) and an air manometer (model PCL-200 D from Omega, pressure range 0–65 kPa). A smart hydrogel was synthesized and cleaned as described above, a circular biopsy tool was used to cut a disc-shaped sample of appropriate diameter, and the sample was then transferred while in a deswollen state to the sensing surface of the pressure transducer using tweezers. The sensor cap with chosen wire mesh was attached to the sensor base by tightening three screws that were adjusted to impose an axial compressive stress on the hydrogel in the sensor. The sensor was then inserted into a large covered environmental bath containing PBS buffer at room temperature with known ionic strength (0.05 M or 0.15 M) and pH value (6.8 or 7.4). This bath also contained a magnetic stirrer used to minimize external mass transfer resistance to the sensor. Sensor response tests were performed by either injecting buffered saline solution into the environmental bath, or by rapidly switching the sensor into another environmental bath of differing ionic strength, and then noting the time-dependent response of the pressure transducer. The time-dependent pressure signal was captured with an Agilent data acquisition system.

2.4. Free-swelling tests

Hydrogels from the same synthesis batch were used in both the free-swelling tests and in the sensor response tests. Furthermore, in order to make the external mass transfer resistance as similar as possible, the same environmental bath was used in both types of response tests, with the same degree of stirring. In the free-swelling test procedure, hydrogel samples were pre-conditioned by soaking in PBS buffer until reaching equilibrium, and then transferred into the appropriate environmental bath. Periodically, a hydrogel sample was withdrawn and rapidly weighed after removing excess surface water by light blotting with a laboratory tissue. The time-dependent hydrogel sample weight W was monitored in this way until a steady value was obtained. The time-dependent swelling ratio Q was calculated as W/W_d , where W_d is the weight of the same hydrogel sample when completely dry. Dry weights were determined by weighing samples after several days of drying in a laboratory oven at 55 °C.

2.5. Thermodynamic analysis and predicted effect of initial hydrogel pressure

A simple working equation for the chemomechanical sensor can be derived by combining the standard model for the swelling of polyelectrolyte hydrogels [9,13–16] with the standard model for membrane osmometry [16]. This equation is by no means exact, but it nonetheless useful as qualitative guide to the trends that can be expected. For an unconfined polyelectrolyte hydrogel, the total free energy of swelling ΔF_{tot} contains three contributions: a negative contribution associated with the mixing of water with polymer segments, a negative contribution associated with the mixing of water with counterions, and a positive contribution associated with the stretching of the hydrogel network [13–16]. The osmotic swelling pressure Π is obtained by differentiating ΔF_{tot} with respect to moles of water [13–15]:

$$\Pi = - \left(\frac{\delta \Delta F_{\text{tot}} / \delta n_1}{V_1} \right) = \frac{(\mu_{1,0} - \mu_1)}{V_1} \quad (1)$$

In Eq. (1), V_1 is the molar volume of water, n_1 is the number of moles of water, μ_1 is the chemical potential value for water in the hydrogel at ambient pressure, and $\mu_{1,0}$ is the chemical potential value for water in the reference solution that surrounds the hydrogel. Hence $\Pi = 0$ for the unconfined hydrogel at equilibrium. However, Π can be increased above zero by compressing the hydrogel inside the chemomechanical sensor, thereby increasing the thermodynamic pressure of the hydrogel so that it exceeds that in the surrounding solution by an amount P . This is the same principle used in reverse osmosis or in membrane osmometry, and thus the standard thermodynamic equation for a membrane osmometer [16] may be applied here:

$$P = \Pi = \frac{(\mu_{1,0} - \mu_1)}{V_1} \quad (2)$$

The content of Eq. (2) is that the chemical potential of water in the hydrogel may be less than that in the surrounding solution (both calculated at ambient pressure), provided that the pressure in the hydrogel exceeds that in the surrounding solution by an amount $P = \Pi$. In a chemomechanical sensor response test, we must have $\Delta P = \Delta \Pi$, where Π is manipulated by varying environmental pH or ionic strength, and ΔP is measured by the piezoresistive diaphragm. Restricting attention to an ionic strength response test at fixed pH ≈ 7 , Π is a function of environmental ionic strength I and hydrogel swelling ratio Q , $\Pi = \Pi(I, Q)$. For example, osmotic deswelling experiments were performed on hydrogels with the same nominal composition as in the current study [9], and the results for Π from

this previous study are well fit by the empirical equation:

$$\Pi = A Q^{-2} - B \quad (3)$$

Here A and B are constants determined empirically for a given choice of reference solution: $A = 5591$ kPa and $B = 93.1$ kPa at $I = 0.15$ M; $A = 5286.7$ kPa and $B = 38.5$ kPa at $I = 0.05$ M. Suppose we perform a sensor response test in which ionic strength I is suddenly reduced from $I_0 = 0.15$ M to $I_f = 0.05$ M. This increases the chemical potential of the surrounding water ($\mu_{1,0}$), or, equivalently, increases Π . In the ideal case, ΔP will increase by an amount $\Delta \Pi_0 = \Pi(I_f, Q_i) - \Pi(I_0, Q_i)$, where Q_i is the initial swelling ratio just before the start of the sensor response test. However, in practice, the piezoresistive sensor will respond to an effective Π change that is less than this, due to mechanical compliance that allows a slight increase in the hydrogel swelling ratio within the sensor. Hence the actual signal ΔP measured by piezoresistive diaphragm in a ionic strength response test is given by:

$$\Delta P = \Delta \Pi_0 - \Delta \Pi_1 = [\Pi(I_f, Q_i) - \Pi(I_0, Q_i)] - [\Pi(I_f, Q_f) - \Pi(I_f, Q_i)] \quad (4)$$

where Q_f is the final swelling ratio of the hydrogel in the sensor, $Q_f > Q_i$. The first term on the right hand side of Eq. (4) is the response of an ideal chemomechanical sensor with no mechanical compliance, and the second term is the correction for hydrogel swelling within the sensor. The postulated path of the hydrogel during the response test for a hydrogel loaded in the sensor at ambient pressure P_0 is shown schematically as $A \rightarrow B \rightarrow C$ in Fig. 2. In Fig. 2, $\Delta \Pi_0$ is the vertical distance between points A and B, $\Delta \Pi_1$ is the vertical distance between points B and C, and the signal ΔP is the vertical distance between points A and C. Fig. 2 was constructed using Eq. (3) for Π , and assuming a linear proportionality between pressure and hydrogel swelling ratio:

$$P = H(Q - Q_0) \quad (5)$$

where H is the effective spring constant of the container that confines the hydrogel in the sensor, and Q_0 is the swelling ratio that gives zero gage pressure. It is obvious from Fig. 2 that the signal ΔP increases with increase in H , the slope of the line P vs. Q . However, ΔP becomes independent of H when H is sufficiently large; that is, when the line P vs. Q in Fig. 2 approaches the vertical. Now

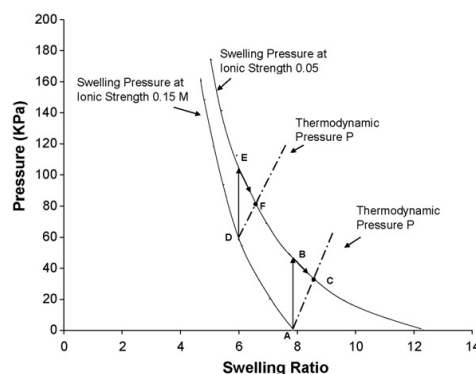


Fig. 2. Schematic diagram showing postulated path of hydrogel thermodynamic state during two sensor response tests, both tests involving the same reduction in environmental ionic strength, but with differing values of the initial pressure on the hydrogel. The two solid curves summarize the measured results from Ref. [9] for hydrogel swelling pressure vs. swelling ratio Q and the two dashed-dot lines are hypothetical curves for piezoresistive sensor pressure P vs. Q . The sensor response signal is the vertical distance between points A and C (zero loading pressure) or D and F (high loading pressure).

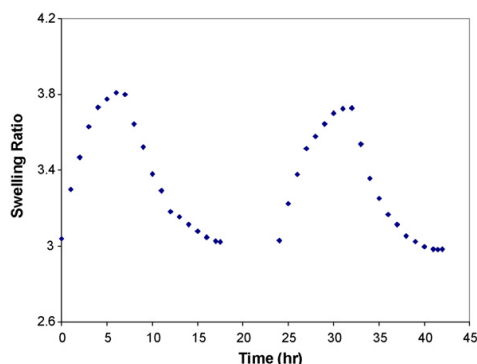


Fig. 3. Time-dependent pH response of free-swelling hydrogel (initial thickness $\approx 400 \mu\text{m}$) in PBS buffer at fixed ionic strength (0.15 M). Initial environmental pH value was 7.4, pH was suddenly decreased to 7.15 at time = 0, suddenly increased to 7.4 at time = 7 h, and then the cycle was repeated.

consider an ionic strength response test in which the hydrogel is loaded into the sensor at an elevated pressure P_{high} , $P_{\text{high}} > P_0$. In this case, the hydrogel may follow the path shown schematically in Fig. 2 as $D \rightarrow E \rightarrow F$. Eq. (4) still applies and may be used to compare the sensor response starting at P_{high} with the sensor response starting at P_0 . In the former case, the initial value of Π is of course higher due to hydrogel compression, but what matters for the signal is $\Delta\Pi_0$, and Eq. (3) predicts that $\Delta\Pi_0$ has essentially the same value at loading pressures of P_{high} and P_0 . The effective spring constant H may be larger for the test performed starting at P_{high} , which would tend to increase the sensor signal. On the other hand, Eq. (3) predicts that the osmotic modulus $\kappa = -Q\partial\Pi/\partial Q$, a measure of the resistance of the hydrogel to the loss of water by squeezing, increases with decreasing Q . If this is the case, then $\Delta\Pi_1$ will be larger for the sensor response test performed starting at P_{high} , which will tend to reduce the sensor signal (see Eq. (4)). As shown in Fig. 2, the predicted sensor signal is expected to be slightly less for sensor response tests performed at elevated loading pressure. However, this analysis is based on Eq. (4), which uses a single parameter H to characterize the effective constraint of the chamber and the piezoresistive diaphragm on the hydrogel, when in reality the elastic properties of the chamber and the diaphragm are anisotropic. We have also assumed that H is independent of loading pressure and hydrogel swelling ratio.

3. Results

3.1. Free-swelling tests

The synthesized HPMa/DMA/TEGDMA hydrogels are pH-responsive because they contain pendant tertiary amines (on DMA) that become protonated at sufficiently low environmental pH value, thereby temporarily increasing the osmotic swelling pressure Π of the hydrogel. The osmotic swelling pressure can also be temporarily increased by reducing the environmental ionic strength at fixed pH, which increases the chemical potential of the surrounding water. In either case, the temporary increase in Π is compensated for by swelling of the unconfined gel, and by some combination of swelling and increase in pressure P for the gel in the sensor (see Eq. (4)). From previous work on hydrogels of the same composition [8], the water content of the unconfined hydrogel varies with pH primarily in the transition pH range between 7.0 and 8.0. Fig. 3 shows the time-dependent change in the swelling ratio Q of the unconfined gel when the external pH value is cycled between 7.4 and 7.15 at fixed ionic strength in PBS buffer. As expected, Q is

higher at the lower pH value (by about 25%), and the free-swelling response is both reversible and reproducible, albeit very slow. Fig. 4 shows the time-dependent change in the swelling ratio Q of the unconfined gel when the external ionic strength is cycled between 0.15 M and 0.05 M at fixed pH equal 7.4. As expected, Q is higher at the lower ionic strength value (by about 33%), and the response is once again reversible and reproducible. Comparing Figs. 3 and 4, the most obvious difference is the time scale of the response, which is about 50 times slower for the pH change than for the ionic strength change, even though the initial hydrogel thickness is the same and amount of swelling is similar. Siegel has already reported that hydrogels of similar composition can exhibit very slow pH response kinetics [17]. For our purposes, the key conclusions to be drawn from Fig. 3 are (1) the degree of protonation along the hydrogel backbone increases with decreasing pH and (2) the pH response time is so long for hydrogels of thickness $400 \mu\text{m}$ that drift of the pressure baseline is likely in the chemomechanical sensor. Thus we exclusively consider ionic strength sensor response in the following. The perceptive reader may also notice that the shape of the time-dependent response curve is different in Figs. 3 and 4. The time-dependent ionic strength response of the unconfined hydrogel accurately obeys the 2nd order kinetic model of Quintana [18–19], whereas the time-dependent pH response does not, nor does the time-dependent sensor response given below. Hence for qualitative comparison of response kinetics, we define τ_{50} as the time at which the change in the swelling ratio or the change in the swelling pressure reaches 50% of its long time value. In Fig. 4, τ_{50} is about 3 min for both swelling and deswelling, whereas τ_{50} is about 2.25 h for swelling and 3.5 h for deswelling in Fig. 3. The free-swelling response times are unaffected by changes in the width of the square samples (1–2.3 cm) at fixed initial thickness ($400 \mu\text{m}$).

3.2. Sensor response tests

In order to obtain good performance of the chemomechanical sensor (Fig. 1) in response to a reduction in environmental salt concentration (or pH), we must employ a porous membrane that allows rapid diffusive transport, and yet does not allow the gel to fully swell to its unconfined volume or to exude through the pores in the membrane. Since the membrane design parameters needed to achieve this are unknown, we begin by investigating sensor performance with off-the-self wire cloth meshes used as membranes. Fig. 5(a) shows an SEM micrograph of one particular stainless steel wire cloth mesh used as the permeable membrane in the sensor. The micrograph confirms that the mesh is highly regular with the

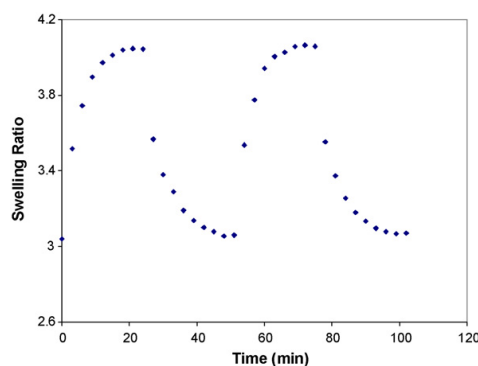


Fig. 4. Time-dependent ionic strength response of free-swelling hydrogel (initial thickness $\approx 400 \mu\text{m}$) in PBS buffer at fixed pH 7.4. Initial environmental ionic strength value (I) was 0.15 M, I was suddenly decreased to 0.05 M at time = 0, suddenly increased to 0.15 M at time = 24 min, and then the cycle was repeated.

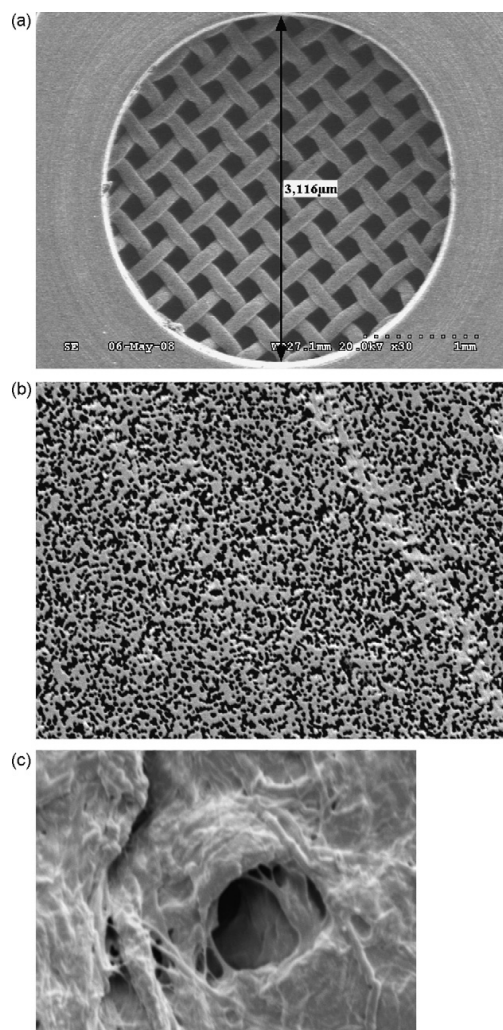


Fig. 5. (a) SEM image of stainless steel 80 mesh wire cloth inside of chemomechanical sensor; (b) SEM image of nanoporous polyester membrane (Oxyphen AG) prior to its use in sensor with wire cloth membrane in some of the sensor tests (field of view = 35 μm in width); (c) SEM image of nonporous cellulosic paper membrane (Oxyphen AG) prior to its use in sensor with wire cloth membrane in some of the sensor tests (field of view = 35 μm in width).

parameters expected for 80 mesh wire: size of opening 178 μm , wire diameter 135 μm , open area 31%. The ionic strength response of the sensor used with this mesh is given in Fig. 6. Fig. 6 shows the swelling pressure as a function of time during cyclic variations in environmental ionic strength value I between 0.15 M and 0.05 M at fixed pH equal 6.8. In this experiment, a hydrogel was first transferred in a deswollen state from a PBS bath at $I=0.15$ M into the sensor, and then the sensor cap was tightened until the pressure signal increased by 11 kPa above the ambient value. The observed sensor response in Fig. 6 is rapid and reversible, even for the first swelling cycle, provided that the hydrogel is subjected to several free-swelling cycles before loading into the sensor as recommended by Guenther et al. [20]. However, in some cases (2nd and 3rd cycles in Fig. 6), the sensor exhibits a slight overshoot mea-

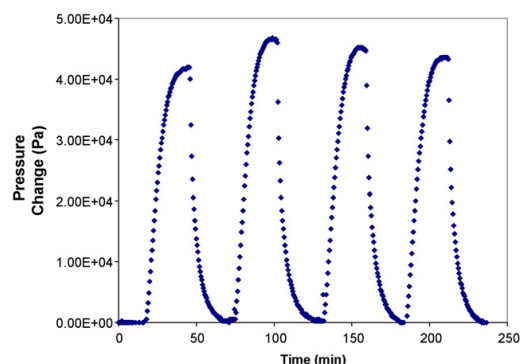


Fig. 6. Time-dependent change in pressure (relative to baseline pressure) measured by chemomechanical sensor of Fig. 1 in response to change in ionic strength I at fixed pH 6.8 in PBS buffer. The initial environmental ionic strength value was 0.15 M, I was suddenly decreased to 0.05 M at time = 17 min, suddenly increased to 0.15 M at time = 45 min, and then the cycle was repeated three times (single layer 80 mesh wire, baseline = initial, loading pressure = 11,000 Pa).

sured to be of order 5% in response to the decrease in environmental strength. This phenomenon was previously reported by Herber et al. [11], who suggested that once the peak pressure is reached, a small amount of salt transfers out of the hydrogel, thereby reducing hydrogel swelling pressure Π . The response time τ_{50} in Fig. 6 is 6.4 min for swelling, and 2.3 min for deswelling, which may be compared with 3 min for both swelling and deswelling in Fig. 4. Thus confinement of the hydrogel in our chemomechanical sensor both increases the mean response time (at least for ionic strength changes), and produces an asymmetry between the kinetics of swelling and deswelling.

3.3. Influence of initial hydrogel pressure on the magnitude of the sensor response

In Section 2.5, thermodynamic arguments were used to predict the effect on ionic strength response of an increase in the hydrogel loading pressure, defined as the initial value of the gage pressure P prior to a sensor response test. This quantity can be adjusted by tightening or loosening the screws that attach the sensor cap to the sensor base, thereby increasing the pressure exerted by the porous membrane on the gel. The predicted effect of the hydrogel loading pressure was tested by cycling the environmental ionic strength twice between 0.15 M and 0.05 M, and measuring the response of the sensor at two different values of the loading pressure. The results obtained are shown in Fig. 7, where the initial pressure values for the two cycles, from left to right in Fig. 7, are 11 kPa and 19 kPa. As a rough approximation, according to Eq. (3), an increase in loading pressure from 11 kPa to 19 kPa compresses the initial hydrogel volume by about 5%. As shown in Fig. 7, the sensor response magnitude increases from 40 kPa to 61 kPa. Thus the sensor sensitivity increases significantly with increasing loading pressure, in disagreement with the predictions put forth in Section 2.5. In between the two cycles in Fig. 7, one also observes that tightening of the sensor screw cap causes a temporary jump in pressure that relaxes to a plateau before the start of the next cycle.

One possible explanation for the discrepancy between theory and the experimental results in Fig. 7 is that the effective spring constant H was assumed to be constant in Section 2.5, independent of hydrogel swelling ratio and hydrogel loading pressure. The value of H characterizes the effective stiffness of the chamber used to confine the hydrogel in the sensor, and as such will be affected by any compliance associated with the membrane or piezoresistive

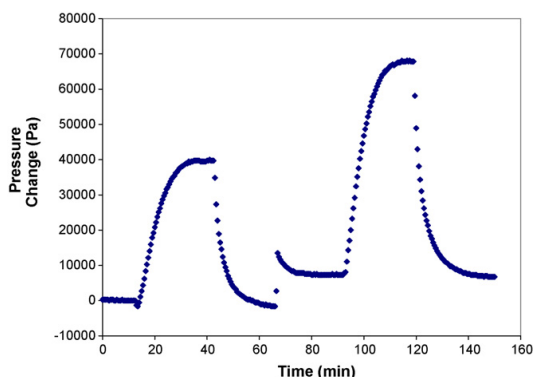


Fig. 7. The effect of hydrogel loading pressure on the sensor response to ionic strength changes at fixed pH 6.8 in PBS buffer. The ionic strength was cycled between 0.15 M and 0.05 M, and the change in pressure (relative to baseline) was measured with the initial pressure on the hydrogel adjusted to 11 kPa for the first cycle, and 19 kPa for the second cycle (single layer 80 mesh wire, baseline pressure = 11,000 Pa).

diaphragm, or by the presence of any free space in the chamber. Our calibration measurements show that the stiffness of the piezoresistive diaphragm is independent of pressure over a very wide pressure range as expected for silicon, but this may not be the case for the wire cloth mesh. The initial deflection of the wire cloth membrane is of course larger if the response test is performed at an elevated loading pressure value. If the stiffness of the wire cloth mesh increases with increasing deflection, this could explain the observed increase in sensor response magnitude with increase in initial pressure. In order to test this hypothesis, we repeated the ionic strength response test of Fig. 7 after replacing the 80 mesh wire cloth membrane with a 40 mesh wire cloth, which is much stiffer. The 40 mesh wire cloth is approximately twice as thick as the 80 mesh wire cloth (405 μm vs. 290 μm), has a wire diameter of 265 μm , a mean mesh opening of 381 μm , and an open area of 36%. Fig. 8 shows the results obtained. Even though the 40 mesh wire cloth is stiffer than the 80 mesh wire cloth, sensitivity to ionic strength response is less when the sensor is deployed using the 40 mesh wire cloth membrane. Fig. 8 also confirms that the sensor response magnitude increases with increasing hydrogel loading pressure. Thus the increase in the sensor response magnitude with increasing initial loading pressure cannot be explained by an increase in mesh stiffness with mesh deflection.

3.4. Use of two-layer membranes in the sensor

According to the results in Fig. 8, the chemomechanical sensor is less sensitive when used with the 40 mesh wire cloth membrane than with the 80 mesh wire cloth membrane, even though the 40 mesh wire cloth membrane is stiffer. A possible explanation for this surprising result is that the hole size or open area of the 40 mesh wire cloth is too large, and hence the hydrogel partially exudes through the mesh while swelling, thereby reducing sensor sensitivity. One would like to vary the wire mesh opening while holding the mesh stiffness constant, but this is not possible because mesh opening and mesh stiffness both decrease with increasing mesh number. In order to circumvent this problem, we explore the use of two-layer membranes in the sensor. The function of the outer layer is to provide stiffness, whereas the inner layer has a smaller pore size and thus prevents the hydrogel from exuding through the mesh. The first two-layer membrane explored was obtained by combining 40 mesh stainless steel wire cloth with 200 mesh stainless steel wire cloth (thickness = 100 μm , mean opening = 74 μm ,

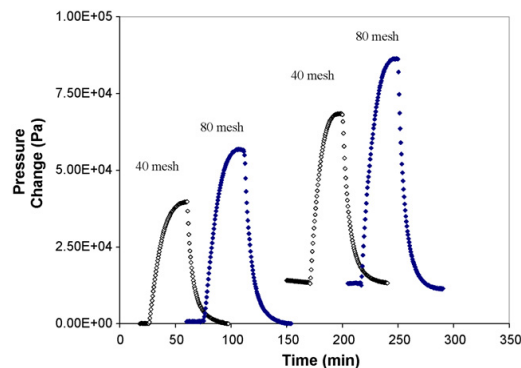


Fig. 8. Influence of wire mesh and initial hydrogel loading pressure on sensor response to ionic strength change at fixed pH 7.4 in PBS buffer. The ionic strength was cycled between 0.15 M and 0.05 M, and the pressure (relative to baseline) was measured with the hydrogel constrained by: single layer 40 mesh wire (\circ); single layer 80 mesh wire (filled diamonds). The initial pressures on the hydrogel were: 9500 Pa (first cycle with 40 mesh); 23,000 Pa (2nd cycle with 40 mesh); 11,500 Pa (first cycle with 80 mesh), 24,000 Pa (second cycle with the 80 mesh), baseline pressure = 9500 Pa for experiments with 40 mesh, 11,500 Pa for experiments with 80 mesh.

wire diameter = 58 μm , open area = 29%). This combination was a failure. Sensor sensitivity was actually less when the sensor was used with the 40/200 mesh combination than with the 40 mesh wire cloth membrane alone, perhaps because of poor adhesion between the two stainless steel layers. Much better sensor performance was obtained when the 80 mesh stainless steel wire cloth mesh was combined with the nanoporous Oxyphen PET membrane (thickness 20 μm , pore size 0.1 μm , open area 15%, see Fig. 5(b) for SEM image). As shown in Fig. 9, the sensitivity of the sensor to ionic strength change increases dramatically when the nanoporous membrane is added as an inner layer to the 80 mesh stainless steel wire cloth. However, mixed results are obtained when the nanoporous membrane is added to the 40 mesh wire cloth: sensor sensitivity is improved, but sensor reproducibility is worsened. A possible explanation for this is that the Oxyphen PET membrane is so thin and flexible that it can partially exude through the large 40 mesh openings (381 μm), but cannot exude through the smaller 80 mesh openings (178 μm). With the 40 mesh wire cloth, better results are obtained with a cellulosic paper inner layer that is thicker and stiffer than the nanoporous Oxyphen PET membrane. The dry thickness of the paper layer is 80 μm , four times that of the Oxyphen membrane. Unlike the Oxyphen, no nanopores were etched in the paper membrane, but in the SEM images (Fig. 5(c)), one observes an occasional micropore. As shown in Fig. 10, the sensitivity of the sensor to ionic strength change increases dramatically when the paper membrane is added as inner layer to the 40 mesh stainless steel wire cloth. This was not unexpected. The unexpected result in Fig. 10 is the improvement in response time that also occurs, particularly with respect to deswelling kinetics. Fig. 11 shows the effect on sensor performance of adding the nanoporous paper membrane to the 80 mesh wire cloth membrane. Fig. 11 confirms that the introduction of the nonporous paper layer improves both sensor ionic strength response kinetics and sensor sensitivity.

The data of Table 1 provides a summary of the response time values τ_{50} observed for both freely swelling hydrogels and for the chemomechanical sensor of Fig. 1 deployed with various combinations of porous membranes and at various loading pressures. The table also includes values for the magnitude of the sensor response. In all cases the results were measured with hydrogels of initial thickness approximately 400 μm subjected to cyclic changes in ionic strength between 0.05 M and 0.15 M at fixed pH. The batch-to-batch

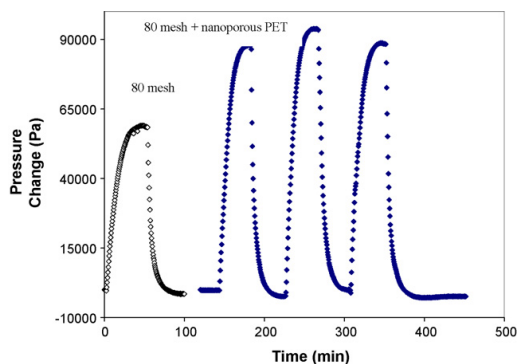


Fig. 9. The effect of adding a nanoporous polymer layer on sensor response to ionic strength change at fixed pH 7.4 in PBS buffer. The ionic strength was cycled between 0.15 M and 0.05 M, and the pressure change (relative to baseline) was measured with the hydrogel constrained by: single layer 80 mesh wire (\diamond); single layer 80 mesh wire plus nanoporous polymer (filled diamonds). The initial pressures on the hydrogel were: 10,500 Pa (single layer 80 mesh); 10,500 Pa (80 mesh + polymer), baseline pressure = 10,500 Pa.

variation in hydrogel swelling pressure response is of order 5 kPa, which is the principle source of sensor experimental uncertainty. When the paper or PET membrane was used as inner layer, it was difficult to adjust the loading pressure to a pre-determined value. Hence sensor tests with different membrane configurations were unfortunately often performed at different loading pressures. Several trends are apparent. The mean response time of the sensor (i.e. average τ_{50} value, swelling and deswelling) is almost always greater than that of the identical free-swelling hydrogel. Undoubtedly the hydrogel in the sensor swells less than a free-swelling hydrogel, because the porous membrane and the piezoresistive diaphragm oppose swelling in the axial direction. In fact, Toomey et al. [21] showed that a smart hydrogel attached to a surface in such a way that lateral swelling is prevented has a smaller volume response than an unattached hydrogel. This being the case, one might have expected the sensor response time to be smaller

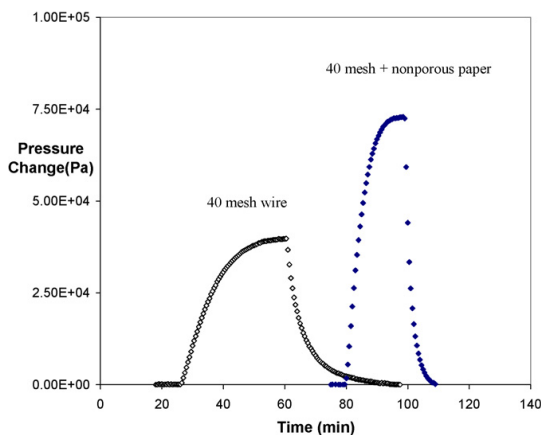


Fig. 10. The effect of adding a nonporous paper layer on sensor response to ionic strength change at fixed pH 7.4 in PBS buffer. The ionic strength was cycled between 0.15 M and 0.05 M, and the pressure change (relative to baseline) was measured with the hydrogel constrained by: single layer 40 mesh wire (\diamond); single layer 40 mesh wire plus paper (filled diamonds). The initial pressures on the hydrogel were: 9500 Pa (single layer 40 mesh); 7500 Pa (40 mesh + paper), baseline = initial loading pressure for both cycles.

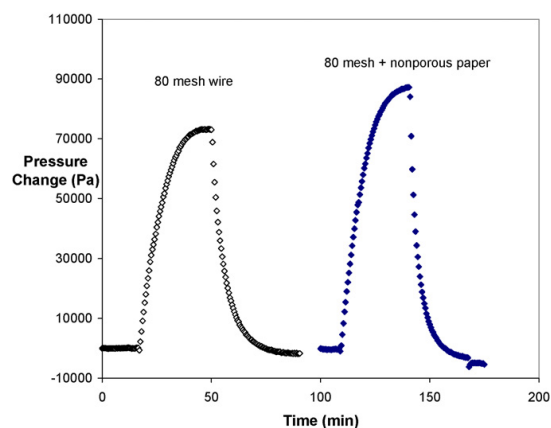


Fig. 11. The effect of adding a nonporous paper layer on sensor response to ionic strength change at fixed pH 7.4 in PBS buffer. The ionic strength was cycled between 0.15 M and 0.05 M, and the pressure change (relative to baseline) was measured with the hydrogel constrained by: single layer 80 mesh wire (\diamond); single layer 80 mesh wire plus paper (filled diamonds). The initial pressures on the hydrogel were: 24 kPa (single layer 80 mesh); 19 kPa (80 mesh + paper membrane), baseline = initial loading pressure for both cycles.

than that of a free-swelling hydrogel. A possible explanation for this is that the hydrogel in the sensor has only one exposed surface through which diffusion can occur, unlike the freely swelling hydrogel. The swelling response time of the sensor is always larger than the deswelling response time. An increase in the hydrogel loading pressure invariably increases the sensitivity of the sensor used with any type of porous membrane, and also reduces the mean response time. The sensor response time for the swelling half-cycle is reduced to a much greater extent by an increase in loading pressure than the sensor response time for the deswelling half-cycle. Introduction of either the nanoporous Oxyphen (Fig. 9) or the nonporous paper (Fig. 10) as an inner membrane layer substantially increases sensor sensitivity. However, the effect on the sensor response kinetics is less certain, and analysis of the data is complicated by the necessity of comparing results at different loading pressures. Introduction of the nanoporous Oxyphen PET membrane or the nonporous paper to the 80 mesh wire cloth improves sensor sensitivity without substantially changing the mean response time. The Oxyphen PET membrane could not be used with the 40 mesh wire cloth, as noted previously. Introduction of the nonporous paper to the 40 mesh wire cloth substantially decreases the mean response time, primarily by reducing the time constant for the deswelling half-cycle (Fig. 10, Table 1). In fact, the smallest average response time (swelling plus deswelling) is obtained when the sensor is deployed with a two-layer membrane consisting of a 40 mesh stainless steel wire cloth and the nonporous paper membrane. This is the only sensor configuration that gives response kinetics as fast or faster than that of a freely swelling hydrogel.

4. Discussion

For a fixed change in ionic strength, our simple model (Section 2.5, Fig. 2) predicts that the change in osmotic swelling pressure $\Delta\pi_0$ is largely independent of the initial state of compression of the hydrogel. Hence it is very surprising that the sensor response signal is observed to increase with loading pressure under all conditions (Figs. 7 and 8, Table 1). The two most likely sources of error in the model are (1) the use of Eq. (3) to calculate $\Delta\pi_0$ and (2) the assumption that the spring constant H in Eq. (5) is independent of Q and loading pressure. Eq. (3) is based on osmotic deswelling

Table 1
Ionic strength response times and response magnitudes of sensor with various membrane configurations.

Porous membrane	pH	Loading pressure (kPa)	Response pressure (kPa)	Mean response time (min)	Swelling half time (min)	De-swelling half time (min)
Free-swelling gel	7.4	N/A	N/A	3.1	3.25	3.0
Free-swelling gel	6.8	N/A	N/A	2.8	2.9	2.6
80 mesh wire	7.4	10	55	6	8	4
80 mesh wire	7.4	23	69	5.6	7.1	4.1
80 mesh plus nonporous paper	7.4	7	54	5.5	8.5	2.5
80 mesh plus nonporous paper	7.4	18	83	5.1	7.5	2.7
40 mesh wire	7.4	9	38	5.7	7.8	3.5
40 mesh wire	7.4	16	47	5.2	6.3	4.1
40 mesh wire	7.4	22	52	5.1	5.8	4.4
40 mesh plus nonporous paper	7.4	8	51	3	4.6	1.4
40 mesh plus nonporous paper	7.4	10	69	2.7	3.9	1.4
80 mesh wire	7.4	11.5	57	6.5	9.5	3.5
80 mesh wire	7.4	21	65	4.9	6.5	3.3
80 mesh plus nanoporous polymer	7.4	13.5	92.5	5.15	6.1	4.2
80 mesh plus nanoporous polymer	7.4	24	112	4.9	4.6	5.2

measurements performed several years ago on hydrogels of similar composition [9], and thus we do not expect it to be quantitatively accurate here for hydrogels synthesized much more recently under slightly different reaction conditions. Nonetheless, the prediction that $\Delta I/I_0$ is a weak function of loading pressure in the range of loading pressures studied (5–30 kPa) is probably qualitatively accurate, given that theoretical analysis based on the Donnan model [13] leads to the same prediction. The assumption that H is independent of loading pressure is much more suspect. The value of H characterizes the effective stiffness of the chamber used to confine the sensor, $H = dP/dQ$. If there is free space available in the sensor chamber at low values of the loading pressure, then the hydrogel can expand laterally into the free volume without increasing P , and H is correspondingly low at low swelling ratios. However, when the hydrogel swells enough to fill all the free space, the value of H will increase to a much higher value reflecting the true stiffness of the membrane and the piezoresistive diaphragm. Thus the true plot of P vs. Q in Fig. 2 should probably be a curve with a slope that increases dramatically above a critical swelling ratio. An increase in loading pressure will reduce this critical swelling ratio by reducing the amount of free space initially available, thereby reducing the compliance correction $\Delta I/I_1$ and increasing the sensor signal ΔP (see Eq. (4)). This likely explains the observed increase in sensor sensitivity with increasing loading pressure. Furthermore, if the true stiffness of the stainless steel mesh greatly exceeds the osmotic modulus (Section 2.5) of the gel, then the signal becomes insensitive to the mesh stiffness. Apparently the initial compression of the hydrogel was never sufficient to completely remove all the free space initially available, because the sensor response signal increases with loading pressure over the entire range of loading pressures studied (5–50 kPa).

If the hydrogel can expand laterally into free space without deflecting the piezoresistive diaphragm, then the response time τ_{50} derived from the P signal may not reflect the true response time of the hydrogel. This may explain why an increase in loading pressure also improves the response time of the sensor. To some extent, this improvement may be attributable to the reduction in gel thickness with initial gel compression, which reduces the diffusion path length. However, using Eq. (3), one predicts that the reduction in thickness is only of order 10% for a loading pressure range increase of 20 kPa. Furthermore, one would expect the reduction in diffusion path length to affect the swelling and deswelling response times similarly. In practice, sensor response time for the swelling half-cycle is reduced to a much greater extent by an increase in loading pressure. For example, with hydrogel loading at a pressure of 11.5 kPa in the sensor with the 80 mesh wire cloth (Table 1), the τ_{50} value for swelling greatly exceeds that for deswelling (9.5 min vs. 3.5 min), whereas the two τ_{50} values become more nearly equal at

a loading pressure of 21 kPa (6.5 min vs. 3.3 min). This implies that the presence of free space in the sensor chamber at low loading pressures is partly responsible for the asymmetry in the time-dependent response curve between swelling and deswelling. This can be explained as follows. The membrane and the piezoresistive diaphragm exhibit mechanical forces that oppose swelling and accelerate deswelling. During the swelling half-cycle, the hydrogel expands laterally to fill all available free space in the sensor before the outward deflection of the piezoresistive diaphragm is complete. On the other hand, during deswelling the piezoresistive diaphragm completes its return to its equilibrium position before the hydrogel finishes contracting laterally within the sensor. Hence the apparent time constant τ_{50} derived from the pressure signal is larger for swelling than for deswelling. An increase in the hydrogel loading pressure increases sensor sensitivity and decreases the apparent asymmetry between swelling and deswelling kinetics by reducing the amount of lateral swelling within the sensor.

If the membrane pores are too large, then the hydrogel can swell by exuding through the pores without deflecting the piezoresistive diaphragm. The effect of this will be similar to that of lateral swelling within the sensor chamber: a reduction in $H = dP/dQ$, an increase in the compliance correction $\Delta I/I_1$, and a decrease in the sensor signal ΔP (see Eq. (4)). We have indirect evidence that this is the case: introduction of a nanoporous or nonporous inner layer substantially increases the sensitivity of the sensor used with the 80 mesh wire cloth (Fig. 9) and with the 40 mesh wire cloth (Fig. 10). We believe that the inner membrane layer increases sensitivity by preventing the hydrogel from exuding through the holes in the stainless steel mesh. Unfortunately, we cannot image the interface between a steel mesh and the hydrogel in a meaningful way, because the interface rearranges and the contact pressure changes when the sensor is transferred from the aqueous solution to the vacuum chamber of the SEM. The 80 mesh wire cloth has a square pore opening of 178 μm with 31% open area. While this may seem like a very coarse mesh, it is not out of line with the porous membranes used in previous studies of chemomechanical sensors: 600 μm pore size and 24% open area by Trinh et al. [12], 50 μm pore size and 31% open area by Herber et al. [11]. Of course the optimum pore size will vary to some extent with hydrogel mechanical properties, and different hydrogels have been used in all studies of chemomechanical sensors from different laboratories published to date.

The PET Oxyphen nanoporous membrane and the nonporous paper membrane are both too flexible to be used in the sensor without a stainless steel mesh to provide rigidity. Thus a two-layer membrane is best for optimizing the sensitivity of our sensor. Surprisingly, it may also be best for optimizing the sensor response time, at least for ionic strength changes. The diffusive permeability of a two-layer membrane with a nanoporous inner layer is surely

much less than that of a single stainless steel 80 mesh cloth with a pore opening of 178 μm , and yet the average sensor response time is approximately the same (Fig. 9 and Table 1). Perhaps introduction of the Oxyphen PET layer eliminates the time required for the hydrogel to exude through and retract from the holes in the steel mesh, and this is more important to the response kinetics than the decrease in diffusive permeability. The most puzzling results pertain to the use of the nonporous paper (Fig. 5(c)) as an inner membrane layer on the stainless steel wire cloths. Introduction of the paper layer improves sensor sensitivity by preventing the hydrogel from exuding through the openings in the steel mesh. Not surprisingly, the effect is more pronounced with the 40 mesh (Fig. 10) than with the 80 mesh (Fig. 11), because the 40 mesh is coarser. However, the paper layer is fairly thick, and hence its use in the sensor increases the diffusion path length by over 25%, assuming that the water-swollen paper does not penetrate into the hydrogel. Nonetheless, use of the paper layer with the 80-mesh wire does not substantially change sensor response time, and its use with the 40-mesh wire actually reduces sensor response time, primarily by reducing the time constant for deswelling (Fig. 10). It is puzzling that the nonporous paper seems to offer so little resistance to mass transfer. However, this is another indication that we are studying a kinetic regime in which the time-dependent mechanical properties of the membrane are far more important than its mass transfer resistance. Furthermore, membrane mass transfer resistance is governed by the product of the membrane thickness and the permeability, where the latter is the product of the diffusivity and the solubility of the diffusing species [22]. Water is the principal diffusant in our experiments, and the solubility of water is much lower in PET than in paper (see below). Hence even though the paper layer is at least four times thicker than the Oxyphen PET layer, the difference in mass transfer resistance may be much less. The hydrophilicity of the paper layer probably also explains the observation that use of the paper layer enhances the asymmetry of the time-dependent sensor response curve, whereas use of the PET layer does not. The Oxyphen PET membrane is hydrophobic and absorbs little water when immersed in PBS buffer. On the other, the weight of the dry nonporous paper membrane doubles when placed in PBS buffer, with little dependence on ionic strength between 0.15 M and 0.05 M. Hence, when subjected to squeezing mechanical forces within the chemomechanical sensor, the paper membrane can reduce its volume by expelling water, whereas the PET membrane cannot. Thus the paper membrane is slightly compressible and contributes an elastic (osmotic) force that opposes hydrogel swelling and accelerates hydrogel deswelling, thereby enhancing the asymmetry of the sensor response curve.

5. Conclusions

The chemomechanical sensor exhibits a reversible and reproducible response to environmental ionic strength change with all of the membranes studied, and at all values of the hydrogel loading pressure. However, the choice of the membrane and the value of the loading pressure strongly affect sensor sensitivity and sensor response kinetics. If the hydrogel is loaded at pressures close to ambient, then sensor sensitivity is relatively low, and the time-dependent response is highly asymmetric between swelling and deswelling. This occurs because the membrane and the piezoresistive diaphragm exhibit mechanical forces that oppose swelling and accelerate deswelling, and also because the gel can swell laterally into a small amount of free space within the sensor. An increase in the hydrogel loading pressure increases sensor sensitivity and decreases the apparent asymmetry between swelling and deswelling kinetics by reducing the amount of lateral swelling within the sensor. The stiffness of a stainless steel mesh used as a

porous membrane is of little importance to sensor response, probably because this stiffness greatly exceeds the osmotic modulus of the hydrogel. On the other hand, the steel mesh pore size is very important, and this pore size is too large for almost all of the stainless steel wire cloth meshes commonly available. This can be rectified by introducing an inner membrane layer (nanoporous PET or nonporous paper) to prevent the hydrogel from exuding through the stainless steel mesh, thereby increasing sensor sensitivity. Surprisingly, the average sensor response time is not increased by the introduction of either type of inner membrane layer, a result that indicates that the response time is more sensitive to the membrane's time-dependent mechanical properties than to its diffusive permeability. The permeability of the nonporous paper membrane appears to be larger than expected due to its high affinity for water. In addition, because the hydrophilic paper layer absorbs a large quantity of water, it can be compressed by squeezing. Hence when the paper membrane is used as an inner layer on the stainless steel mesh, this introduces an additional elastic force that affects sensor response kinetics by opposing swelling and accelerating deswelling.

Acknowledgements

The authors thank Prashant Tathireddy, Loren Rieth, Michael Orthner, Box Cox, Seok Lew, and Mike Knutson for their assistance on this project, Ferenc Horkay of NIH for useful discussions, and Andreas Koch of Oxyphen AG for the donation of nanoporous membranes. This project was supported by the National Institutes of Health NHLBI/NIBIB Grant # 5R21EB008571-02.

References

- [1] S.H. Gehrke, Synthesis, equilibrium swelling, kinetics, permeability and applications of environmentally responsive gels, *Adv. Polymer Sci.* 110 (1993) 81–144.
- [2] I.Y. Galaev, B. Mattiasson, Smart polymers and what they could do in biotechnology and medicine, *Trends Biotechnol.* 17 (1999) 335–340.
- [3] N.A. Peppas, J.Z. Hilt, A. Khademhosseini, R. Langer, Hydrogels in biology and medicine: from molecular principles to biotechnology, *Adv. Mater.* 18 (2006) 1345–1360.
- [4] D.J. Beebe, J.S. Moore, J.M. Bauer, Q. Yu, R.H. Liu, C. Devadoss, B.-H. Jo, Functional hydrogel structures for autonomous flow control inside microfluidic channels, *Nature* 404 (2000) 588–590.
- [5] A. Richter, G. Paschew, S. Klatt, J. Lienig, K.-F. Arndt, H.-J.P. Adler, Review on hydrogel-based pH sensors and microsensors, *Sensors* 8 (2008) 561–581.
- [6] M. Lei, A. Baldi, E. Nuxoll, R.A. Siegel, B. Ziaie, A hydrogel-based implantable micromachined transponder for wireless glucose measurement, *Diab. Technol. Therap.* 8 (2006) 112–122.
- [7] T. Miyata, N. Asami, T. Uragami, Preparation of an antigen-sensitive hydrogel using antigen-antibody bindings, *Macromolecules* 32 (1999) 2082–2084.
- [8] D.-Y. Jung, J.J. Magda, I.S. Han, Catalase effects on glucose-sensitive hydrogels, *Macromolecules* 33 (2000) 3332–3336.
- [9] I.S. Han, M.-H. Han, J. Kim, S. Lew, Y.J. Lee, F. Horkay, J.J. Magda, Constant-volume hydrogel osmometer: a new device concept for miniature biosensors, *Biomacromolecules* 3 (2002) 1271–1275.
- [10] Z.A. Strong, A.W. Wang, C.F. McConaghy, Hydrogel-actuated capacitive transducer for wireless biosensors, *Biomed. Microdevices* 4 (2002) 97–103.
- [11] S. Herber, J. Eijkel, W. Olthuis, P. Bergveld, A. van den Berg, Study of chemically induced pressure generation of hydrogels under isochoric conditions using a microfabricated device, *J. Chem. Phys.* 121 (2004) 2746–2751.
- [12] Q.T. Trinh, C. Gerlach, J. Sorber, K.-F. Arndt, Hydrogel-based piezoresistive pH sensors: design, simulation and output characteristics, *Sens. Actuators, B Chem.* 117 (2006) 17–26.
- [13] P.J. Flory, *Principles of Polymer Chemistry*, Cornell University Press, Ithaca, New York, 1953.
- [14] K. Dusek, W. Prins, Structure and elasticity of non-crystalline polymer networks, *Adv. Polymer Sci.* 6 (1969) 1–102.
- [15] F. Horkay, I. Tasaki, P.J. Basser, Osmotic swelling of polyacrylate hydrogels in physiological salt solutions, *Biomacromolecules* 1 (2000) 84–90.
- [16] J.M. Prausnitz, R.N. Lichtenthaler, E.G. de Azevedo, *Molecular Thermodynamics of Fluid-Phase Equilibria*, 3rd ed., Prentice Hall, Upper Saddle River, New Jersey, 1999.
- [17] R.A. Siegel, Hydrophobic weak polyelectrolyte gels: studies of swelling equilibria and kinetics, *Adv. Polymer Sci.* 109 (1993) 233–267.

- [18] J.R. Quintana, N.E. Valderruten, I. Katime, Synthesis and swelling kinetics of poly(dimethylaminoethyl acrylate methyl chloride quaternary-co-itaconic acid) hydrogels, *Langmuir* 15 (1999) 4728–4730.
- [19] B. Zhao, J.S. Moore, Fast pH- and ionic strength-responsive hydrogels in microchannels, *Langmuir* 17 (2001) 4758–4763.
- [20] M. Guenther, D. Kuckling, C. Corten, G. Gerlach, J. Sorber, G. Suchanek, K.-F. Arndt, Chemical sensors based on multiresponsive block copolymer hydrogels, *Sens. Actuators, B Chem.* 126 (2007) 97–106.
- [21] R. Toomey, D. Freidank, J. Ruhe, Swelling behavior of thin, surface-attached polymer networks, *Macromolecules* 37 (2004) 882–887.
- [22] R.B. Bird, W.E. Stewart, E.N. Lightfoot, *Transport Phenomena*, 2nd ed., John Wiley, New York, 2002.

Biographies

Genyao Lin is a graduate student in Materials Science & Engineering at the University of Utah. He received a B.S. degree in polymer science & engineering in 2006 from Zhejiang University, P.R.C.

Seok Chang is a research professor in Materials Science & Engineering at the University of Utah. He received a B.S. degree in chemistry in 1981 from Hanyang University, Korea, an M.S. degree in chemistry in 1984 from Hanyang University, and a Ph.D. in chemistry in 1993 from the University of North Carolina. His areas of interest include synthesis of smart materials and organometallic chemistry.

Cheng-Hao Kuo is a graduate student in Materials Science & Engineering at the University of Utah. He received a B.S. degree in materials & minerals resources engineering in 2001 from the National Taipei University of Technology, R.O.C.

Jules Magda is an associate professor in Chemical Engineering and in Materials Science & Engineering at the University of Utah. He received his B.S. in chemical engineering in 1979 from Stanford University, and his Ph.D. in chemical engineering and materials science in 1986 from the University of Minnesota in Minneapolis. His areas of interest include stimuli-responsive hydrogels and biomedical sensors for treatment of diabetes and obesity.

Florian Solzbacher is Director of the Microsystems Laboratory at the University of Utah and an associate professor in Electrical and Computer Engineering with adjunct appointments in Materials Science and Bioengineering. His research focuses on harsh environment microsystems and materials, including implantable, wireless microsystems but also high temperature and harsh environment compatible micro sensors. Prof. Solzbacher received his M.Sc. EE from the Technical University Berlin in 1997 and his Ph.D. from the Technical University Ilmenau in 2003. He is co-founder of several companies such as I2S Micro Implantable Systems, First Sensor Technology and NFocus. He is Chairman of the German Association for Sensor Technology AMA, and serves on a number of company and public private partnership advisory boards. He is author of over 100 journal and conference publications, 5 book chapters and 13 pending patents.

CHAPTER 3

OSMOTIC SWELLING PRESSURE RESPONSE OF SMART HYDROGELS SUITABLE FOR CHRONICALLY IMPLANTABLE GLUCOSE SENSORS

Reprinted by permission from Elsevier

Sensors and Actuators B: Chemical 144 (2010) 332-336



Contents lists available at ScienceDirect

Sensors and Actuators B: Chemical

journal homepage: www.elsevier.com/locate/snb

Short communication

Osmotic swelling pressure response of smart hydrogels suitable for chronically implantable glucose sensors

G. Lin^a, S. Chang^b, H. Hao^c, P. Tathireddy^d, M. Orthner^d, J. Magda^{a,b,*}, F. Solzbacher^{a,d,e}^a Department of Materials Science & Engineering, University of Utah, Salt Lake City, UT 84112, USA^b Department of Chemical Engineering, University of Utah, Salt Lake City, UT 84112, USA^c Department of Chemical Engineering, Northwest University, Xi'an 710069, PR China^d Department of Electrical & Computer Engineering, University of Utah, Salt Lake City, UT 84112, USA^e Department of Bioengineering, University of Utah, Salt Lake City, UT 84112, USA

ARTICLE INFO

Article history:

Received 17 July 2009

Received in revised form 27 July 2009

Accepted 28 July 2009

Available online 8 August 2009

Keywords:

Glucose sensor

Hydrogel

Piezoresistive sensor

Smart material

ABSTRACT

In the last few years, a new type of glucose-sensitive hydrogel (GSH) has been developed that shrinks with increasing glucose concentration due to the formation of reversible crosslinks. The first osmotic swelling pressure results measured for any member of this new class of GSH are reported, so that their suitability for use in sensors combining pressure transducers and smart gels can be evaluated. Comparison is also made with results obtained for an older type of GSH that expands with increasing glucose concentration due to an increase in the concentration of counterions within the gel. The newer type of GSH exhibits both faster kinetics and weaker fructose interference, and therefore is more suitable for *in vivo* glucose sensing.

© 2009 Elsevier B.V. All rights reserved.

1. Introduction

In recent years, there has been a considerable effort to develop enzyme-free glucose-sensitive hydrogels (GSHs) with enhanced selectivity for glucose relative to fructose [1–8]. A GSH is a crosslinked polymer network that reversibly changes its volume in response to changes in environmental glucose concentration [9]. By coupling a GSH of micron-scale thickness to a method for detecting the volume change, such as optical or pressure measurements, one can obtain an implantable glucose sensor suitable for diabetic patients [1,4,7–8,10]. If the GSH is enzyme free, then the sensor response will be independent of blood oxygen level. By contrast, the widely studied electrochemical glucose sensors that rely on the enzyme *glucose oxidase* require special measures to overcome the blood oxygen deficit [11], such as the use of glucose-restrictive membranes [12]. The vast majority of enzyme-free GSH developed to date employ the glucose-binding moiety phenylboronic acid (PBA). The first generation of PBA-containing GSH, of a type first synthesized about 15 years ago, have volumes that increase with increasing glucose concentration [13–22]. This increase occurs because glucose binding favors the charged form of boronic acid. Hence when the environmental glucose concentration

increases, the fraction of charged boronic acid groups increases, thereby increasing the osmotic contribution of counterions that swell the hydrogel. Unfortunately, PBA will bind any molecule containing a cis-diol, and in fact the binding affinity of PBA for fructose exceeds that for glucose by a factor of 40 [23]. Hence finding a means for enhancing the glucose-selectivity of enzyme-free GSH is considered a high priority, even though physiological glucose concentrations far exceed those of fructose [24].

The second generation of GSH, of a type first synthesized about 5 years ago, have volumes that decrease with increasing glucose concentration [1–8,25]. This decrease occurs because glucose simultaneously binds to two PBA moieties within the gel, thereby forming a reversible crosslink (bis-boronate–sugar complex) that increases the entropic penalty associated with chain stretching [7]. This penalty can be reduced by chain contraction, hence the gel shrinks with increasing glucose-mediated crosslinking. Fructose, unlike glucose, contains only one set of cis-diols and thus cannot bind to two PBA moieties simultaneously. However, PBA must have the correct stereochemistry for glucose to reversibly crosslink the gel. This correct stereochemistry is achieved by attaching PBA to the hydrogel in the ortho position [1,4,5], or by incorporating protonated tertiary amines in the hydrogel adjacent to the PBA [3,7–8,25]. The cationic tertiary amines stabilize the charged form of boronic acid, even in the absence of sugars, so that almost all of the added glucose participates in reversible crosslinking [23]. Fructose molecules can still bind to PBA moieties in the gel, one at a time, but this has a relatively minor effect on the swelling pressure

* Corresponding author at: Department of Materials Science & Engineering, University of Utah, Salt Lake City, UT 84112, USA. Tel.: +1 801 581 7536.
E-mail address: jj.magda@utah.edu (J. Magda).

because most of the boronic acid groups are already charged. Hence the glucose-selectivity of the second generation of GSH greatly exceeds that of the first.

Surprisingly, as far as we know, there have been no reports of the osmotic swelling pressure Π for any member of the second generation of GSH. The osmotic swelling pressure Π is defined as the derivative of the hydrogel free energy of swelling ΔF_{tot} with respect to moles of water [26,27]:

$$\Pi = -\frac{\partial \Delta F_{\text{tot}} / \partial n_1}{V_1} = \frac{\mu_{1,0} - \mu_1}{V_1} \quad (1)$$

In Eq. (1), V_1 is the molar volume of water, n_1 is the number of moles of water, μ_1 is the chemical potential value for water in the hydrogel at ambient pressure, and $\mu_{1,0}$ is the chemical potential value for water in the reference solution that surrounds the hydrogel. The value of ΔF_{tot} includes contributions from the boronic acid counterions and the glucose crosslinks mentioned above. As discussed in detail in a recent publication within this journal [28], Π is a measure of the force that a given GSH can exert on a pressure sensor, or equivalently, of the force that a given GSH can exert when used as an autonomous actuator [19]. Hence, in the following, we report for the first time the glucose-dependent Π value in physiological saline solution (PBS buffer) for one particular member of the second generation of GSH, namely the hydrogel with composition developed by Tierney et al. [7]. The goal is to evaluate the suitability of this GSH for use in chemomechanical sensors that combine smart hydrogels and pressure transducers. It should be noted that Tierney et al. have already shown that this GSH exhibits adequate glucose response in blood plasma [8]. We also investigate Π for a hydrogel with composition developed by Gu [23], a hydrogel belonging to the first generation of GSH.

2. Experimental methods

2.1. Materials

The monomers used for preparation of the gels were obtained as follows: acrylamide (AAM, Fisher Scientific), *N,N*-methylenebisacrylamide (BIS, Sigma–Aldrich), 3-acrylamidophenylboronic acid (3-APB, Frontier Scientific, Logan, UT), and *N*-(3-dimethylaminopropyl acrylamide (DMAPAA Polyscience). The monomers were used as received. Ammonium peroxydisulfate (APS, Sigma–Aldrich), *N,N,N',N'*-tetramethylethylenediamine (TEMED, Sigma–Aldrich), *D*(+)-glucose (Mallinckrodt Chemicals), *D*(–)-fructose (Sigma–Aldrich), dimethyl sulfoxide (DMSO, Sigma–Aldrich), 4-(2-hydroxyethyl)piperazine-1-ethanesulfonic acid (HEPES, Sigma–Aldrich), and Delbecco's phosphate-buffered saline solution (PBS, Sigma–Aldrich) were also used as received. Market grade wire cloth mesh (type 304 stainless steel, 80 mesh, wire opening 178 μm , open area 31%) was obtained from Small Parts, Inc., Miramar, FL, USA.

2.2. Hydrogel synthesis

A GSH (composition 1) containing AAM/3-APB/DMAPAA/BIS at a nominal mole ratio of 80/8/10/2 was prepared by free radical crosslinking copolymerization. This composition and the synthesis procedure followed were the same as in Tierney et al. [7], with the exception that we used a different reaction initiator and accelerator, namely thermal free radical initiator APS and TEMED. This use of APS and TEMED is not expected to markedly change hydrogel properties. In brief, stock solutions were prepared of AAM and BIS in 1 mM HEPES buffer. Appropriate amounts of the two stock solutions were mixed in a vial with DMAPAA and TEMED. In order to dissolve 3-APB into the pregel solution, 10 vol% of DMSO was added into the vial. The free radical initiator APS was introduced after

purging the vial with N_2 gas for 10 min, after which the pregel solution was rapidly injected into a cavity (thickness 400 μm) between two square plates (polycarbonate and poly(methyl methacrylate)) of surface area 60 cm^2 . The total monomer concentration in the pregel solution was 12.7 wt%. After approximately 12 h of reaction at room temperature, the hydrogel slab was removed from the mold and washed for at least two days with deionized water and PBS buffer (pH 7.4, ionic strength 0.15 M) before testing. A similar procedure was used to prepare a GSH (composition 2) containing AAM/3-APB/BIS at a nominal mole ratio of 80/20/0.25, with the principal difference being the replacement of HEPES buffer/DMSO with 1 M NaOH. The total monomer concentration in the pregel solution was 30.2 wt%. This GSH has a composition very similar to a hydrogel studied by Gu [23]. In sugar-free PBS buffer at physiological pH and ionic strength, GSH (composition 1) contains 88 wt% water, and GSH (composition 2) contains 58 wt% water).

2.3. Sensor construction and sensor response tests

As analyzed in detail in a recent publication in this journal [28], the osmotic swelling pressure Π of a smart hydrogel can be obtained by confining it between a porous membrane and the diaphragm of a miniature pressure transducer. In such a sensing scheme, a change in the environmental glucose concentration, as sensed through the pores of the membrane, changes Π (see Eq. (1)) which must at equilibrium equal the mechanical pressure measured by the pressure transducer. Fig. 1 shows a sketch of the chemomechanical sensor that was used. The sensor consists of a piezoresistive pressure transducer (model EPB-501-5P, Entran, Inc., Fairfield, NJ, USA) with a cylindrical stainless steel sensing area (diameter 3.18 mm) completely covered with a hydrogel film of thickness $\approx 400 \mu\text{m}$. The hydrogel is held in place in the sensor by a cap with a top surface that consists of a replaceable porous membrane through which mass transfer can occur. In our previous work [28], we investigated membranes having various pore sizes and porosities, and found that use of a stainless steel wire cloth mesh (mesh size 80, wire opening 174 μm , 31% open area) gave acceptable results for Π measurements in PBS buffer. Therefore the same porous mesh was used to obtain all the results presented here. A GSH was synthesized and cleaned as described

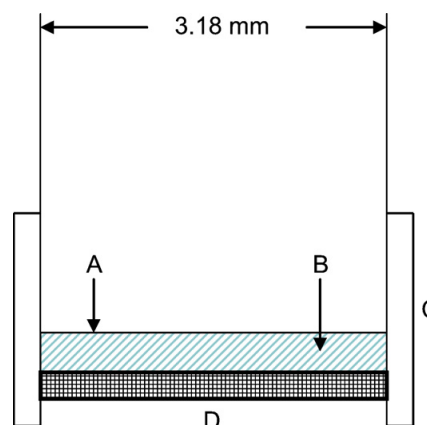


Fig. 1. Preliminary version of the chemomechanical sensor used in this study. A piezoresistive pressure transducer with a cylindrical sensing area (A) is completely covered with a disc-shaped hydrogel film (B) of approximate thickness 400 μm . The hydrogel is held in place by a cap (C) that has a top surface which is a replaceable wire mesh/porous membrane (D) (from Ref. [28]).

above, a circular biopsy tool was used to cut a disc-shaped sample of appropriate diameter, and the sample was then transferred from sugar-free PBS buffer (pH 7.4, ionic strength 0.15 M) to the sensing surface of the pressure transducer using tweezers. The sensor cap with wire mesh was attached to the sensor base by tightening three screws that were adjusted to impose an axial compressive stress on the hydrogel in the sensor. The sensor was then inserted into a large covered environmental bath containing PBS buffer at room temperature and physiological pH and ionic strength. This bath also contained a magnetic stirrer used to minimize external mass transfer resistance to the sensor. Sensor response tests were performed by either injecting solutions of glucose with or without fructose into the environmental bath and then noting the time-dependent response of the pressure transducer, or by rapidly switching the sensor into another environmental bath at the same ionic strength and pH but with no sugar. The time-dependent pressure signal was captured with an Agilent data acquisition system.

3. Results and discussion

3.1. The glucose-dependent swelling pressure response: magnitude and kinetics

In order to ensure good mechanical contact with the pressure transducer at all glucose concentrations, GSH (composition 1) was transferred from sugar-free buffer into the sensor at a high loading pressure of approximately 20 kPa, which is approximately 60% of the transducer full-scale value. From measurements of the change in optical path length by Tierney et al. [7], this hydrogel is expected to shrink with increasing glucose concentration. Fig. 2 shows the measured change in swelling pressure Π when the hydrogel is exposed to a cyclic variation in glucose concentration between zero and 5 mM at physiological pH and ionic strength. As expected, Π is lower at higher glucose concentration, and the change in Π is observed to be reversible and surprisingly large, almost 9 kPa or 1750 Pa per mM of glucose. We are aware of only one previous Π measurement for a GSH, in this case for a GSH that swells with increasing glucose concentration. Lei et al. subjected this first generation GSH to an increase in glucose concentration from 0 to 20 mM, and measured an increase in Π of only 3 kPa [29]. For GSH (composition 1), Fig. 3 contains a plot of the equilibrium Π response vs. glucose concentration over the range of physiological interest for diabetic patients, 0–20 mM. The swelling pressure increases monotonically

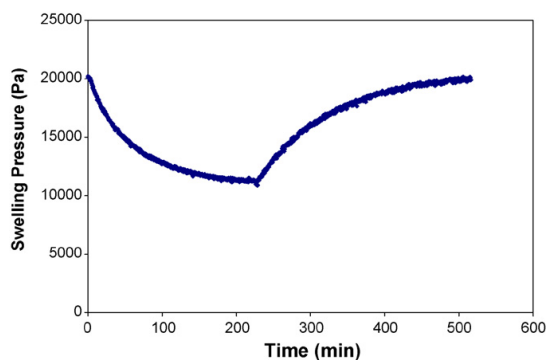


Fig. 2. Time-dependent response of the osmotic swelling pressure in response to change in glucose concentration from zero to 5 mM then back to zero. Measurements were made at room temperature in PBS buffer at physiological pH and ionic strength using GSH (composition 1) in the sensor of Fig. 1.

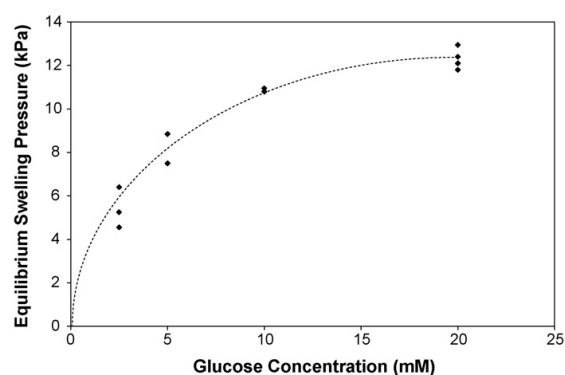


Fig. 3. Magnitude of the equilibrium change in swelling pressure vs. glucose concentration, as measured at room temperature in PBS buffer at physiological pH and ionic strength using GSH (composition 1) in the sensor of Fig. 1 (average error bar magnitude 0.6 kPa). The dashed curve is given as a guide to the eyes only.

with glucose concentration, but unfortunately the equilibrium response curve appears to saturate near 20 mM glucose. Presumably this occurs because all of the glucose binding sites become occupied at high external glucose concentration. This is unsurprising, given that the mole fraction of PBA in this hydrogel is only about 0.08. Fig. 4 shows the fit of the time-dependent swelling curve in Fig. 2 to a first-order-kinetics model. The fit is excellent, and this was observed to be the case (R -squared values 0.92–0.98) for all of the time-dependent swelling and deswelling curves for this GSH (composition 1). There was no obvious dependence of the first-order time constant τ on glucose concentration. The average values were $\tau = 60 \pm 15$ min for deswelling, and $\tau = 75 \pm 15$ min for swelling. Though the relative uncertainty in the τ values is large, nonetheless deswelling appears to be slightly faster than swelling, probably because the membrane and the piezoresistive diaphragm exhibit mechanical forces that oppose swelling and accelerate deswelling.

3.2. Interference by fructose

The normal physiological level of fructose is approximately 500 times smaller than that of glucose (8 μ M vs. 5.5 mM, respectively) [24]. Nonetheless, potential interference is important because the affinity of PBA for fructose is 40 times greater than that for

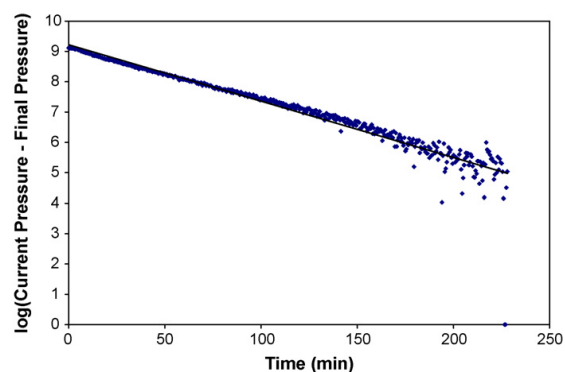


Fig. 4. Fit of the time-dependent decrease in swelling pressure in Fig. 2 to an exponential decay. The value of the first-order-time constant is 54 min.

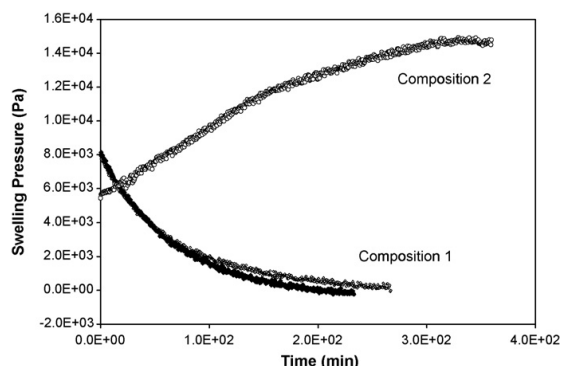


Fig. 5. Time-dependent response of the swelling pressure measured at room temperature in PBS buffer at physiological pH and ionic strength using the sensor of Fig. 1 with GSH (composition 2) (upper curve) and GSH (composition 1) (two lower curves). At time equal zero, the sugar concentration was suddenly increased from zero to: 5 mM glucose (unfilled symbols); 5 mM glucose plus 0.1 mM fructose (filled symbols).

glucose [23], hence normal fructose levels could cause a glucose-measurement error of ca. 10%. Fig. 5 compares the measured response of Π for GSH (composition 1) to PBS solutions containing 5 mM glucose and PBS solutions containing 5 mM glucose plus 0.1 mM fructose. As noted previously, this GSH shrinks with increasing glucose concentration due to the formation of reversible crosslinks formed when glucose binds simultaneously to two PBA moieties, whereas fructose cannot mediate crosslinks. Hence addition of 0.1 mM fructose has no discernible effect on the sensor response in Fig. 5. Fig. 5 also shows the measured response of Π for GSH (composition 2) to PBS solutions containing 5 mM glucose. In contrast to GSH (composition 1), this hydrogel does not contain pendant tertiary amines and hence is expected to swell with increasing glucose concentration. One observes in Fig. 5 that the measured Π value of GSH (composition 2) responds to the increase in glucose concentration in a direction which is opposite to that of GSH (composition 1). The magnitude of the equilibrium response is slightly greater for GSH (composition 2) than for GSH (composition 1) (9.2 kPa vs. 8 kPa). However, the response time of GSH (composition 2) in Fig. 5 is clearly larger than that of GSH (composition 1). The time-dependent response curve of GSH (composition 2) in Fig. 5 does not fit a first- or second-order model. Defining τ_{60} as the time at which hydrogel response reaches 60% of its final value, and τ_{90} as the time at which hydrogel response reaches 90% of its final value, then $\tau_{60} = 140$ min and $\tau_{90} = 260$ min for GSH (composition 2) in Fig. 5. In comparison, $\tau_{60} = 60$ min and $\tau_{90} = 175$ min for GSH (composition 1). Furthermore, the measured Π value of GSH (composition 2) is much more responsive to fructose than to glucose, as shown in Fig. 6. Fig. 6 contains the time-dependent response of Π for both types of GSH to PBS solutions containing 5.0 mM fructose. After 1 h, the Π response of GSH (composition 1) in Fig. 6 has already reached an equilibrium value of 1.9 kPa, which is four times smaller in magnitude than the equilibrium response of the same gel to an equivalent concentration of glucose (Fig. 3). On the other hand, after 1 h, the Π response of GSH (composition 2) is still increasing in Fig. 6, and the magnitude of the response of this gel to 5.0 mM fructose is already at least 1.6 times greater than the response to an equivalent concentration of glucose (Fig. 5). We speculate that the small short-time drop in Π observed for GSH (composition 2) in Fig. 6 arises from the osmotic effect of fructose on the environmental solution that occurs immediately after fructose injection and before fructose diffuses into the gel and binds.

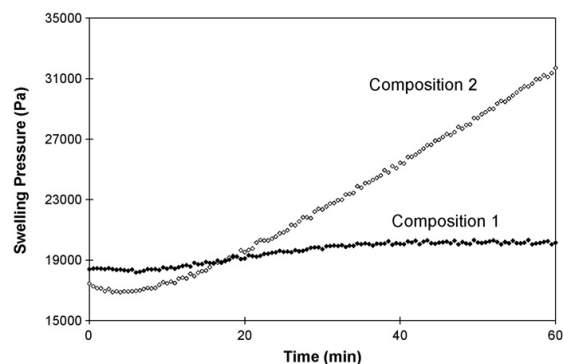


Fig. 6. Time-dependent response of the swelling pressure to 5 mM fructose as measured in PBS buffer at room temperature and at physiological pH and ionic strength with sensor of Fig. 1 using: GSH (composition 1) – filled symbols; GSH (composition 2) – open symbols.

4. Conclusions and perspectives

For both glucose-sensitive hydrogels studied (GSH composition 1 and GSH composition 2), the magnitude of the osmotic swelling pressure response to glucose is surprisingly large, and easily detectable using custom-designed microfabricated pressure sensors. For example, near the normal glucose level in the body (5.5 mM), the sensitivity of GSH (composition 1) is approximately 1750 Pa per mM of glucose. Since microfabricated pressure sensors are available with resolutions of order 1 mbar, this implies a chemo-mechanical glucose sensor resolution of 0.06 mM (1.2 mg/dl), which is more than adequate for a chronically implantable glucose sensor [11,30]. GSH (composition 1) also exhibits minimal fructose interference and reasonably fast kinetics, with a first-order time constant of about 65 min at room temperature. GSH (composition 2), an older type of hydrogel that swells rather than shrinks with increasing glucose concentration, has slower kinetics and much greater fructose interference. GSH (composition 1) was first developed by Tierney et al. [7], who placed it on the tip of a fiber optic sensor and measured glucose-dependent changes in optical path length in PBS buffer and in blood plasma. Tierney et al. report that the swelling kinetics of GSH (composition 1) are four times faster at body temperature than at room temperature [8], so we can expect a similar reduction in the first-order-time constant of our chemo-mechanical glucose sensor. Additional reduction in response time can no doubt be obtained by reducing the thickness of the GSH in the sensor from 400 μm or by introducing pores. In the future, we plan to construct a MEMS glucose sensor [29,31] which is a micro-fabricated chemomechanical sensor and that will use the same or a similar GSH. The only deficiency of GSH (composition 1) is the reduction in sensitivity observed at higher glucose concentrations, near 20 mM. This can probably be rectified by synthesizing a hydrogel with a greater mole fraction of glucose-binding moieties.

Acknowledgement

This project was supported by the National Institutes of Health NHLBI/NIBIB Grant # 5R21EB008571-02.

References

- [1] V.L. Alexeev, A.C. Sharma, A.V. Goponenko, S. Das, I.K. Lednev, C.S. Wilcox, D.N. Finogold, S.A. Asher, High ionic strength glucose-sensing photonic crystal, *Anal. Chem.* 75 (2003) 2316–2323.

- [2] A.M. Horgan, A.J. Marshall, S.J. Kew, K.E.S. Dean, C.D. Creasey, S. Kabilan, Crosslinking of phenylboronic acid receptors as a means of glucose selective holographic detection, *Biosens. Bioelectron.* 21 (2006) 1838–1845.
- [3] G.K. Samoei, W. Wang, J.O. Escobedo, X. Xu, H.-J. Schneider, R.L. Cook, R.M. Strongin, A chemomechanical polymer that functions in blood plasma with high glucose selectivity, *Angew. Chem. Int. Ed.* 45 (2006) 5319–5322.
- [4] X. Yang, M.-C. Lee, F. Sartain, X. Pan, C.R. Lowe, Designed boronate ligands for glucose-selective holographic sensors, *Chem. Eur. J.* 12 (2006) 8491–8497.
- [5] X. Yang, X. Pan, J. Blyth, C.R. Lowe, Towards the real-time monitoring of glucose in tear fluid: holographic glucose sensors with reduced interference from lactate and pH, *Biosens. Bioelectron.* 23 (2008) 899–905.
- [6] F. D'Hooge, D. Rogalle, M.J. Thatcher, S.P. Perera, J.M.H. van den Elsen, A.T.A. Jenkins, T.D. James, J.S. Fossey, Polymerisation resistant synthesis of methacrylamido phenylboronic acids, *Polymer* 49 (2008) 3362–3365.
- [7] S. Tierney, S. Volden, B.T. Stokke, Glucose sensors based on a responsive gel incorporated as a Fabry-Perot cavity on a fiber-optic readout platform, *Biosens. Bioelectron.* 24 (2009) 2034–2039.
- [8] S. Tierney, B.M.H. Falch, D.R. Hjelme, B.T. Stokke, Determination of glucose levels using a functionalized hydrogel-optical fiber biosensor: toward continuous monitoring of blood glucose in vivo, *Anal. Chem.* 81 (2009) 3630–3636.
- [9] S.H. Gehrke, Synthesis, equilibrium swelling, kinetics, permeability and applications of environmentally responsive gels, *Adv. Polym. Sci.* 110 (1993) 81–144.
- [10] I.Y. Galaev, B. Mattiasson, Smart polymers and what they could do in biotechnology and medicine, *Trends Biotechnol.* 17 (1999) 335–340.
- [11] H.E. Koschwanetz, W.M. Reichert, In vitro, in vivo and post explanation testing of glucose-detecting biosensors: current methods and recommendations, *Biomaterials* 28 (2007) 3687–3703.
- [12] R. Gifford, J.J. Kehoe, S.L. Barnes, B.A. Kornilayev, M.A. Alterman, G.S. Wilson, Protein interactions with subcutaneously implanted biosensors, *Biomaterials* 27 (2006) 2587–2598.
- [13] S. Kitano, I. Hisamitsu, Y. Koyama, K. Kataoka, T. Okano, Y. Sakurai, Effect of the incorporation of amino groups in a glucose-responsive polymer complex having phenylboronic acid moieties, *Polym. Adv. Technol.* 2 (1991) 261–264.
- [14] S. Kitano, K. Kataoka, Y. Koyama, T. Okano, Y. Sakurai, Glucose-responsive complex formation between poly(vinyl alcohol) and poly(*N*-vinyl-2-pyrrolidone) with pendent phenylboronic acid moieties, *Makromol. Chem. Rapid Commun.* 12 (1991) 227–233.
- [15] K. Kataoka, H. Miyazaki, T. Okano, Y. Sakurai, Sensitive glucose-induced change of the lower critical solution temperature of poly[*N,N*-dimethylacrylamide-*co*-3-(acrylamido)phenylboronic acid] in physiological saline, *Macromolecules* 27 (1994) 1061–1062.
- [16] K. Kataoka, H. Miyazaki, M. Bunya, T. Okano, Y. Sakurai, Totally synthetic polymer gels responding to external glucose concentration: their preparation and application in on-off regulation of insulin release, *J. Am. Chem. Soc.* 120 (1998) 12694–12695.
- [17] F.H. Arnold, W. Zheng, A.S. Michaels, A membrane-moderated conductometric sensor for the detection and measurement of specific organic solutes in aqueous solutions, *J. Membr. Sci.* 167 (2000) 227–239.
- [18] R. Badugu, J.R. Lakowicz, C.D. Geddes, Ophthalmic glucose sensing: a novel monosaccharide sensing disposable and colorless contact lens, *Analyst* 129 (2001) 516–521.
- [19] A. Baldi, Y. Gu, P.E. Loftness, R.A. Siegel, B. Ziaie, A hydrogel-actuated smart microvalve with a porous diffusion barrier back-plate for active flow control, in: *Proc. IEEE Intl. Conference on MEMS*, Jan 20–24, Las Vegas, NV, 2002, pp. 105–107.
- [20] T.D. James, S. Shinkai, Artificial receptors as chemosensors for carbohydrates, *Top. Curr. Chem.* 218 (2002) 159–200.
- [21] Y.-J. Lee, S.A. Pruzinsky, P.V. Braun, Glucose-sensitive inverse opal hydrogels: analysis of optical diffraction response, *Langmuir* 20 (2004) 3096–3106.
- [22] M.V. Kuzimenkova, A.E. Ivanov, C. Thammakhet, L.I. Mikhailovska, I.Y. Galaev, P. Thavarungkul, P. Kanatharana, B. Mattiasson, Optical responses, permeability and diol-specific reactivity of thin polyacrylamide gels containing immobilized phenylboronic acid, *Polymer* 49 (2008) 1444–1454.
- [23] Y. Gu, Ph.D. Thesis, University of Minnesota, 2003.
- [24] T.H. Kawasaki, H. Akanuma, T. Yamanouchi, Increased fructose concentrations in blood and urine in patients with diabetes, *Diabetes Care* 25 (2002) 353–357.
- [25] S.K. Mujumdar, Ph.D. Thesis, University of Minnesota, 2008.
- [26] P.J. Flory, *Principles of Polymer Chemistry*, Cornell University Press, Ithaca, NY, 1953.
- [27] K. Dusek, W. Prins, Structure and elasticity of non-crystalline polymer networks, *Adv. Polym. Sci.* 6 (1969) 1–102.
- [28] G. Lin, S. Chang, C.-H. Kuo, J. Magda, F. Solzbacher, Free swelling and confined smart hydrogels for applications in chemomechanical sensors for physiological monitoring, *Sens. Actuators B: Chem.* 136 (2009) 186–195.
- [29] M. Lei, A. Baldi, E. Nuxoll, R.A. Siegel, B. Ziaie, A hydrogel-based implantable micromachined transponder for wireless glucose measurement, *Diabetes Technol. Ther.* 8 (2006) 112–122.
- [30] T. Koschinsky, L. Heinemann, Sensors for glucose monitoring: technical and clinical aspects, *Diabetes Metab. Res. Rev.* 17 (2001) 113–123.
- [31] X. Huang, S. Li, J.S. Schultz, Q. Wang, Q. Lin, A MEMS affinity glucose sensor using a biocompatible glucose-responsive polymer, *Sens. Actuators B: Chem.* 140 (2009) 603–609.

Biographies

Genyao Lin is a graduate student in Materials Science & Engineering at the University of Utah. He received a B.S. degree in Chemistry & Engineering in 2006 from Zhejiang University of Technology, P.R.C. His research area is synthesis and testing of stimuli-responsive hydrogels.

Seok Chang is a research associate professor in Chemical Engineering at the University of Utah. He received a B.S. degree in chemistry in 1981 from Hanyang University, Korea, an M.S. degree in chemistry in 1984 from Hanyang University, and a Ph.D. in chemistry in 1993 from the University of North Carolina. His areas of interest include synthesis of smart materials and organometallic chemistry.

Hong Hao is a professor in Chemical Engineering at the Northwest University in Xi'an, PR China. Her principal area of research interest is biodegradable polymers. In 2008, she was a Visiting Research Fellow in Chemical Engineering at the University of Utah.

Prashant Tathireddy received a bachelor's degree in Chemical Technology from the Osmania University, Hyderabad, India in 1997. He was a project leader at Computer Maintenance Corporation Private Limited, Hyderabad, India till 1999. He received a Ph.D. degree in Chemical Engineering in June 2005 from University of Utah. He later joined the Microsystems Laboratory at the University of Utah as a post-doctoral fellow and worked in that position till 2007. He received a Fraunhofer fellowship award in 2007 and was posted as a guest scientist at the Fraunhofer Institute for Biomedical Engineering (IBMT), St. Ingbert, Germany. He currently holds a position as research assistant professor in the department of Electrical & Computer Engineering at Utah. He has previously contributed to disciplines such as microfluidics and material characterization using impedance spectroscopy while his current research focuses on design, fabrication process development and testing of implantable medical microdevices or BioMEMS. This includes design and development of electronic packaging and new encapsulation techniques of medical devices for chronic use.

Michael Orthner is a graduate student in Electrical & Computer Engineering at the University of Utah. He received a B.S. degree in Materials Science & Engineering in 2004 and an M.S. degree in Materials Science & Engineering in 2006, both at the University of Utah. He is currently developing a MEMS based platform to detect the swelling pressures of analyte specific hydrogels, including a novel sensor design.

Jules Magda is associate professor of Chemical Engineering and Materials Science & Engineering at the University of Utah. He received his B.S. in Chemical Engineering in 1979 from Stanford University, and his Ph.D. in Chemical Engineering and Materials Science in 1986 from the University of Minnesota in Minneapolis. His research areas of interest include rheology, stimuli-responsive hydrogels and biomedical sensors for treatment of diabetes and obesity.

Florian Solzbacher is director of the Microsystems Laboratory at the University of Utah and an associate professor in Electrical and Computer Engineering with adjunct appointments in Materials Science and Bioengineering. His research focuses on harsh environment microsystems and materials, including implantable, wireless microsystems but also high temperature and harsh environment compatible microsensors. Prof. Solzbacher received his M.Sc. EE from the Technical University Berlin in 1997 and his Ph.D. from the Technical University Ilmenau in 2003. He is co-founder of several companies such as I2S Micro Implantable Systems, First Sensor Technology and NFocus. He is the Chairman of the German Association for Sensor Technology AMA, and serves on a number of company and public private partnership advisory boards. He is author of over 100 journal and conference publications, 5 book chapters and 13 pending patents.

CHAPTER 4

OPTIMIZATION OF GLUCOSE SENSITIVE HYDROGELS

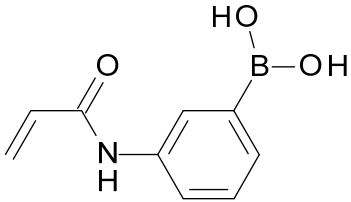
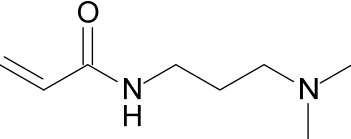
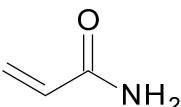
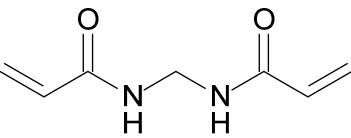
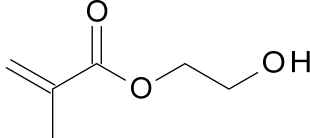
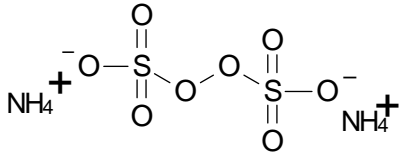
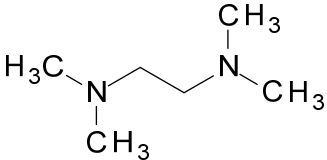
FOR SENSOR APPLICATIONS

4.1 Introduction

This chapter concerns the optimization of glucose-sensitive hydrogels for sensor applications. All the osmotic swelling pressure data described herein were obtained using the same method and identical macrosized sensor as described in chapters 2 and 3. First of all, an attempt was made to synthesize 2-Methacrylamido phenylboronic acid which is not commercially available, and glucose-sensitive hydrogels based on this monomer. 2-Acrylamidophenylboronic acid (2-APB) has been reported to be able to form an intramolecular 6-membered ring which stabilizes the 2-Acrylamidophenylboronic acid in its charged form at physiological pH 7.4, and hydrogels containing 2-APB show high glucose selectivity [1]. Furthermore, 2-Acrylamidophenylboronic acid is believed to be relatively pH independent because of the intramolecular stable 6-membered ring microenvironment structure that is less responsive to external pH change [1,2]. Although 2-Methacrylamido phenylboronic acid (2-MPBA) was successfully synthesized here, no desired glucose-sensitive hydrogels containing this monomer were obtained, probably because of the poor solubility of 2-MPBA in the solvents used. Acknowledging that 2-MPBA could not be used to synthesize glucose-sensitive hydrogels and that the

glucose-sensitive hydrogels reported in chapter 3 were later found to be pH dependent, attention was shifted to the optimization of glucose-sensitive hydrogels (GSHs) reported in chapter 3 by varying the pre-gel chemical compositions. In chapter 3, we have demonstrated that osmotic swelling pressure response of polyampholytic glucose-sensitive hydrogels (GSHs) containing 3-acrylamido phenylboronic acid and a tertiary amine could be used to obtain novel chemomechanical glucose sensors with high selectivity towards glucose over fructose. However, slight physiological pH changes that may occur in the body have been ignored in the previous chapter. Results indicate that reduced pH interference on glucose response can be achieved by designing a hydrogel where the hydrogel's isoelectric point (IEP) pH is close to physiological pH 7.4. Lastly, novel glucose-sensitive hydrogels employing hydroxyethylmethacrylate (HEMA), instead of acrylamide, as the major monomer were synthesized and glucose-response tests were also performed in the preliminary version of the chemomechanical sensor as shown in Fig. 1.7. Comparison is also made with results obtained with glucose-sensitive hydrogels (GSHs) containing acrylamide as the major component. Results suggest that GSHs containing HEMA as the major composition exhibit unexpected two-step deswelling process, which is contributed to the lower equilibrium water content of the hydrogel. Consequently, lower water content indicates shorter distance between two functional boronic acid moieties and more likely to form crosslink with glucose. This two-step deswelling process may be can also be found in other members of shrinking glucose sensitive hydrogels under appropriate conditions as glucose-mediated crosslinking and skin layer formation appears to be the mechanism. The chemical structures of various materials involved in this chapter are shown in Table 4.1.

Table 4.1. Materials chemical structures

Acronym	Name	Chemical structure
3-APB	3-Acrylamidophenylboronic acid	
DMAPAA	N,N-Dimethylaminopropyl acrylamide	
AAM	Acrylamide	
BIS	N,N-methylenebisacrylamide	
HEMA	2-Hydroxyethylmethacrylate	
APS	Ammonium persulfate	
TEMED	Tetramethylethylenediamine	

4.2 Synthesis of 2-(Methacrylamido)phenylboronic acid (2-MPBA) and glucose-sensitive hydrogels (GSHs)

4.2.1 Materials

The materials used in the synthesis are as follows. 2-(Methacrylamido)phenylboronic acid pinacol ester (Frontier Scientific, Logan, UT), Potassium hydrogen difluoride (KHF₂, Fluka Analytical), Lithium hydroxide monohydrate (LiOH·H₂O, Sigma-Aldrich), Diethyl ether (Sigma-Aldrich). Ethyl acetate, sodium sulfate, and acetonitrile were purchased from Mallinckrodt Chemicals. Acetone was obtained from VWR International. All chemicals were used as received without further purification.

4.2.2 Experimental methods

The synthesis procedures followed here were basically the same as reported by D'Hooge et al. [3], with the only exception being that we used a different starting material, namely 2-(Methacrylamido)phenyl boronic acid pinacol ester. The overall synthesis procedure is shown in Fig. 4.1.

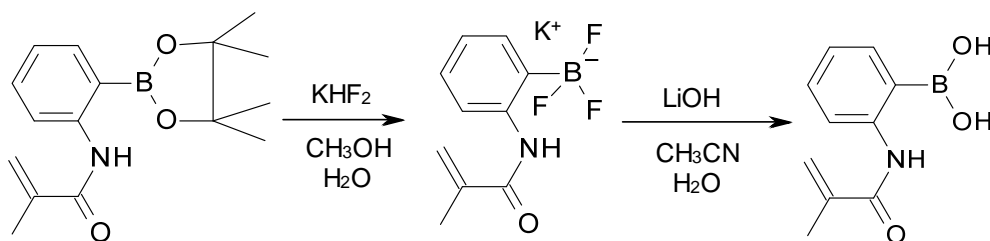


Fig. 4.1. Synthesis of 2-(Methacrylamido) phenylboronic acid.

Briefly, to a plastic beaker of about 50 ml in volume, 316 mg 2-(Methacrylamido)phenylboronic acid pinacol ester along with the mixture of 8 ml methanol and 8 ml water were added. Subsequently, 515.5 mg KHF_2 was added in one portion and the obtained mixture in the beaker covered with parafilm was stirred overnight at room temperature. After overnight reaction, the obtained slurry solution was evaporated to dryness at room temperature ($<30^\circ\text{C}$) by reducing the pressure with a vacuum pump, redissolved in hot acetone and then filtered. The obtained filtrate was evaporated in vacuum, and subjected to trituration with ether for three times, to obtain white solids.

The obtained white solids were stirred with a mixture of 10 ml acetonitrile and 5 ml water, 184.8 mg $\text{LiOH}\cdot\text{H}_2\text{O}$ was added thereafter and the obtained mixture was stirred overnight at room temperature. To the mixture 20 ml saturated ammonium hydrochloride and 5 ml 1N hydrochloric acid were added. The solution was extracted with ethyl acetate three times, and subsequently the obtained extracts were subjected to dehydration by adding sodium sulphate, filtering, evaporating, and then drying again in vacuum, thereby obtaining white solids.

4.2.3 NMR results

^1H NMR spectra were measured on a 400 MHz spectrometer in CD_3OD and are noted in parts per million with respect to the peak for TMS (chemical shift=0). The ^1H NMR spectra results on the reaction product are listed in Fig. 4.2. Comparison is also made with published data on 2-(Methacrylamido) phenylboronic acid [3] as listed in Table. 4.2.

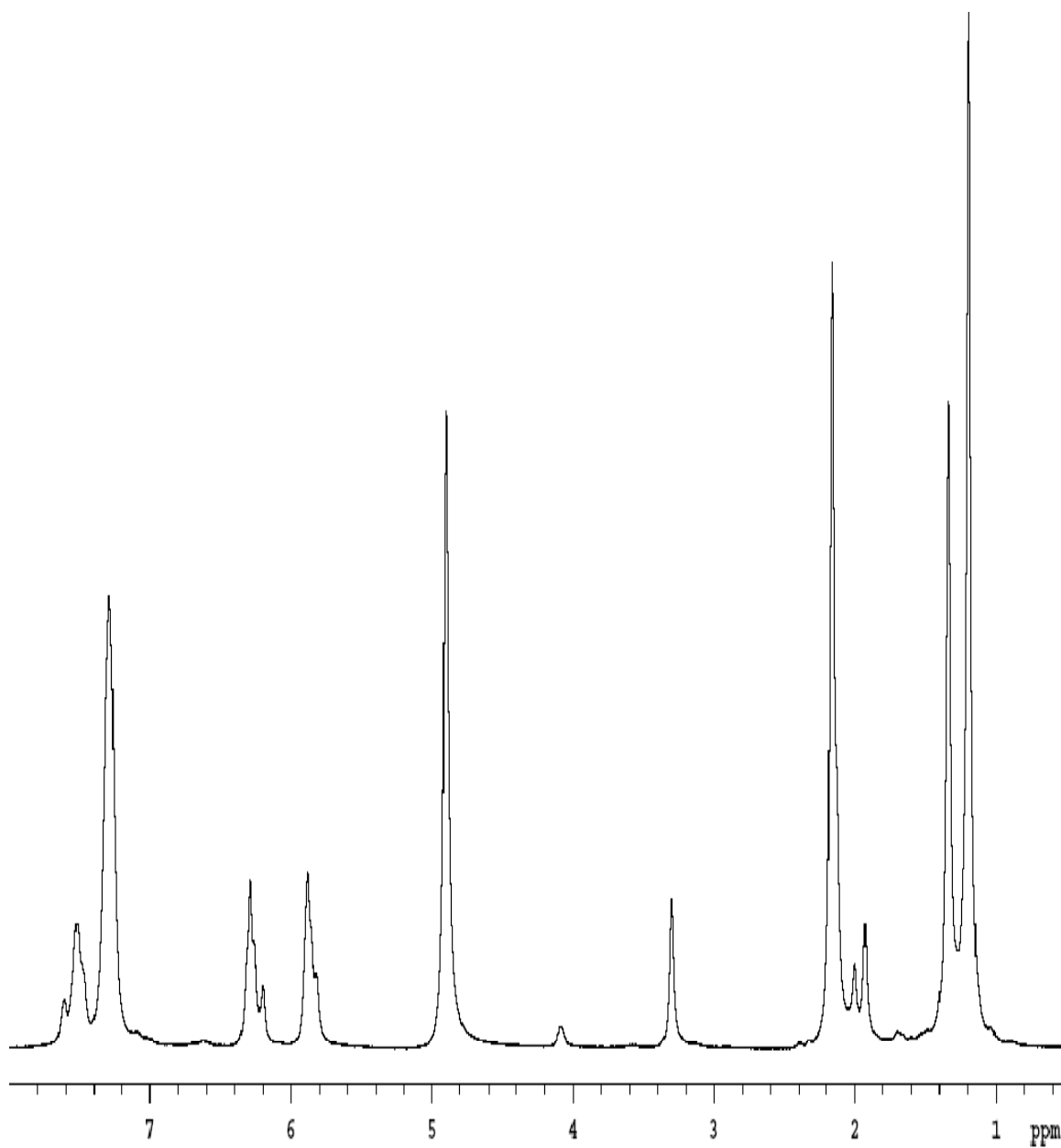


Fig. 4.2. ^1H NMR results for 2-(Methacrylamido) phenylboronic acid (2-MPBA).

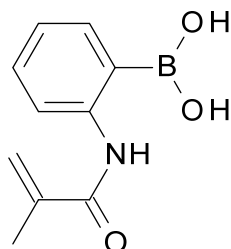


Table 4.2. Comparison of ^1H NMR results for synthesized 2-(Methacrylamido) phenylboronic acid with published data [3], numbers in the parenthesis indicate the area of that specific peak after integration.

^1H NMR	Methacryl -CH ₃	Methacryl C=CH ₂	Ar (CH) ₄
Published	2.05 (3H)	5.76 (1H),	7.2 (3H),
chemical shifts			
and integration [3]		6.16 (1H)	7.4 (1H)
Measured	2.16 (3.1H)	5.88 (1H),	7.29 (3.17H),
chemical shifts			
and intergration		6.29 (0.97H)	7.51(1.01H)

As seen in Table 4.2, the obtained ^1H NMR results are in good agreement with the published results, indicative of the successful synthesis of 2-(Methacrylamido) phenylboronic acid.

4.2.4 Synthesis of 2-(Methacrylamido) phenylboronic acid

(2-MPBA) based hydrogels

Glucose-sensitive hydrogels were synthesized in the same manner as the pH-sensitive hydrogels and glucose-sensitive hydrogels containing 3-Acrylamido phenylboronic acid (3-APB) discussed previously in chapter 2 and 3. Namely pregel solution containing appropriate amount of 2-(Methacrylamido) phenylboronic acid (2-MPBA) and other monomers was injected into the cavity between two square plates separated by a Teflon spacer of $400\ \mu\text{m}$ thickness. Glucose-sensitive hydrogels were synthesized by free radical solution copolymerization in the presence of redox initiator (APS+TEMED) at room temperature.

Table 4.3 lists the attempted approaches to synthesize glucose-sensitive hydrogels containing 2-(Methacrylamido) phenylboronic acid (2-MPBA). Unfortunately, no glucose-sensitive hydrogels (GSHs) with good mechanical properties were obtained. Extremely weak and/or phase separated hydrogels, as shown in Table 4.2, were observed at best, and none of these glucose-sensitive hydrogels were mechanically tough enough to generate osmotic swelling pressure change in our macrosized piezoresistive pressure sensor (see Fig. 1.7). In some cases, the obtained hydrogels were so weak that they broke apart in water without agitation.

Table 4.3. Experimental attempts to synthesize glucose-sensitive hydrogels (GSHs) containing 2-(Methacrylamido) phenylboronic acid (2-MPBA).

Pregel Chemical Compositions (mmole)	Solvents and total monomer weight concentration	Initiator System	Results
2-MPBA:AAM:BIS =0.3:1.2:0.0075	300 μ L NaOH(1M/L) 500 μ L water 15.6 wt%	APS: 0.5 mg TEMED: 2.5 μ L	2-MPBA could not completely dissolve in solvents. No hydrogel was formed after 24 h.
2-MPBA:AAM:BIS: Glucose =0.1:0.4:0.005:0.5	DMSO 600 μ L 5.6 wt%	APS:1 mg TEMED: 2.5 μ L	2-MPBA completely dissolved in DMSO, but no hydrogel was obtained after 24 h.
2-MPBA:AAM:BIS =0.05:1:0.005	75 μ L NaOH(1M/L) 500 μ L water 250 μ L Methanol 9.6 wt%	APS:1 mg TEMED: 2.5 μ L	2-MPBA completely dissolved in the solvents. White hydrogel was formed with very poor mechanical strength.
2-MPBA:AAM:BIS =0.05:1:0.01	50 μ L NaOH(1M/L) 600 μ L Methanol 13.8 wt%	APS:1 mg TEMED: 2.5 μ L	2-MPBA completely dissolved in solvents. An extremely weak and white hydrogel was formed after 24 h. The gel was so weak that it broke apart in water.

These failed synthesis attempts might be due to a poor solubility of 2-MPBA in aqueous solutions used, as evidenced by the fact that 2-MPBA could not be completely dissolved in equimolar NaOH solution. The use of DMSO alone or the combination of NaOH with methanol appears to be able to completely dissolve 2-MPBA, however, only extremely weak hydrogels were attained at the best. This incomplete polymerization or no polymerization at all may be partially due to the chemical structure of 2-MPBA, namely the presence of a methyl group (CH₃) immediately adjacent to the double bond not present in the similar monomer previously synthesized [1]. This methyl group might have a steric hindrance effect on the opening of the double bond and on the approach of other monomers, thereby decreasing the chance of polymerization with other monomers. Furthermore, this extra methyl group, as compared to 2-acrylamidophenylboronic acid investigated by Lowe et al. [1], makes the monomer more hydrophobic and more difficult to dissolve in aqueous solutions.

4.3 Investigation of polyampholytic glucose-sensitive hydrogels

based on AAM, DMAPAA and 3-APB

The data presented in this section is basically an extension of chapter 3, as the hydrogels involved enjoy the same monomers with the only difference being the mole ratios.

As pointed out earlier, fructose interference for phenylboronic acid based glucose-sensitive hydrogels can be addressed by either using 2-acrylamidophenylboronic acid or by introducing a tertiary amine group to the vicinity of 3-acrylamidophenylboronic acid. However, slight physiological pH changes that may occur in the body have been ignored by the developers of many potential glucose sensors,

including chemomechanical sensors, especially for those glucose sensors based on glucose sensitive hydrogels employing tertiary amine and 3-acrylamidophenylboronic acid [4].

Results show that glucose-sensitive hydrogels (GSH) based on acrylamide, DMAPAA and 3-APB, are responsive to pH change. Furthermore, this pH effect is significant, with about 40% difference in swelling pressure response to 5 mM glucose concentration increase observed at pH 7.18 and pH 7.4 in PBS buffer with ionic strength of 0.15 M. This shows the importance of designing a hydrogel that exhibits negligible pH interference. Alternatively, one can design a sensor array, incorporated with smart hydrogels tailored for pH and glucose signal, so that the glucose signal can be deconvoluted from other physiological changes.

In this section, attention is paid to glucose-sensitive hydrogels containing 3-acrylamidophenylboronic acid and amine groups, which are polyampholytic hydrogels that contain both positive and negative fixed charges along the polymer backbone. The pH dependent pressure response of this hydrogel is explored within the piezoresistive pressure transducer. Also, antipolyelectrolyte behavior was observed and was used to check the isoelectric point (IEP) of the hydrogels. Results indicate that a GSH having an IEP close to pH 7.4 exhibits less pH dependence than a GSH having an IEP far from 7.4. Therefore, we would like the IEP of the hydrogel closer to physiological pH 7.4 in order to minimize the pH dependence of the glucose sensor. This IEP shift can be achieved by varying the chemical composition of the glucose sensitive hydrogels, such as by varying the mole ratio between cationic tertiary amine and anionic boronic acid moieties within the GSH.

4.3.1 Glucose-sensitive hydrogels and pH interference

Glucose-sensitive hydrogels presented herein were synthesized in the same manner as the ones in chapter 3. For the glucose-sensitive hydrogels containing 3-APB:DMAPAA:AAM:BIS at a nominal mole ratio of 8:10:80:2, the same composition as the one reported in chapter 3, pH interference is not negligible. As observed in Fig. 4.3, 5 mM glucose concentration increase induced a 40% larger swelling pressure response signal at pH 7.4 than pH 7.18.

This sensitivity difference may be explained by the fact that higher pH indicates more charged forms of boronic acid and less uncharged forms of boronic acid. Hence addition of same amount of glucose brings about less crosslinking within the hydrogel at pH 7.18 than pH 7.4. Meanwhile, glucose may also participate in binding with the uncharged form of boronic acid which would increase the osmotic pressure of the hydrogel and promote swelling, and thus reduce the magnitude of the deswelling signal. In addition, potential hydrogel swelling pressure difference at pH 7.4 and pH 7.18 in PBS buffer at physiological ionic strength of 0.15M in the absence of glucose may also contribute to the signal difference.

Following the same procedures used to obtain the pH dependent glucose response signals of Fig. 4.3, 5 mM glucose induced deswelling signal at other pH values were obtained and are plotted vs. pH in Fig. 4.4. As seen in Fig. 4.4, the magnitudes of osmotic swelling pressure responses for the glucose-sensitive hydrogels are dependent on the pH values investigated. Therefore, measures should be taken to reduce or minimize this pH dependent signal.

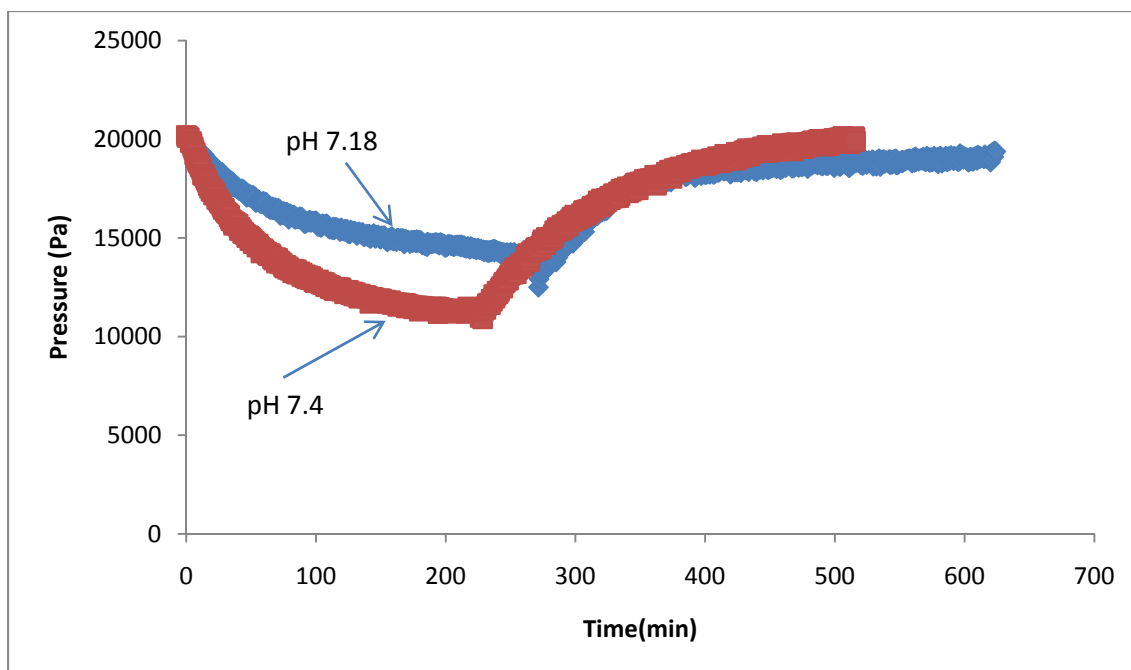


Fig. 4.3. Glucose-sensitive hydrogels (3-APB:DMAPAA:AAM:BIS=8:10:80:2) subjected to 5 mM glucose reversibility test in 0.15 M PBS at pH 7.4 and pH 7.18. Glucose concentration was suddenly increased from 0 to 5 mM at time zero and switched back to 0 after equilibrium was obtained.

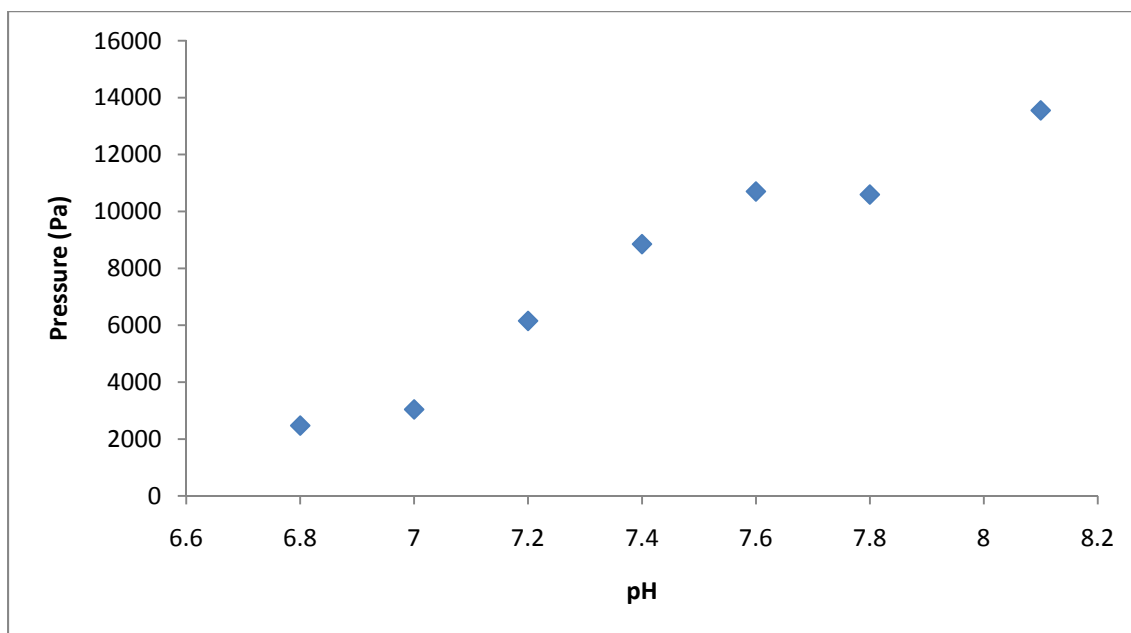


Fig. 4.4. For the same GSH investigated in Fig. 4.3, magnitude of swelling pressure decrease in response to 5 mM glucose administration in 0.15 M PBS as a function of pH.

To evaluate how much pressure change can be induced by the direct osmotic effect on the water surrounding the GSH from glucose, rather than the crosslinking effect of glucose, NaCl reversibility tests were performed to roughly assess the osmotic effect from glucose. As illustrated in Fig. 4.5, addition of 20 mM NaCl to the solution surrounding the sensor induced only about 1300 Pa change of pressure. In contrast, 5 mM glucose induced a pressure change of 8800 Pa, as noted in Fig. 4.3. Therefore, 5 mM glucose induced pressure decrease is largely due to the crosslinking effect, not the osmotic effect on the surrounding water from glucose.

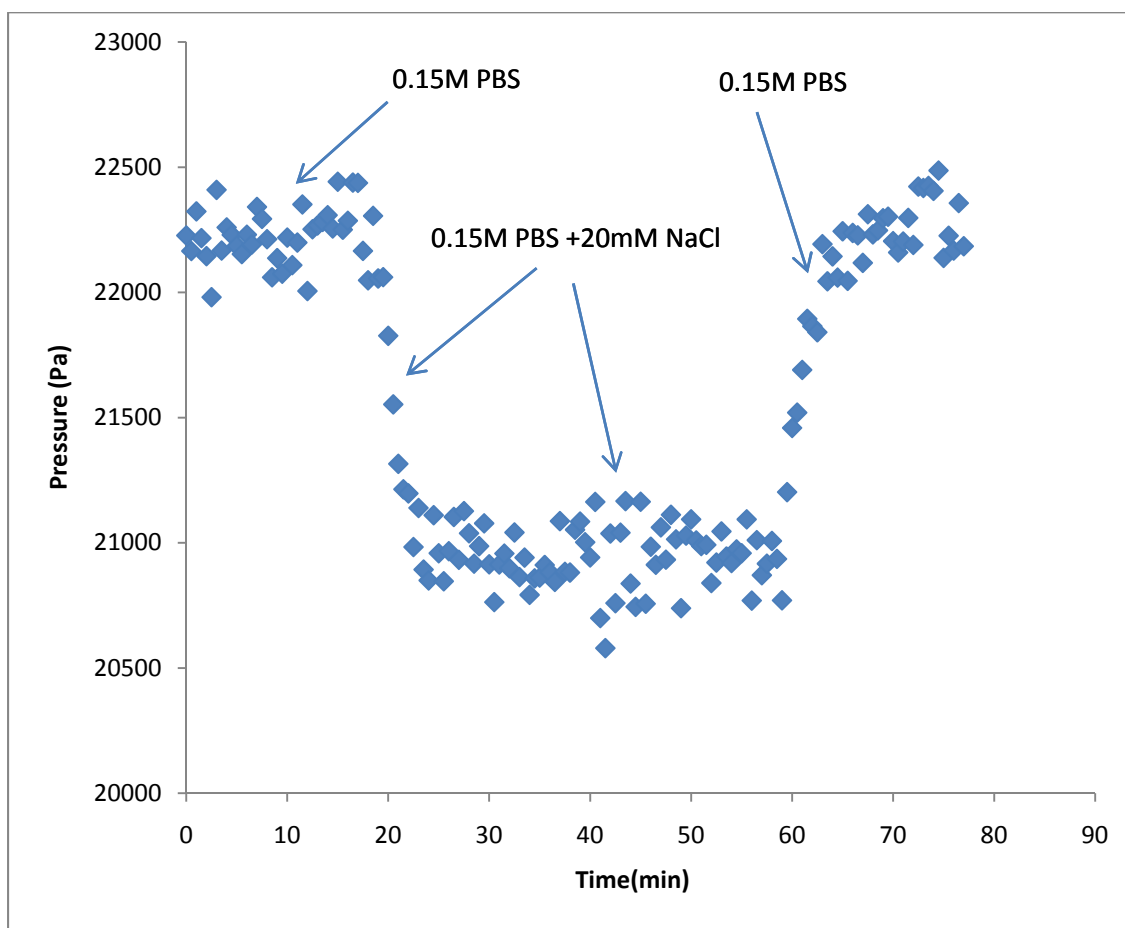


Fig. 4.5. Response of macrosize sensor containing GSHs (8:10:80:2) subjected to NaCl reversibility tests in PBS buffer at physiological pH 7.4.

4.3.2 Glucose-sensitive hydrogels and the isoelectric point

For polyampholytic hydrogels, the isoelectric point (IEP) refers to the pH where equal amounts of positive charge and negative charge are present along the polymer backbone [5]. Most hydrogels shrink with increase in the environmental ionic strength value. As seen in Fig. 4.6, the glucose-sensitive hydrogel exhibits interesting antipolyelectrolyte behavior, characterized by an increase in hydrogel swelling pressure with increasing ionic strength from 0.15 M to 0.25 M. This occurs because the increase in environmental ionic strength increasing the degree of screening between the positive and negative charges on the polymer backbone [5]. Antipolyelectrolyte behavior for polyampholytic gels is usually observed near the pH value of the isoelectric point (IEP). Fig. 4.6 indicates the IEP of the hydrogel is around pH 9.5, as this was the pH used to obtain Fig. 4.6.

Fig. 4.7 demonstrates the swelling pressure change of the same glucose sensitive hydrogel subjected to pH change only without any glucose involved. In Fig. 4.7, swelling pressures are plotted relative to the value at pH 7.4. One can see that the minimum swelling pressure of the hydrogel is observed at pH around 9.2, indicative of the IEP of the hydrogel. This is consistent with the observed antipolyelectrolyte behavior at pH 9.5. At IEP, equal amount of positive and negative charges are present in the hydrogel polymer chains. In this case, counterions in the solution do not have to diffuse into the hydrogel to maintain the neutrality of the hydrogel, which results in minimum counterions concentration within the hydrogels and minimum hydrogen swelling pressure.

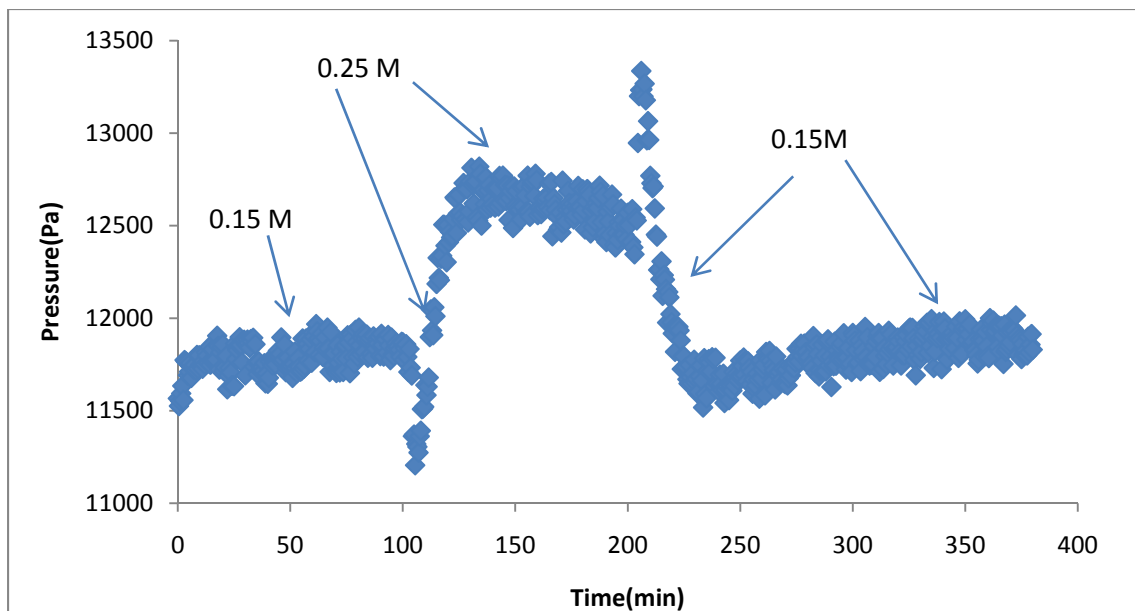


Fig. 4.6. GSH(8:10:80:2) subjected to ionic strength change between 0.15 M and 0.25 M in PBS buffer at pH 9.5. Ionic strength was suddenly increased from 0.15 M to 0.25 M at time 103 min and switched back to 0.15 M at time 204 min. Antipolyelectrolyte behavior is observed.

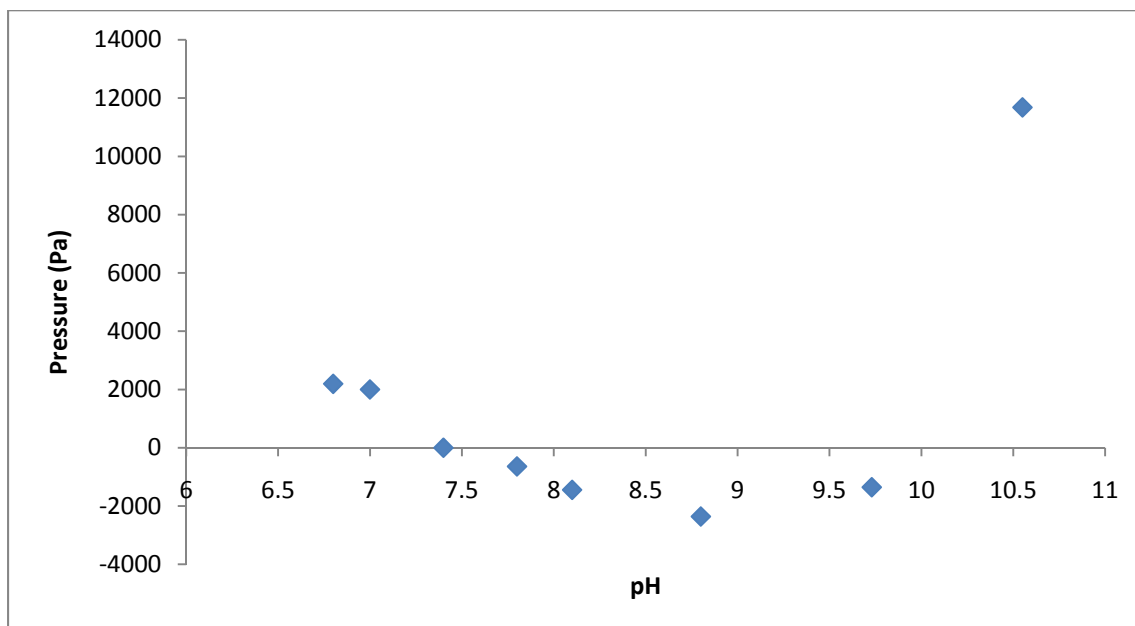


Fig. 4.7. Response of macrosized sensor containing GSH (8:10:80:2) subjected to pH change in 0.15 M PBS buffer plotted against pH with pressure at 7.4 used as the reference value.

4.3.3 Glucose-sensitive hydrogels with different isoelectric points

As seen in Fig. 4.7, if one can shift the IEP of hydrogel closer to pH 7.4, then we can expect less pH interference in the body where the pH may vary in the vicinity of pH 7.4. Meanwhile, many applications of hydrogels in the biomedical field require hydrogels having good biocompatibility. For polyampholytic hydrogels, if only charge is taken into consideration, the optimal biocompatibility can be expected at the isoelectric point [6]. Therefore, for in vivo sensor applications, it is desirable to design a glucose sensitive

The change of hydrogel IEP can be accomplished by varying the chemical composition of the pregel solution. As seen in Fig. 4.8, the IEP of the hydrogel was shifted from about 9.2 to about 7.5 when the chemical composition of the hydrogel was varied from (3-APB:DMAPAA:AAM:BIS) 8:10:80:2 to 10:2.5:80:2. For glucose sensitive hydrogels (GSH) with mole ratio of 8:10:80:2 at pH 7.4, the hydrogel backbone is in a net positive charge state because pH 7.4 is only barely above the pKa value of boronic acid, and thus a significant fraction of boronic acid groups are not negatively charged. In order to bring about equal amount of anions and cations in the polymer backbone at pH 7.4, the ratio of PBA to DMAPAA has to be increased as PBA confers negative charge and DMAPAA contributes positive charge to the hydrogel backbone. Based on this rationale, the synthesis of GSH containing 3-APB:DMAPAA:AAM:BIS at a mole ratio of 10:2.5:80:2 was performed. For this new GSH, which has an IEP of about 7.5, as illustrated in Fig. 4.8, 5 mM glucose response tests were performed at pH 7.4 and pH 7.18 in 0.15 M PBS buffer to evaluate if the change of IEP will reduce pH dependent glucose sensitivity.

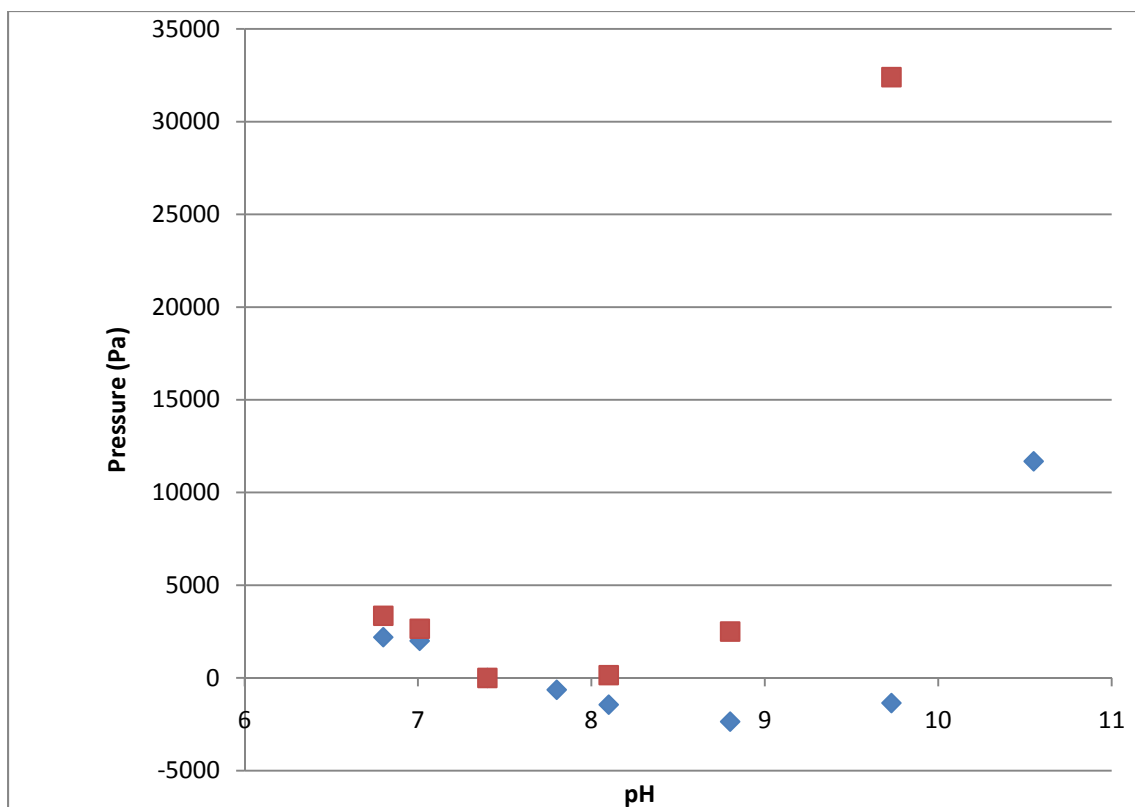


Fig. 4.8. Comparison of two glucose-sensitive hydrogels (GSHs) in macrosize sensor subjected to pH change only in 0.15 M PBS buffer. Solid diamond symbols and solid square symbols represent GSHs containing mole ratios of 8:10:80:2 and 10:2.5:80:2 (3-APB:DMAPAA:AAM:BIS), respectively.

Fig. 4.9 shows the results of 5 mM glucose response at pH 7.18 and pH 7.4 for the hydrogel having an IEP about 7.5. As observed in Fig. 4.9, there is no significant difference in the deswelling signal between pH 7.18 and 7.4 upon 5 mM glucose administration. This is in sharp contrast to the behavior observed in Fig. 4.3 for the glucose-sensitive hydrogel containing 8/10/80/2 composition, which has about 40% difference in deswelling signal for the same pH change as opposed to only about 6% difference seen in Fig. 4.9. These results indicate that by shifting the isoelectric point (IEP) of the hydrogel close to pH 7.4, one can significantly reduce the inference from pH change, at least for pH change from 7.18 to 7.4.

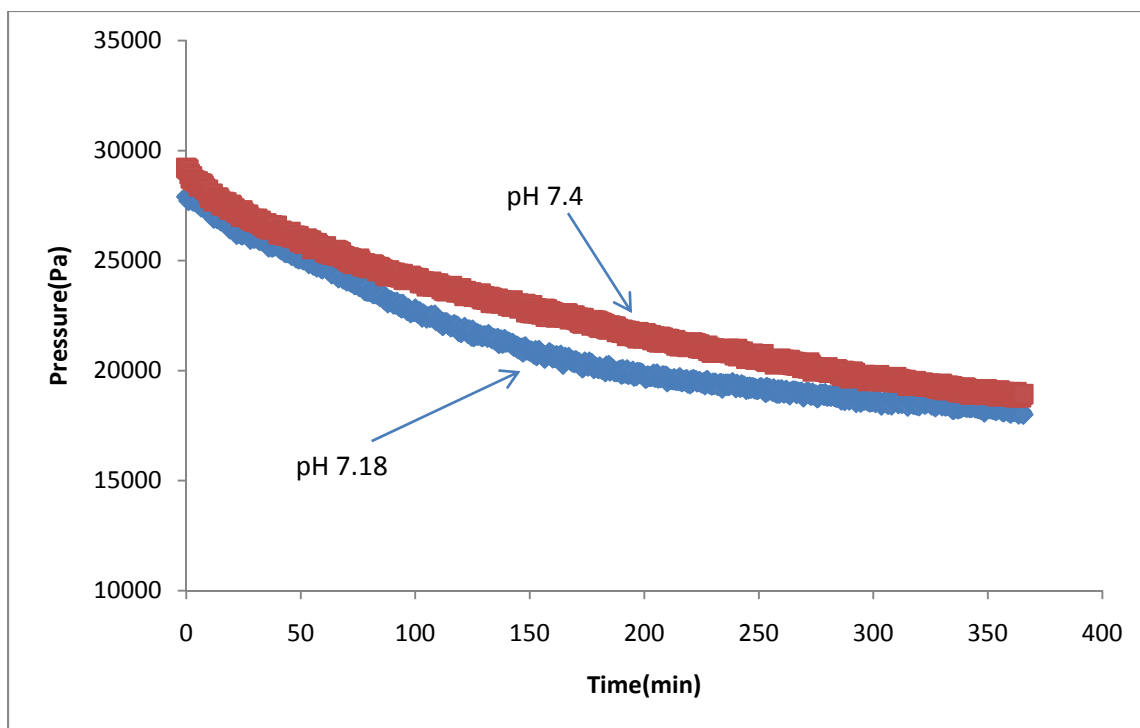


Fig. 4.9. Response curves of macrosized sensor containing glucose-sensitive hydrogels (3-APB:DMAPAA:AAM:BIS=10:2.5:80:2) subjected to increase in glucose concentration from zero to 5 mM in 0.15 M PBS at pH 7.4 and pH 7.18.

In Fig. 4.9, one also notes that both the pH 7.18 and pH 7.4 curves obey first order kinetics with $R^2 = 0.96$ (first order constant = 111 min) and 0.91 (first order constant = 107 min), respectively. It should be noted that two curves in Fig. 4.3 also obey first order kinetics with first order constant 87 min and 54 min for deswelling at pH 7.18 and 7.4, respectively. Therefore, the hydrogel with 10/2.5/80/2 exhibits slower kinetics than hydrogel with 8/10/80/2 composition. One possible explanation might be related to the observation that the permeability of a polyampholytic hydrogel membrane exhibits a minimum at the IEP, and increases as the pH deviates from the IEP [7]. At the IEP, maximum attractive forces between positive charge and negative charge can be obtained and this renders a minimum degree of swelling. An increase in ionic strength reduces the

maximum attractive forces and thus the hydrogel swells and permeability increases.

4.3.4 Glucose sensitive hydrogels and two-step deswelling behavior

Further glucose response tests were performed using the macrosize sensor for the glucose-sensitive hydrogels with 10/2.5/80/2 composition. As seen in Fig. 4.10, as expected, a 20 mM glucose concentration increase induces a larger pressure response than that of 5 mM glucose concentration increase. The unexpected result in Fig. 4.10 is that the 20 mM glucose response curve shows a two-step deswelling process with a sharp decrease in deswelling rate occurring about 10 min after glucose administration. This phenomenon was observed at two different hydrogel loading pressures in response to 20 mM glucose administration, as indicated in Fig. 4.10.

One may argue that this occurs because of the immediate osmotic effect on the water surrounding the gel from 20 mM glucose administration before glucose diffuses into the hydrogel and causes shrinking. At first glance this argument seems possible as the osmotic effect from 20 mM glucose occurs first. However, as demonstrated in Fig. 4.11, this two-step deswelling phenomenon was not observed in a glucose-sensitive hydrogel containing a smaller mole ratio of PBA to amine under the same experimental test. Thus the appearance of the two-step deswelling is not due to the immediate osmotic effect from 20 mM. One also notices in Fig. 4.10 that the two-step deswelling is glucose concentration dependent, as it was observed for 20 mM glucose concentration increase but not for 5 mM increase.

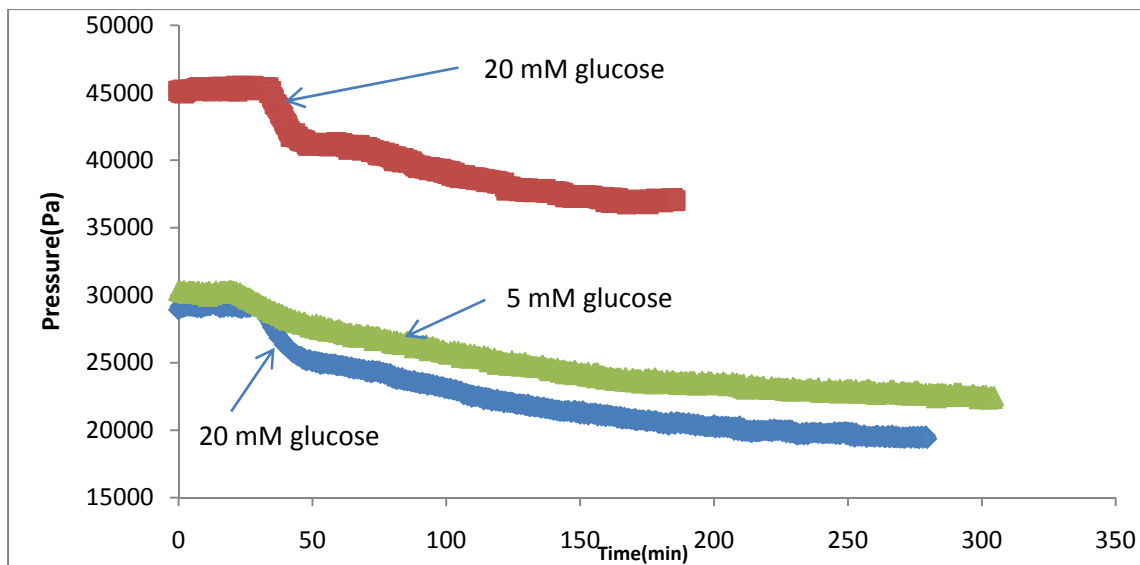


Fig. 4.10. Time-dependent pressure change of macrosized sensor containing a GSH (3-APB:DMAPAA:AAM:MBA=10:2.5:80:2) in response to glucose addition at physiological pH 7.4 in PBS buffer. The hydrogel was initially in PBS buffer without glucose, and the solution glucose concentration was suddenly increased to 5 mM or 20 mM glucose at the time when the first change of slope occurs. 20 mM glucose tests were performed at two different values of initial loading pressures.

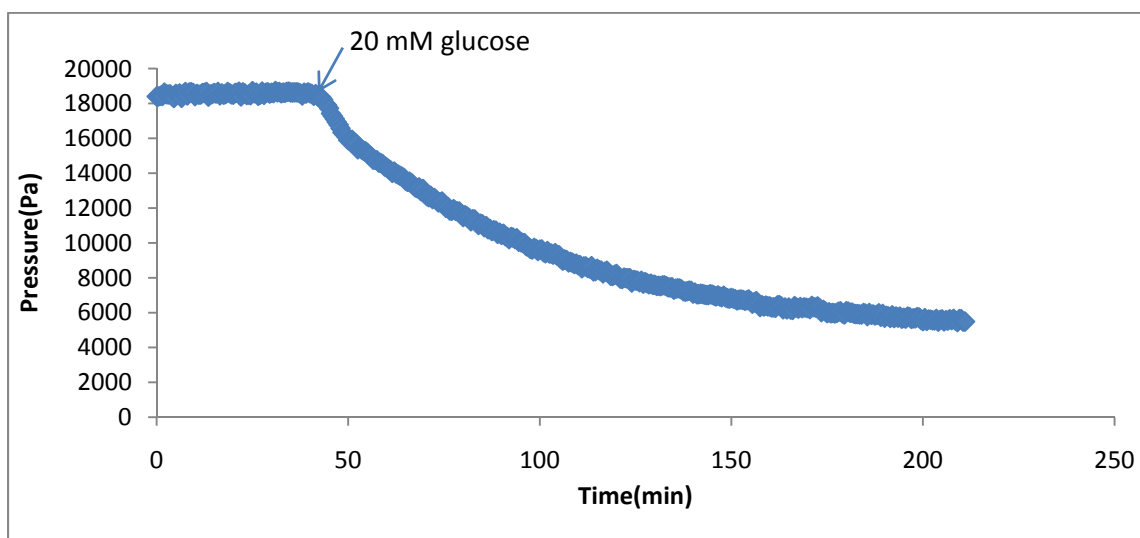


Fig. 4.11. Time-dependent pressure change of macrosized sensor containing a GSH (3-APB:DMAPAA:AAM:BIS=8:10:80:2) in response to glucose concentration change at fixed pH 7.4 and ionic strength 0.15 M in PBS buffer. Initially the GSH was in PBS buffer without glucose, and the glucose concentration was suddenly increased to 20 mM at the time located by the arrow in the plot.

A possible explanation for this two-step deswelling phenomenon is skin layer formation on the outer surface of the hydrogels in the sensor due to glucose-mediated crosslinking. The formation of a skin layer substantially retards further diffusion of the glucose into the hydrogel and thus the retarded deswelling or two-step deswelling phenomenon appears. In this scenario, each-glucose binds simultaneously to two boronic acids and forms a crosslinker, too many crosslinkers formed on the outer surface of the hydrogels cause the outer layer to shrink abruptly and collapse before the glucose diffusion to the inner part of the hydrogel can occur. This substantial difference in glucose crosslinker density between the outer surface of the hydrogel and the interior of the hydrogel induces the formation of the skin layer. In fact, this skin layer formation in glucose-sensitive hydrogels has been reported previously by Akira et al. [8], who suggested that the skin layer formation was responsible for the two-step deswelling phenomenon. In their case, however, the glucose sensitive hydrogel swelled with increasing glucose concentration and involved no DMAPAA or glucose crosslinks. This occurred because the dissociation of complex between glucose and the phenylboronates led to the dehydration of the gel surface which results in the formation of the collapse or skin layer. Here we observed for the first time that hydrogels that shrink with increasing glucose concentration also exhibit a two-step deswelling process. Additionally, the glucose-sensitive hydrogels (GSHs) also exhibit high glucose selectivity towards glucose over fructose. To further investigate the hypothesis that skin layer formation is responsible for the two-step deswelling, glucose sensitive hydrogels containing various chemical compositions were studied and the results obtained are listed in Table 4.4.

Table 4.4. Various GSHs of higher acrylamide content subjected to various glucose deswelling tests, where “no” indicates no two-step deswelling was observed and “yes” indicates two-step deswelling was observed in 0.15 M PBS at pH 7.4.

GSH mole ratio (3-APB:DMAPAA:A AM:BIS)	2.5 mM Glucose	5 mM Glucose	10 mM Glucose	20 mM Glucose	Water content Wt%
8:10:80:2	No	No	No	No	88%
10:8:80:2	No	No	No	No	86%
13.6:4.4:80:2	N/A	No	N/A	Yes	73.8%
4:14:80:2	No	No	No	No	91.7%
10:2.5:80:2	No	No	No	Yes	78.8%

As seen in Table 4.4, two trends can be identified. Two-step deswelling phenomenon is dependent on the mole ratio of 3-APB as well as glucose concentration. First of all, for hydrogels containing a low 3-APB/DMAPAA ratio such as 8:10, no two-step deswelling was observed at all glucose concentrations investigated. Secondly, for hydrogels containing a higher 3-APB/DMAPAA ratio such as 10:2.5 or 13.6:4.4, two-step deswelling was observed at high glucose concentrations such as 20 mM, but no two-step deswelling was observed at low glucose concentrations such as 5 mM. What determines the appearance of two-step deswelling appears to be the glucose crosslinking density difference between the outer surface layer of the hydrogels and the interior of the hydrogels. In other words, the glucose-mediated crosslink density gradient normal to the surface of the hydrogel dictates the magnitude of two-step deswelling. For hydrogels having a low 3-APB/DMAPAA ratio, not enough boronic acid groups are available for glucose to form a high glucose-mediated crosslink density and this applies to all the glucose concentrations studied. For hydrogels having a high 3-APB/DMAPAA ratio, sufficient boronic acid are available for glucose binding to form crosslinks. In the case of high glucose concentration administration, an initial huge increase in glucose crosslinks on the hydrogel surface renders a skin layer that causes an initial deswelling and also substantially retards glucose permeability to the hydrogel. Over time, glucose gradually diffuses through this dense skin and forms crosslink in the interior of the hydrogels which results in the disappearance of the skin layer and a more homogeneous hydrogel. Upon low glucose concentration administration, however, not enough glucose molecules are available for the formation of dense glucose-mediated crosslinking along the surface of the hydrogel and two-step deswelling kinetics are not present. It should be noted that in

Table 4.4, a GSH containing 13.6:4.4:80:2 composition subjected to an increase in glucose concentration initially exhibits deswelling and then reswelling, as illustrated in Fig. 4.12. What contributes to the reswelling after deswelling might be the complex formation between glucose and one boronic acid moiety, as this complex formation renders the hydrogel more negatively charged and thus the hydrogel swells. Initial deswelling is due to glucose-mediated crosslink formation, which has a much faster kinetics than the complex formation of glucose with the uncharged form of boronic acid [9].

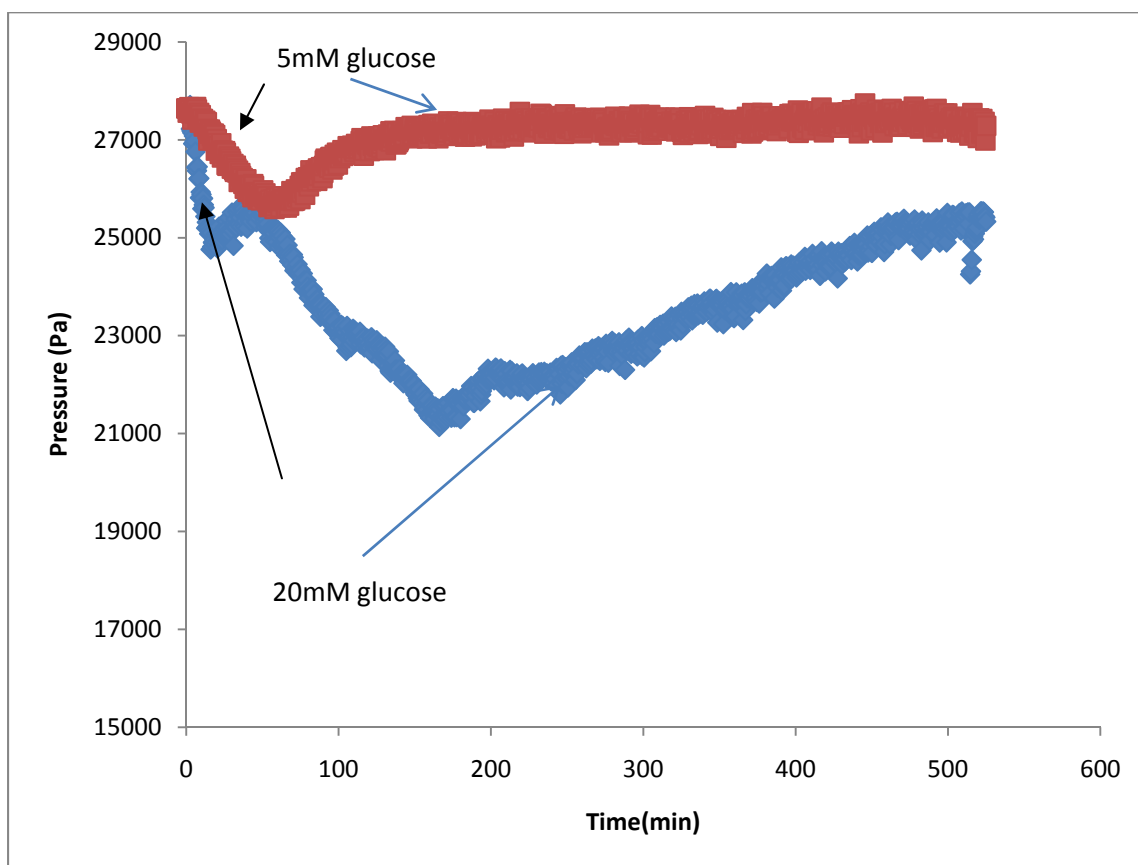


Fig. 4.12. Response of macrosized sensor containing GSH having monomer mole ratio (3-APB:DMAPAA=13.6:4.4) subjected to glucose injection in 0.15 M PBS buffer at pH 7.4. The glucose concentration was suddenly increased from zero to 5 mM (upper curve) and 20 mM (lower curve) glucose at time equal zero.

Another set of GSHs with different chemical compositions further validate the proposed two-step deswelling hypothesis, namely that this 2-step deswelling is related to the mole ratio of 3-APB and the applied glucose concentration, as demonstrated in Table 4.5. A typical deswelling curve for this composition of glucose sensitive hydrogel (GSH) can be found in Fig. 4.13. In Fig. 4.13, one can see that a GSH containing 5:20:60 mole ratio exhibits no two-step deswelling upon 50 mM glucose addition. However, the two-step deswelling kinetics are quite obvious for GSH containing monomer mole ratios 20:20:60. This sharp difference shows that two-step deswelling is 3-APB/DMAPAA mole ratio dependent. For GSH containing 10:20:60 or 20:20:60 mole ratio, one also notices in Fig. 4.13 that the hydrogels shrink almost below the volume of the confining cavity, as evidenced by a near zero swelling pressure at equilibrium.

Table 4.5. Various GSHs of lower acrylamide content subjected to various glucose deswelling tests, where “no” indicates no two-step deswelling was observed and “yes” indicates two-step deswelling was observed.

GSH pregel composition (mole ratio) (3-APB:DMAPAA:AAM:BIS)	5 mM glucose	20 mM glucose	50 mM glucose	Water content
5:20:60:2	No	No	No	93.4%
10:20:60:2	No	No	Yes	90.6%
20:20:60:2	Yes	Yes	Yes	79.5%

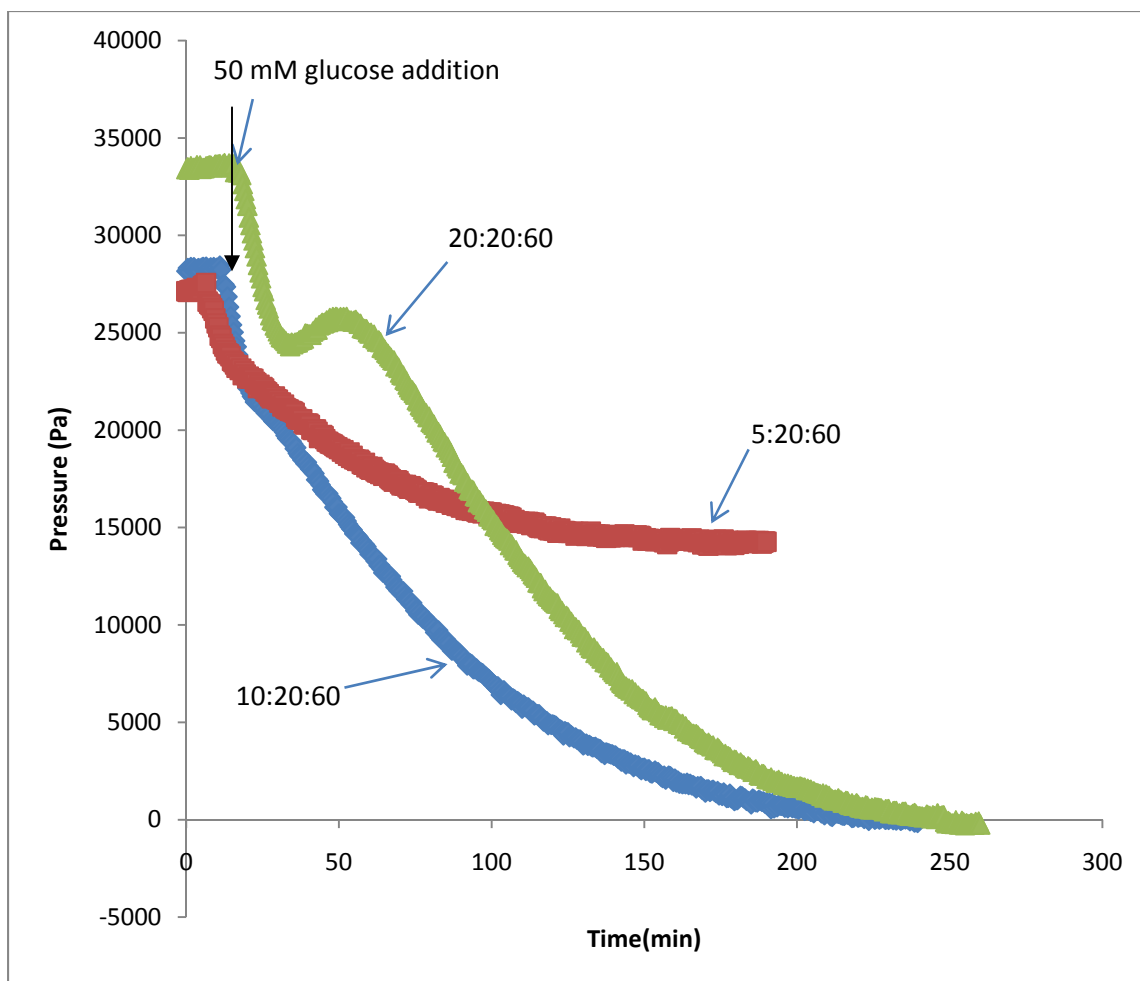


Fig. 4.13. Time dependent response curves of macrosized sensor containing glucose sensitive hydrogels listed in Table 4.5 subjected to increase in glucose concentration from zero to 50 mM. The mole ratio of 3-APB:DMAPAA:AAM is given in the figure legend.

It should be noted that in both Table 4.4 and Table 4.5, the water content of the hydrogel also appears to have an effect on the two-step deswelling phenomenon. If only water content is taken into consideration, less water content seems more likely to cause two-step deswelling, probably because smaller water fraction implies a shorter distance between two boronic acid moieties and thus a greater likelihood of formation of crosslinks mediated by glucose.

In summary, two-step deswelling observed herein is a function of glucose

concentration, mole ratio of 3-APB to DMAPAA, and probably also water content of the hydrogels. All these factors might work synergistically to induce a large glucose crosslinking density gradient into the hydrogel and results in two-step deswelling kinetics. The two-step deswelling behavior might be advantageous for use in a repetitive on-off drug-releasing carrier device with a long interval [8]. Meanwhile, further study is necessary to elucidate the detailed mechanism of this two-step deswelling so that one can tailor the appearance of two-step deswelling kinetics and also manipulate the rate constants.

4.3.5 Glucose-sensitive hydrogel phase separation

This section summarizes when phase separation of hydrogels was observed during synthesis and presents potential approaches to avoid such hydrogel phase separation. Phase separated hydrogels exhibit poor mechanical properties and are unsuitable for generating osmotic swelling pressure change in our chemomechanical sensors. The examined cases are shown in Table 4.6.

Polymerization induced hydrogel phase separation is a phenomenon in which an initially homogeneous pregel solution becomes phase separated during the course of hydrogel polymerization [10]. Generally, a phase-separated hydrogel exhibits opaqueness or is white in color. Consistently, the color of the phase-separated hydrogels is white in our cases. Hydrogel phase separation can be induced by several factors, including the solvent, crosslinking density, solvent-polymer interaction parameter, and the elasticity of the resultant hydrogel polymer network [11,12].

Table 4.6. Glucose-sensitive hydrogels and phase separation during synthesis. The amount of DMSO used in this table was 10 vol% or equal moles of NaOH and 3-APB were used in each synthesis.

Pregel Chemical Compositions (mole ratio) (3-APB:DMAPAA:AAM:BIS, unless otherwise stated)	Solvents and Monomer Concentration wt%	Results
20:20:60:2	DMSO and HEPES 19.4 wt%	White
20:20:60:0.5	DMSO and HEPES 27.2 wt%	Transparent
14.4:3.6:80:2	DMSO and HEPES 12.7 wt%	White
14.4:3.6:80:2	NaOH and HEPES 12.7 wt%	Transparent
10:2.5:80:2	DMSO and HEPES 12.7 wt%	White
10:2.5:80:2	NaOH and HEPES 12.7 wt%	Transparent
3-APB:DMAPAA:HEMA:BIS =8:10:80:2	DMSO and HEPES 21.8 wt%	White
3-APB:DMAPAA:HEMA:BIS =8:10:80:2	NaOH and HEPES 21.7 wt%	Transparent

As seen in Table 4.6, the use of DMSO or 2% crosslinking density induces hydrogel phase separation, whereas the use of NaOH or 0.5% crosslinking density leads to transparent hydrogels. This happens probably because 3-APB is acidic and NaOH is basic, hence the solvating power of NaOH for 3-APB is expected to be better than DMSO for 3-APB. This leads to a more homogenous pregel solution and a transparent hydrogel. This observed result is in agreement with the published literature [11].

Meanwhile, an increase in crosslinking density from 0.5% to 2% also results in a transparent hydrogel becoming opaque and presumably phase separated. This occurs probably because higher elasticity of the hydrogel, due to higher crosslinking density, leads to phase separation during polymerization as reported by Boots et al. [12].

In summary, use of DMSO will lead to opaque hydrogels in some cases, and this can be addressed by using NaOH instead. Higher crosslinker content appears to be more likely to induce phase separation.

4.4 Novel glucose sensitive hydrogels containing

HEMA, DMAPAA and 3-APB

A novel glucose sensitive hydrogel containing 3-APB/DMAPAA/HEMA/BIS with a nominal mole ratio of 8:10:80:2 was synthesized via free radical solution polymerization. All of the GSH for which results have been presented so far in this thesis contained acrylamide as the major component, whereas this novel GSH employs hydroxyethylmethacrylate (HEMA). HEMA has been widely used in biomedical applications such as in contact lenses and HEMA based hydrogels are resistant to degradation by enzyme and pH [13]. In addition, HEMA-based hydrogels are particularly suitable for applications in biological systems due to their essential nontoxicity [14].

Acrylamide, however, has been reported to be toxic, at least according to some studies [15-17]. Glucose-sensitive hydrogels (GSHs) with HEMA as the major component may therefore be expected to be more biocompatible and superior for in vivo applications. As far as we know, synthesis of this novel GSH has not been reported previously in the literature. In our study, the novel GSH was synthesized and coupled with the macrosized piezoresistive pressure sensor to obtain the glucose-dependent swelling pressure response. The results show that the osmotic swelling response of this GSH is suitable for an implantable glucose sensor, albeit for practical application the response time needs to be substantially reduced. Glucose response comparison was also made between this GSH containing HEMA and GSH containing AAM, as reported in chapter 3.

4.4.1 Synthesis and testing

Glucose sensitive hydrogels (GSHs) containing 3-APB/DMAPAA/HEMA/BIS with a nominal mole ratio of 8/10/80/2 were synthesized by free radical solution copolymerization. The procedures followed here were the same as the previous study [18], with the only exception being the use of 1 M NaOH as the solvent instead of DMSO, because the use of DMSO leads to partial phase-separated, fragile, and white hydrogels. The transparent GSHs obtained using NaOH were washed with deionized water for one day and then 0.15 M PBS for several days to remove impurities before testing in the macrosized sensor. The GSH with HEMA as the major component contains 62 wt% water, which is a lot less than that of the similar GSH (88 wt% water) having acrylamide as the major component.

The testing procedures followed were the same as the previous study [18]. Briefly, a disc-shaped smart hydrogel was cut by a biopsy tool and attached to the cylindrical top

surface of a macrosized piezoresistive pressure transducer (see Fig. 1.7). A detachable sensor cap equipped with a rigid porous membrane as the top surface, through which mass transportation can occur, was used to keep the hydrogel within the sensor and to exert an adjustable stress on the hydrogel via tightening or loosening of the three screws attached to the sensor. The chemomechanical sensor with the smart hydrogel confined inside was then inserted into a large covered environmental bath buffer solution in which the glucose concentration was varied by either injecting concentrated glucose solutions or by rapid switching to another large environmental bath with differing glucose concentration. For all the tests involved, 0.15 M PBS buffer with pH 7.4 was used as the buffer to mimic physiological conditions. The time dependent pressure response induced by glucose was captured by a piezoresistive transducer data acquisition system.

4.4.2 Results and discussion

Glucose-sensitive hydrogels (GSHs) subjected to a 5 mM glucose reversibility test in PBS buffer at the physiological pH 7.4 and ionic strength 0.15 M gave the results shown in Fig. 4.14. In Fig. 4.14, one notices a slight slope transition during deswelling and swelling. This slope change was observed at all the glucose concentrations investigated; and this slope change becomes more obvious with increasing glucose concentration. One possible explanation for this phenomenon is the formation of a skin layer due to glucose-mediated crosslinks formed on the surface of the hydrogels, as already discussed in section 4.3.4. In Fig. 4.15, the deswelling half cycle of Fig. 4.14 was analyzed by the first-order kinetics model, and an excellent fit was observed with an R squared value of 0.94.

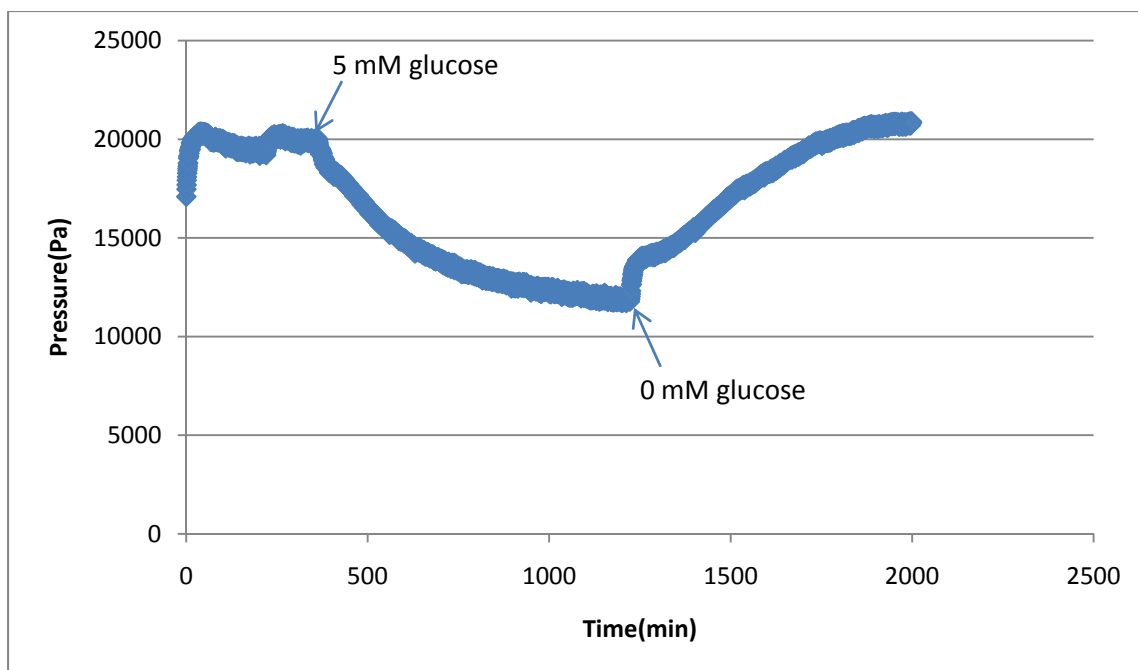


Fig. 4.14. Response of macrosize sensor containing glucose sensitive hydrogel with HEMA as the major component subjected to 5 mM glucose reversibility test in PBS buffer at physiological pH 7.4 and ionic strength 0.15 M. The results were obtained by using the macrosensor of Fig. 1.7.

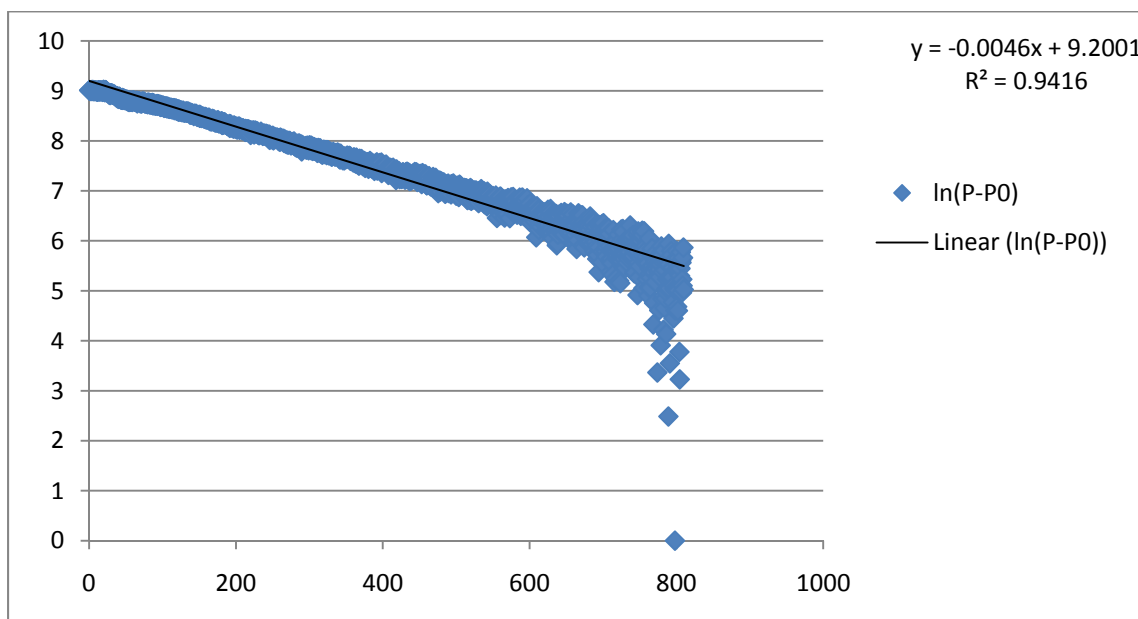


Fig. 4.15. Fit of time dependent deswelling half cycle in Fig. 4.14 to first order kinetics model, with a first order time constant of 217 min.

Following the same procedures as in the 5 mM glucose response test, 2.5, 10, 15 and 20 mM glucose responses tests for the same hydrogel were also performed. The results obtained for various glucose concentrations are shown in Fig. 4.16. Comparison is also made in this figure between this novel GSH and a similar GSH containing AAM as the major component as reported in chapter 3, with the only difference being that the novel GSH contains HEMA, instead of AAM, as the major component.

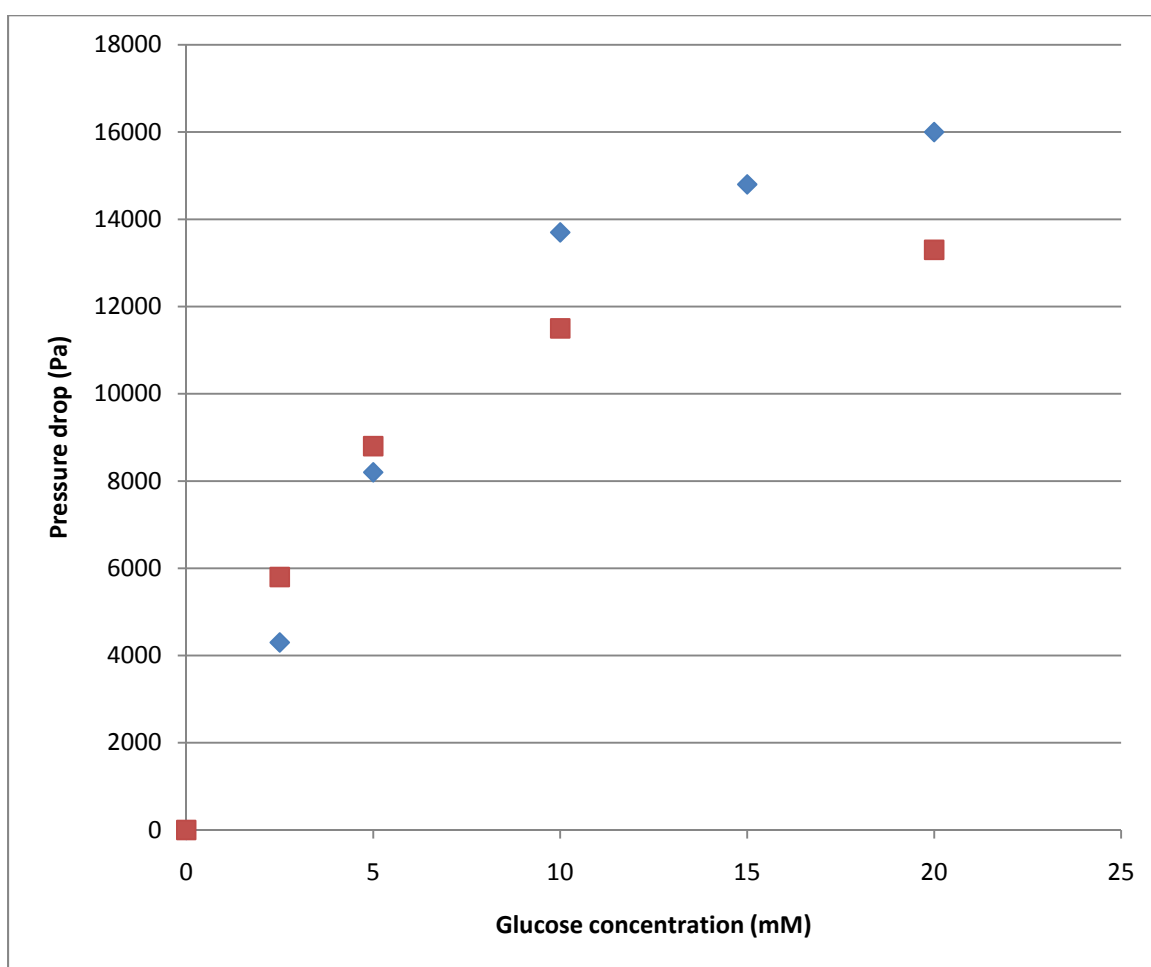


Fig. 4.16. Magnitude of the osmotic-swelling pressure decrease at equilibrium vs. external glucose concentration, as measured using the macrosizer sensor of Fig. 1.7. Filled diamonds correspond to sensor results obtained using a GSH with HEMA as the major component, whereas filled squares correspond to sensor results obtained using a GSH with acrylamide as the major component.

As seen in Fig. 4.17, a striking behavior of the novel HEMA-containing GSH is observed in the deswelling curve after a jump in glucose concentration from zero to 20 mM glucose. It is surprising to observe in Fig. 4.17 the sharp difference in deswelling response between the sensor response curves obtained using two similar GSHs, because both GSHs employ the same amount of APB, DMAPAA, and APB/DMAPAA ratio in the pregel solution. In Fig. 4.17, GSH (HEMA) exhibits two-step deswelling kinetics with a plateau lasting for about 30 min before deswelling occurs again, whereas this is not observed with GSH (AAM).

Different monomer reactivity ratios in different solvents might affect the percentage of monomers incorporated into the GSH backbone, as the synthesis solvent was DMSO for GSH (AAM), whereas NaOH was used for GSH (HEMA). In addition, hydrogel water content might play a significant role in this striking deswelling difference. The GSH (AAM) contains 88 wt% water, as opposed to 62 wt% water for GSH (HEMA). This implies that the average distance between two APB moieties in GSH (HEMA) is shorter than in GSH (AAM), hence a larger probability to form glucose-mediated crosslinks with boronic acid moieties in GSH (HEMA). A larger distance between two APB moieties in GSH (AAM) might result in lower glucose-mediated crosslink density upon glucose administration on the surface of the hydrogel. In addition, a larger water content gives a larger glucose diffusion coefficient in the hydrogel. Therefore, the skin layer forms on the surface of the GSH when HEMA rather than AAM is the major hydrogel component. Indeed, this two-step deswelling was not observed in GSH (AAM) at any of the glucose concentrations studied.

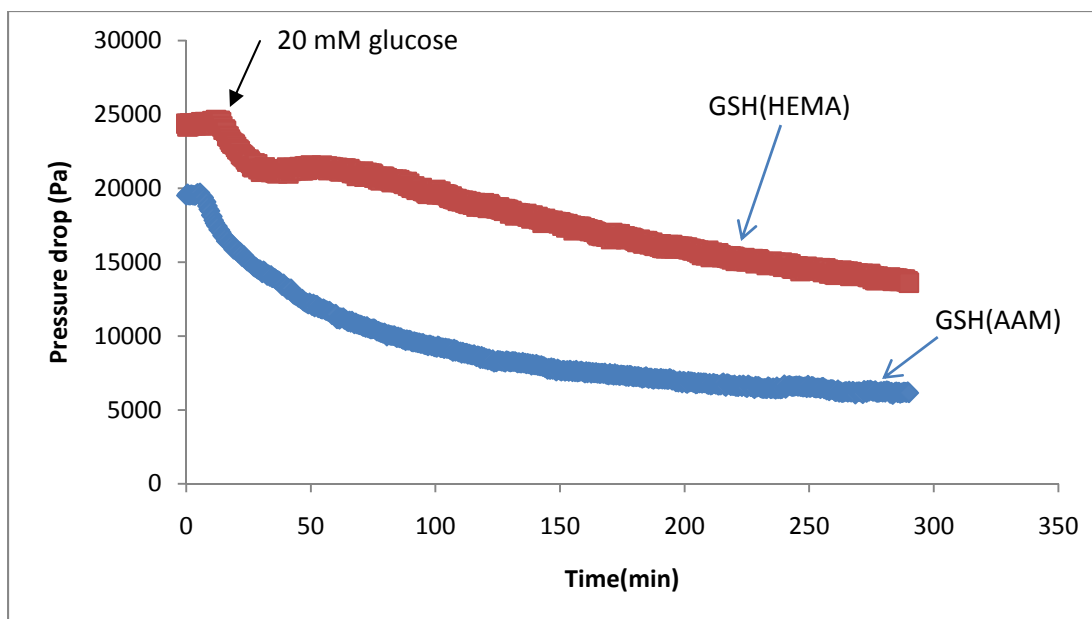


Fig. 4.17. Response of macrosized sensor containing GSHs with HEMA as the major component compared to response of macrosized sensor with AAM as the major component upon increase in glucose concentration from zero to 20 mM glucose in PBS buffer at physiological pH and room temperature. 20 mM glucose was administered at the time when the first slope change is observed.

4.5 Conclusions

Based on the foregoing results, it is possible to make several conclusions. The isoelectric point (IEP) can be shifted to lower pH values by increasing the mole ratio of 3-APB to DMAPAA in the glucose-sensitive hydrogel (GSH). Near the IEP, the glucose response magnitude is less dependent on pH, but the glucose response kinetics are slower. In addition, the GSH exhibits anti-polyelectrolyte behavior.

Glucose sensitive hydrogels employing HEMA as the major component were successfully synthesized and found to be responsive to glucose. The magnitude of the osmotic swelling response of these novel GSHs are suitable for glucose sensing. According to Fig. 4.16, GSHs containing HEMA appear to be more responsive to glucose at high glucose concentration than GSHs containing AAM. However, the macrosized

sensor glucose response time for GSHs containing HEMA is substantially larger than that of GSHs containing AAM (first order time constant 217 min vs. 55 min). The lower water content of GSHs containing HEMA is at least partially responsible for its longer glucose response time. Lastly, at low glucose concentrations, both GSH (HEMA) and GSH (AAM) fit 1st order model kinetics. At high glucose concentrations, however, only GSH (AAM) follows 1st order model kinetics.

Unusual two-step deswelling glucose response curves were discovered for a number of different types of GSHs under certain experimental conditions. The occurrence of the two-step curve is more likely for GSHs having lower water content, greater PBA and HEMA content, and at higher glucose concentrations. It is hypothesized that the two-step kinetics can be attributed to the formation of a low permeability “skin” on the GSH after the exterior portions of the GSH become reversibly crosslinked by glucose.

4.6 References

1. X. Yang, M.C. Lee, F. Sartain, X. Pan, C.R. Lowe, Designed boronate ligands for glucose-selective holographic sensors, *Chem. Eur. J.* 12 (2006) 8491-8497.
2. X. YANG, X. Pan, J. Blyth, C.R. Lowe, Towards the real-time monitoring of glucose in tear fluid: Holographic glucose sensors with reduced interference from lactate and pH, *Biosensors and Bioelectronics* 23 (2008) 899-905.
3. F.D. Hooge, D. Rogalle, M.J. Thatcher, S.P. Perera, J.M. Elsen, A.T. Jenkins, T.D. James, J.S. Fossey, Polymerization resistant synthesis of methacrylamido phenylboronic acids, *Polymer* 49 (2008) 3362-3365.
4. S. Tierney, S. Volden, B.T. Stokke, Glucose sensors based on a responsive gel incorporated as a Fabry-Perot Cavity on a fiber-optic readout platform, *Biosensors and Bioelectronics* 24 (2009) 2034-2039.
5. J.P. Baker, H.W. Blanch, J.M. Prausnitz, Swelling properties of acrylamide-based ampholytic hydrogels: comparison of experiment with theory, *Polymer* 36 (1995) 1061-1069.

6. J. Kopecek. Personal communication 10/19/2009.
7. J. Kopecek, Hydrogels: From soft contact lens and implants to self-assembled nanomaterials, *Journal of Polymer Science: Part A: Polymer Chemistry* 47 (2009) 5929-5946.
8. Akira Matsumoto, Takeyuki Kurata, Daijiro Shiino, and Kazunori Kataoka. Swelling and shrinking kinetics of totally synthetic glucose responsive polymer gel bearing phenylborate derivative as a glucose sensing moiety, *Macromolecules* 37 (2004) 1502-1510.
9. H.G. Dennis, *Boronic acid*, Wiley-VCH Verlag GmbH & Co. KGaA (2005).
10. A.Y. Kwok, E.L. Prime, G.G. Qiao, D.H. Solomon, Synthetic hydrogels 2. Polymerization induced phase separation in acrylamide systems, *Polymer* 44 (2003) 7335-7344.
11. O. Okay, Phase separation in free-radical crosslinking copolymerization: formation of heterogeneous polymer networks, *Polymer* 40 (1999) 4117-4129.
12. H.M.J. Boots, J.G. Kloosterboer, C. Serbutoviez, F.J. Touwslager, Polymerization-induced phase separation. 1. Conversion-phase diagrams, *Macromolecules* 29 (1996) 7683-7689.
13. J.P. Montheard, M. Chatzopoulos, D. Chappard, 2-hydroxyethylmethacrylate HEMA; chemical properties and applications in biomedical fields, *J Macromol Sci Macromol Rev* 32 (1992) 1-34.
14. I. Cifkova, E. Brynda, V. Mandys, M. Stol, Irritation effects of residual products derived from p(HEMA) gels. *Biomaterials* 9 (1988) 372-375.
15. T.O. Garland, M.W. Patterson, Six cases of acrylamide poisoning, *BMJ* 4 (1967) 134-138.
16. H. Igisu, I. Goto, Y. Kawamura, M. Kato, K. Izumi, Y. Kuroiwa, Acrylamide encephaloneuropathy due to well water pollution, *J. Neurol Neurosurg Psychiatry* 38 (1975) 581-584.
17. A.S. Kuperman, Effects of acrylamide on the central nervous system of the cat, *J Pharmacol Exp Ther* 123 (1958) 180-192.
18. G. Lin, S. Chang, H. Hao, P. Tathireddy, M. Orthner, J. Magda, F. Solzbacher, Osmotic swelling pressure response of smart hydrogels suitable for chronically implantable glucose sensors, *Sensors and Actuators B: Chemical* 144 (2010) 332-336.

CHAPTER 5

IN SITU SYNTHESIS OF PH AND GLUCOSE SENSITIVE

HYDROGELS WITHIN MICROFABRICATED

SENSOR ARRAYS

5.1 Introduction

This chapter is concerned with the synthesis and characterization of pH sensitive hydrogels and glucose-sensitive hydrogels for a custom designed microfabricated sensor array. First of all, microfabricated sensor array construction is briefly introduced and proof-of-concept is demonstrated by showing results obtained by integrating pH-sensitive hydrogels with the sensor array and subjected the array to ionic strength variation tests. The incorporated pH-sensitive hydrogels were synthesized and preconditioned in the same manner as in chapter 2, and were not synthesized in situ. Attempts that were made to synthesize the hydrogel in situ within the microfabricated sensor array using the redox initiator system of chapters 2-4 are reviewed. Due to evaporation problems occurring during in situ polymerization, it was found to be necessary to switch to photoinitiation of the reaction, and this approach is discussed next. To assess the effect of the change in initiator system on the hydrogel response properties, comparison is made between results measured using the macrosensor between hydrogels synthesized by photoinitiator and by redox initiator. Thereafter, preliminary results are presented for response of the

microsensor array containing glucose sensitive hydrogels synthesized in situ on the microchip and subjected to glucose variation tests.

5.2 Microfabricated sensor array construction and ionic strength tests for pH sensitive hydrogels

5.2.1 Introduction

The data presented in this section have recently been published [1] and a brief summary of the work we have done will be presented here. As pointed out earlier in the introduction section, the objective of our research is to integrate smart hydrogels with a microfabricated piezoresistive sensor array to obtain biosensors for potential in vivo sensing applications. The sensing mechanism of the biosensor is the osmotic swelling pressure change of hydrogels in a confined state, as shown in Fig. 1.1. The work presented here is a demonstration of the proof-of-concept of such a sensor array in vitro. Ionic strength variation tests were performed to obtain all the data for the integrated sensor array. Although ionic strength variation tests may not be as physiologically significant as other tests such as pH or glucose variation tests, they are already well characterized from macrosized sensor tests (Chapter 2) and have fast response kinetics, making them ideal for preliminary sensor array characterization tests [1].

5.2.2 Sensor construction

The microfabricated piezoresistive sensor consists of three main components. Namely a square silicon sensor array contains four microsensors (2x2) used for the detection of hydrogel swelling pressure, four smart stimuli-responsive hydrogels in contact with the sensor diaphragms and a backing plate that holds the hydrogels in place.

The overall schematic illustration of the “chemomechanical sensors” that we have fabricated is shown in Fig. 5.1. Analyte diffusion paths to the hydrogel in the sensor array were obtained by either introducing pores into the backing plate or introducing pores directly into the piezoresistive diaphragms, as shown in Fig. 5.1. It should be noted that the former method (Fig. 5.1 (a)) has previously been employed to obtain hydrogel-based sensors for measurement of CO₂ concentration [2-5] and pH [6-9]. However, to our knowledge, no hydrogel containing sensors using perforated piezoresistive diaphragms (Fig. 5.1 (b)) have previously been reported. A perforated diaphragm has several advantages. First of all, the design of the pores such as pore size, shape and location can be used to manipulate the stress distribution within the diaphragm allowing the sensor to be tuned to a particular hydrogel [10]. In addition, a semipermeable diaphragm with appropriate pore size scale can be fabricated using a combination of potassium hydroxide (KOH) and deep reactive etching (DRIE) [1].

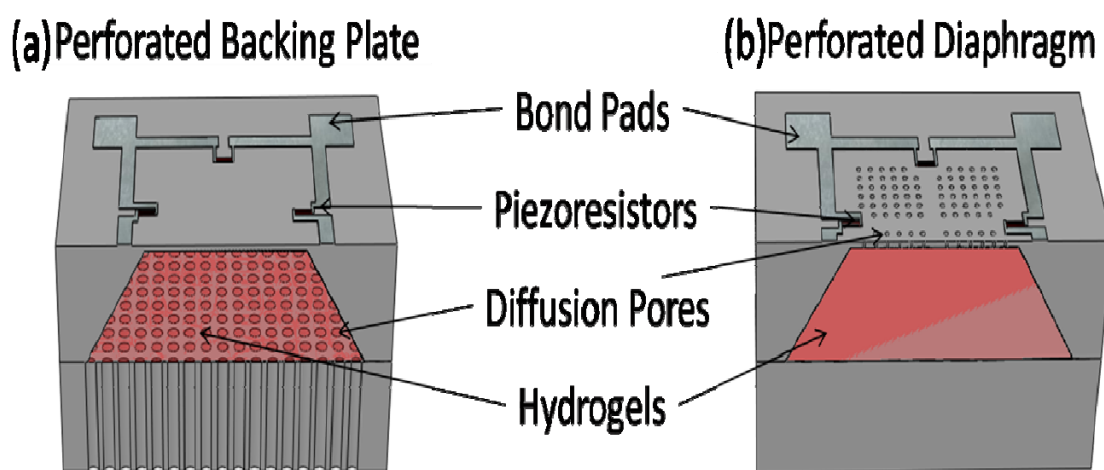


Fig. 5.1. Hydrogel based piezoresistive pressure sensor designs utilizing analyte diffusion pores that are located (a) within the backing plate that hold the hydrogel in place (b) within the piezoresistive diaphragm [1].

The sensor dies in the sensor array were fabricated with both solid and perforated square diaphragms with widths of 1.0, 1.0, 1.25, and 1.5 mm to measure hydrogel swelling pressure, as shown in Fig. 5.2. [1]. The 2x2 array measures approximately 5 mm x 5 mm, and the thicknesses of the diaphragms and the wafer are $15 \pm 3 \mu\text{m}$ and $400 \pm 15 \mu\text{m}$, respectively. Thus the cavity on the backside of the pressure sensor diaphragm has a depth of about $385 \mu\text{m}$. The synthesis, preconditioning, and thickness ($400 \mu\text{m}$) of pH-sensitive hydrogels inserted into the sensor array was the same as reported in chapter 2. After the synthesis and preconditioning, the hydrogels were stored in 0.15 M PBS buffer to ensure they were in a shrunken state before loading into the cavities in contact with the pressure sensor diaphragms in the array.

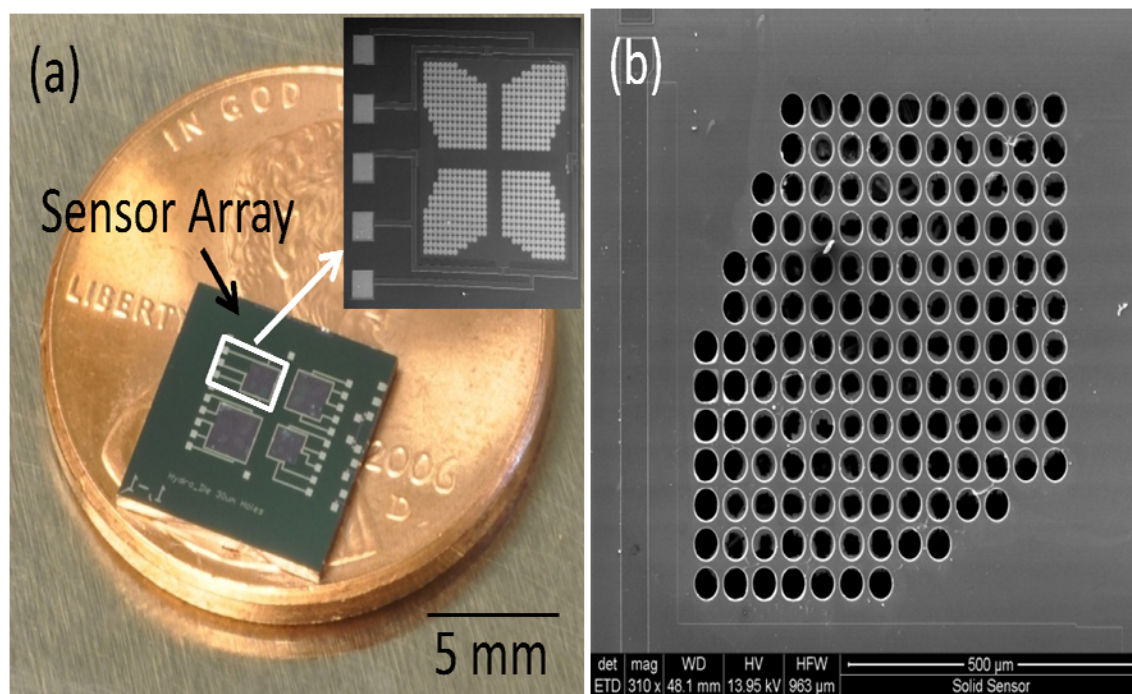


Fig. 5.2. (a) Photograph of perforated diaphragm pressure sensor array. Inset represents a scanning electron microscope (SEM) image of one of the 1mm x 1mm sensors. (b) SEM image showing the pores in the 1 mm x 1 mm sensor diaphragm [1].

The integration of pH-sensitive hydrogels into the sensor array was accomplished by cutting and trimming the hydrogels into squares of thickness $400\ \mu\text{m}$ with lateral dimensions of about $1\ \text{mm} \times 1\ \text{mm}$, $1.25\ \text{mm} \times 1.25\ \text{mm}$ and $1.5\ \text{mm} \times 1.5\ \text{mm}$ and then inserting the hydrogels into the corresponding sensor cavities on the backside of the pressure transducer diaphragms.

The last component of the sensor is the backing plate that holds the hydrogels in place. The backing plates have the same thickness as the wafer ($400 \pm 15\ \mu\text{m}$) and also measure $5\ \text{mm} \times 5\ \text{mm}$, the same lateral dimension as the sensor array, and thus can cover all four hydrogels on the backside of the pressure transducer diaphragms simultaneously. The backing plates were attached to the sensor array using silicone adhesive (NuSil MED 4211, Carpinteria, CA, USA) and allowed to cure for 48 h at room temperature before testing.

5.2.3 Experimental methods

After insertion of pH-sensitive hydrogels into the sensor array and the gluing of the backing plate, the sensor array was subject to appropriate wire bonding using insulated gold wires and sensor passivation using parylene C to give appropriate protection against salts for solution testing [1]. Thereafter, the sensor array was connected to a data acquisition unit (Agilent Technologies, Inc., 34970A, Santa Clara, CA) with the help of a pin latch connector soldered to a custom printed circuit board (PCB). Fig. 5.3 (a) shows the sensor array after wire bonding and parylene C coating that is ready for testing.

The testing solution used was phosphate buffer solution (PBS) at the physiological pH value of 7.4 and ionic strength varied from 0.025 to 0.15 M. The solution was placed

in a 100 ml plastic bottle and the sensor array was directly immersed into the plastic bottle during the test at room temperature without additional agitation, as shown in Fig. 5.3 (b). The data were recorded in real-time by a personal computer connected to the data acquisition system, as shown in Fig. 5.4. The ionic strength change was realized by rapid switching to another plastic bottle containing PBS solution with pH 7.4 and a different ionic strength.

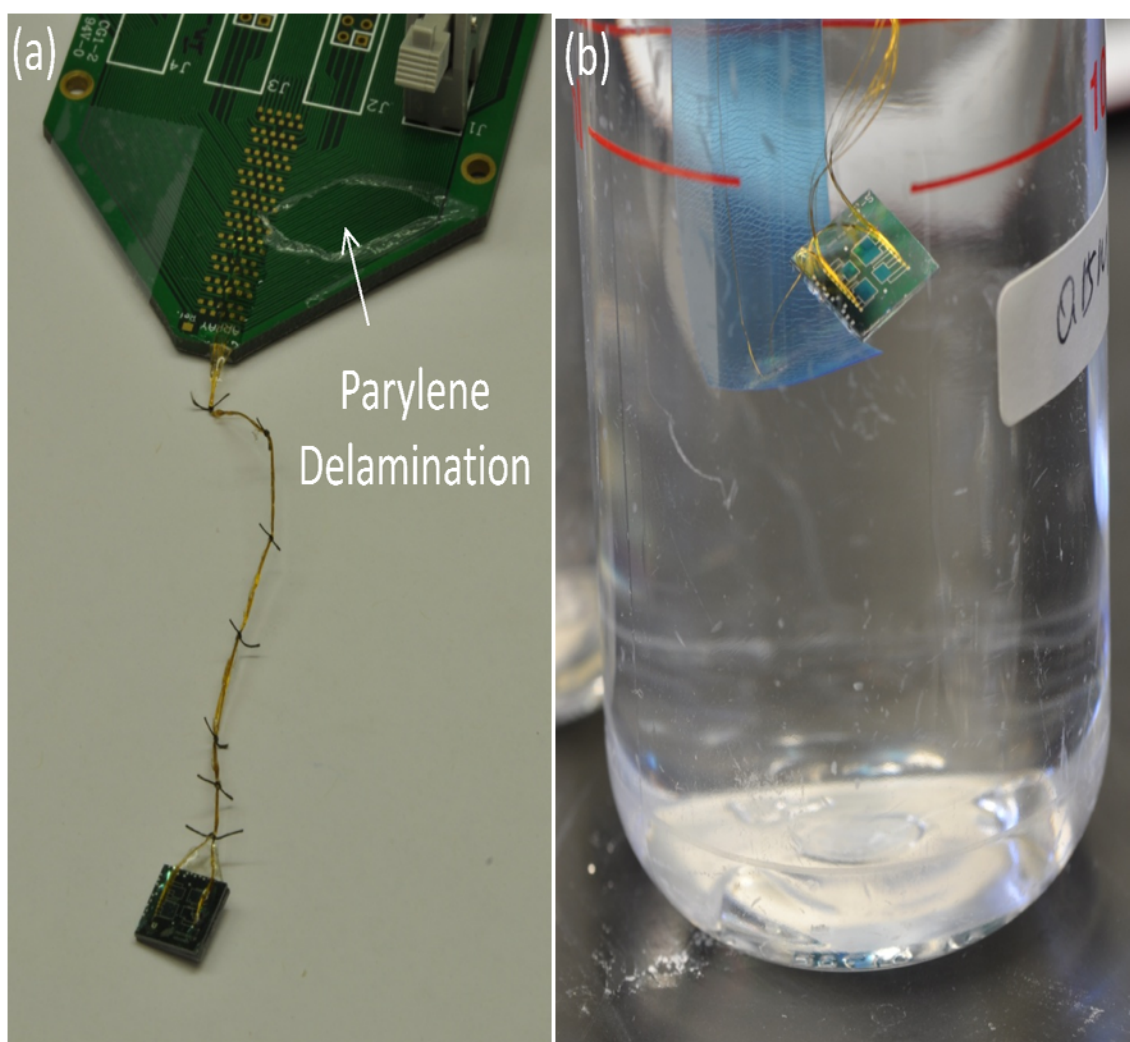


Fig. 5.3. (a) Photographs of sensor assembly after wire bonding and parylene C coating, with insulated wires sutured together to give extra strength and placed in (b) 100ml bottle with PBS buffer solution. Parylene delamination resulted from tape adhesion testing [1].



Fig. 5.4. Overview of the testing apparatus used to obtain sensor output characteristics. The sensor array was inserted into solutions of varying ionic strength and the output voltage signal was measured simultaneously [1].

5.2.4 Results

Ionic strength response tests were performed to assess the performance of the sensor array in vitro in PBS buffer with physiological pH 7.4 and differing ionic strengths. Fig. 5.5 shows the time-dependent voltage response of the four pressure transducer on a given chip with respect to ionic strength variations of PBS buffer for the two different sensor array designs. The first sensor array has a solid diaphragm and a perforated backing plate with pore size of $175\ \mu\text{m}$, open area of 60%, and thickness of $400\ \mu\text{m}$, as shown in Fig. 5.5 (a). The other sensor array has a solid backing plate and a perforated diaphragm with pore size of $40\ \mu\text{m}$, open area of about 64%, and thickness of $15\ \mu\text{m}$, as shown in Fig. 5.5 (b).

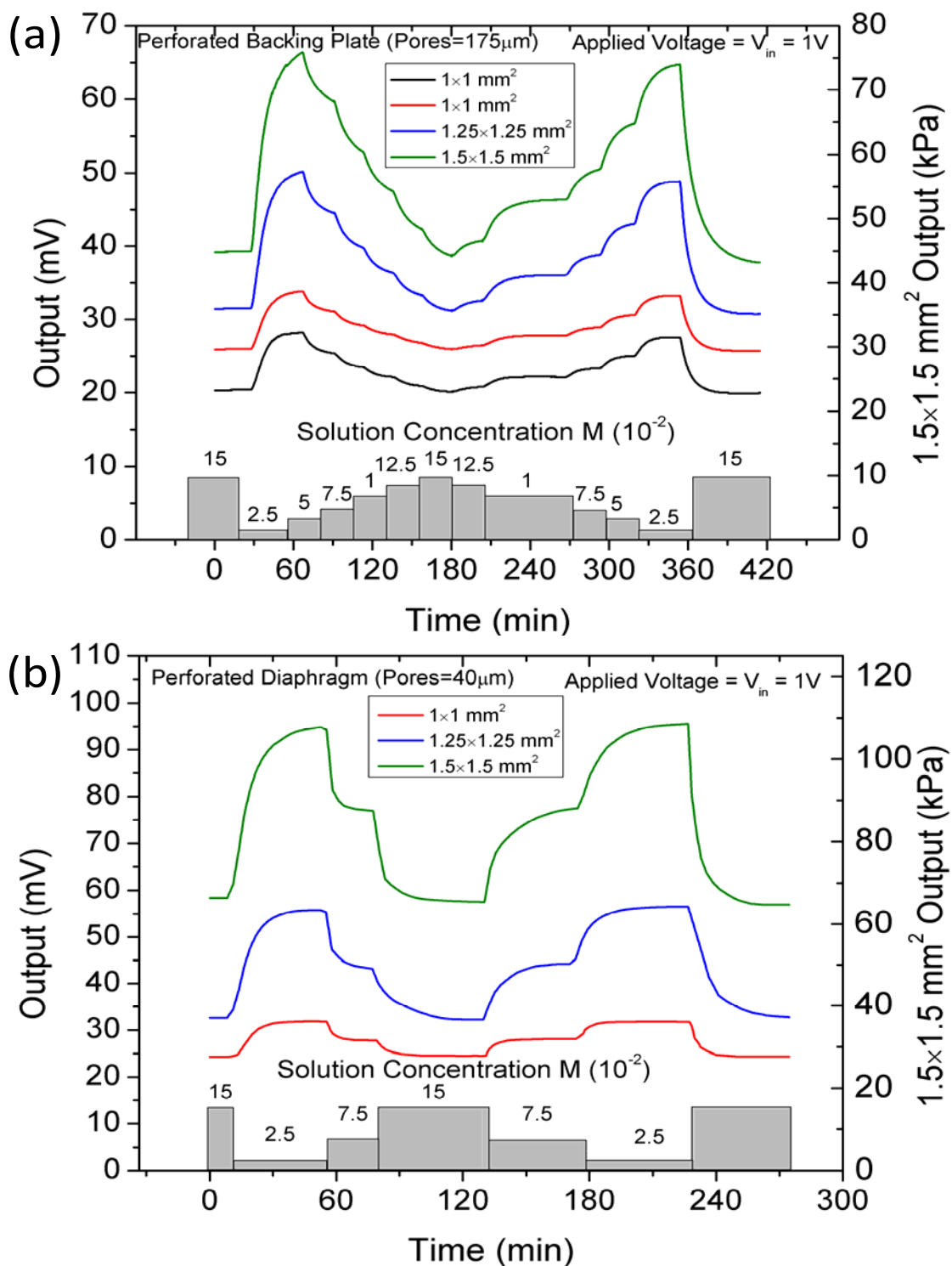


Fig. 5.5. Time dependent ionic strength variation response of the integrated sensor array with (a) solid diaphragm and perforated backing plate (b) perforated diaphragm and solid backing plate. The bar graph gives the time dependence of the ionic strength [1].

As seen in Fig. 5.5, both sensor arrays exhibit reversible response to ionic strength change. Meanwhile, the swelling trend is as expected, namely hydrogels within the sensor array swell at low ionic strength thereby increasing the voltage, and shrinks at high ionic strength thereby decreasing the voltage. Also notice in Fig. 5.5 that the pressure sensor with the largest diaphragm area (1.5 mm x 1.5 mm) has the highest sensitivity, probably because this diaphragm deflects more at a given hydrogel swelling pressure. Comparison of the sensitivity of the two types of sensor arrays in Fig. 5.5 shows that the perforated diaphragm sensors have a higher sensitivity than the solid diaphragm sensors. This higher sensitivity corresponds to higher stress induced in the perforated piezoresistive diaphragm which was designed in such a way to maximize stress within the diaphragm at a given hydrogel swelling pressure [10]. For the sensor with a perforated backing plate (pore size of 175 μm , open area of 60%) and a solid diaphragm size of 1.5x1.5 mm² (Fig. 5.5(a)), the sensitivity upon ionic strength change between 0.15 M and 0.025 M in PBS buffer at pH 7.4 is about 33 kPa, as opposed to the sensitivities of about 55 kPa to 69 kPa observed upon ionic strength change from 0.15 M to 0.05 M in PBS buffer at pH 7.4 (see chapter 2 Table 2.1) in macrosized sensor containing same pH-sensitive hydrogel with a similar porous backing plate (pore size of 178 μm , open area 31%). As compared to the macrosensor, the larger backing plate open area and more compliant diaphragm of the microsensor are responsible for the decreased sensitivity.

5.2.5 Conclusions

In this section, we have demonstrated that integrated sensor arrays could be used to reversibly measure ionic strength variation. Also, for the first time, we demonstrated the proof-of-concept of a novel pressure sensor design with a perforated piezoresistive

diaphragm for analyte diffusion. Further experiments are planned to incorporate glucose-sensitive hydrogels into the sensor array cavities intended for glucoses sensing, which would be more physiologically significant as it is an indicator of the disease diabetes. However, one major limitation of the results in this section is the way the hydrogels were incorporated into the sensor cavities; the hydrogels were synthesized, cut, trimmed and then finally inserted into the cavities. It would be ideal if one could synthesize the smart hydrogels in situ, which would better ensure complete filling of the sensor cavity and minimize human errors involved in insertion of the gels. The following sections of this chapter investigate the in situ synthesis of hydrogels in the microfabricated sensor array.

5.3 In situ synthesis using redox initiator systems

As stated previously, it is advantageous and desirable to synthesize the smart hydrogels in situ within the microfabricated sensor array. In situ synthesis will be the principle difference between the current microfabricated sensor array used to obtain the results in this section and the macroscale sensor (Fig. 1.5) employed to obtain the results in chapters 2-4. For macrosize sensor, the hydrogels were synthesized using redox initiators (APS+TEMED) between two square plates before transfer to the sensor using a biopsy punch and tweezers. For hydrogels synthesis between two square plates (area about 64 cm²), nitrogen gas purging was applied to the pregel solution prior to solution injection between the two square plates in order to remove oxygen which inhibits free radicals. Initial attempts were made to synthesize smart pH-responsive hydrogels in situ on the sensor chip using the redox initiator system. Two sets of redox initiator systems were used. The first set was ammonium persulfate (APS) and TEMED which is the same

as used in chapters 2-4, and the other was the combination of ammonium persulfate (APS) with sodium metabisulfite (SPS). The second initiator system was tried because it has been reported to be able to synthesize hydrogels in the presence of oxygen [10]. The synthesis protocols and results are noted below.

5.3.1 In situ hydrogel synthesis in the air

The stock solution of APS in DI water is 114.3 mg/20 ml and 95.1 mg/20 ml for SPS. To the pregel solution containing all the monomers HPMA/DMA/TEGDMA =70:30:2, appropriate amounts of initiator system stock solution, either APS plus TEMED or APS plus SPS, were added to the mixture. Right after mixing all the chemical components, the mixture was vortexed for several seconds before rapidly transferred to the cavities, about 1 μ L in volume, of an unassembled microfabricated piezoresistive sensor array. The experiments were conducted at room temperature and at ambient conditions.

5.3.2 Results and discussion

No hydrogels were formed in the sensor array cavities, the pregel solutions were still liquid in the cavities 24 h after reaction initiation. This result is mostly likely due to the presence of oxygen in the ambient air, because generally oxygen is a powerful inhibitor for radical polymerization as characterized by a very high inhibition constant Z value, which is defined as follows [12]

$$Z = k_z/k_p \quad (5.1)$$

where k_z and k_p are the rate constants for inhibition and propagation of the

polymerization, respectively. The inhibition mechanism of oxygen can be written as



Oxygen reacts with the active radicals ($M_n \cdot$) to produce the relatively stable peroxy radicals ($M_n - OO \cdot$) that react with themselves or with other propagating radicals through coupling and disproportionation reactions to form inactive products [3]. Sometimes, oxygen can act as initiator instead of inhibitor for the polymerization, however, this usually only occurs at high temperatures where the peroxides become unstable [12].

It is desirable to be able to carry out radical polymerization in the presence of oxygen [4]. Stringent removal of oxygen in the cavities of microfabricated sensor array is difficult, especially considering the high surface area to volume ratio of the microscale cavities. At least two studies have investigated the initiation of free radical polymerization in the presence of oxygen. Orakdogan et al. [11] reported that the redox initiator system SPS plus APS was able to initiate the free radical polymerization to obtain hydrogel in the presence of oxygen. Krzysztof et al. [13] introduced zerovalent metal copper to the system to control the radical polymerization in the presence of oxygen. At first glance these reports seem promising and encouraging as both methods described might be applicable to our in situ synthesis, but after careful scrutiny, it was recognized that both methods are applicable only to a sealed system. The underlying mechanism appears to be that either SPS or the zerovalent metal consumes the existing oxygen first before radical polymerization proceeds. In our synthesis, however, the sensor cavities were continuously exposed to the air and never sealed, thus no obvious polymerization occurred and no hydrogels were obtained.

In summary, oxygen is a strong polymerization inhibitor. Normally pregel solutions have to be purged with inert gas to strictly remove oxygen before polymerization. It is possible to initiate the polymerization and obtain hydrogel in the presence of oxygen, but a sealed system is required.

5.3.3 In situ synthesis in the glove box

In order to address the issue of oxygen contamination, subsequent experiments were performed in a glove box (about 1m³) purged with nitrogen. In this case, the APS plus TEMED redox initiator system was used for the synthesis of both pH and glucose sensitive hydrogels. The same synthesis procedures were followed as described in section 5.3.1, with the only difference being that in situ synthesis was performed inside a glove box instead of ambient air. As expected both pH and glucose-responsive hydrogels were obtained within the sensor cavities.

However, two problems were identified during the synthesis. First of all, it was observed that the pregel solution evaporated substantially, especially the glucose-sensitive hydrogel pregel solution, during the course of synthesis which is about 2 h. This results in sensor cavities incompletely filled with hydrogel and thus not expected to generate swelling pressure on the sensor diaphragm. Secondly, the transfer of the pregel solution to the sensor array cavities is challenging, because polymerization proceeds immediately after the mixing of APS with pregel solution at room temperature, and a finite time is required to transfer the pregel solution containing APS into the sensor cavity. Hence the pregel solution became too viscous to be pipetted into the cavities over the course of transfer.

These observed problems indicate that the use of a redox initiator system is not

ideal for in situ synthesis within a microfabricated sensor array. Therefore, we opt for photoinitiator system to accomplish in situ synthesis as discussed below.

5.4 Photopolymerization of pH sensitive hydrogels

As challenges and problems have been identified during the in situ synthesis of smart hydrogels employing redox initiator systems APS plus TEMED or SPS plus TEMED, a photoinitiation system was attempted for in situ synthesis. The advantages of using photopolymerization are ease of manipulation, very fast initiation rate, and on demand initiation or termination of polymerization by just turning on or off the UV light [12]. The photoinitiation system employed in this work consists of 2,2-Dimethoxy-2-phenylacetophenone and 1-Vinyl-2-pyrrolidinone. The combination of photoinitiator (2,2-Dimethoxy-2-phenylacetophenone) and electron donor (1-Vinyl-2-pyrrolidinone) was used to maximize the energy absorption and radical production [12]. Both chemicals were purchased from Sigma-Aldrich and were used as received.

5.4.1 Synthesis

The photoinitiation method followed here was the same as reported by West et al. [14]. Namely 600mg 2,2-Dimethoxy-2-phenylacetophenone were dissolved in 1 ml of 1-Vinyl-2-pyrrolidinone to obtain the photoinitiator system (600 mg/ml). The amount of photoinitiator system used was 40 $\mu\text{L}/\text{ml}$ of pregel solution. Polyelectrolyte pH sensitive hydrogels containing HPMA/DMA/TEGDMA at a nominal mole ratio of 70:30:2 were synthesized via free radical photopolymerization by irradiating with UV light (365 nm) for 5 min in the presence of the photoinitiator system (40 $\mu\text{L}/\text{ml}$). Hydrogel synthesis

were carried out in the macroscopic mold (thickness 400 μm) between two plates (one glass and one plastic), with UV light transmitted through the glass plate. Concurrently, hydrogel synthesis was performed in the cavities of an unassembled microfabricated sensor array, with UV light applied from the top of the sensor array for 5 min. Both experiments were performed under ambient conditions outside a glove box.

5.4.2 Results

Encouragingly, it was observed that pH-sensitive hydrogels were obtained in the cavities of the unassembled microfabricated sensor chip. This indicated that photopolymerization is feasible for in situ synthesis for microfabricated sensor arrays.

Prior to in situ synthesis in an assembled microfabricated sensor array, pH-sensitive hydrogel synthesized by photopolymerization between two macroscopic plates were tested with the macrosized sensors of chapters 2-4. The tests in the macrosized sensor were performed to ensure that the change in synthesis technique to photopolymerization still yield smart hydrogels responsive to ionic strength change and pH change. The testing procedures for hydrogel in the macrosized sensor are basically the same as described in chapter 2. Briefly, after the hydrogels were detached from the plates, they were kept in 0.15 M PBS buffer solution for about 2 h before subjecting to cyclic ionic strength change testing. The results obtained are shown in Fig. 5.6, where complex response curves are observed, but certain trends do arise. These irregular patterns might be due to the fact that the hydrogels were not preconditioned by DI water and several cycles of cyclic ionic strength change. The ionic strength response between 0.15 M and 0.05 M is obvious in Fig. 5.6, where higher ionic strength leads to hydrogel deswelling, but the magnitude of change upon ionic strength is unexpectedly small.

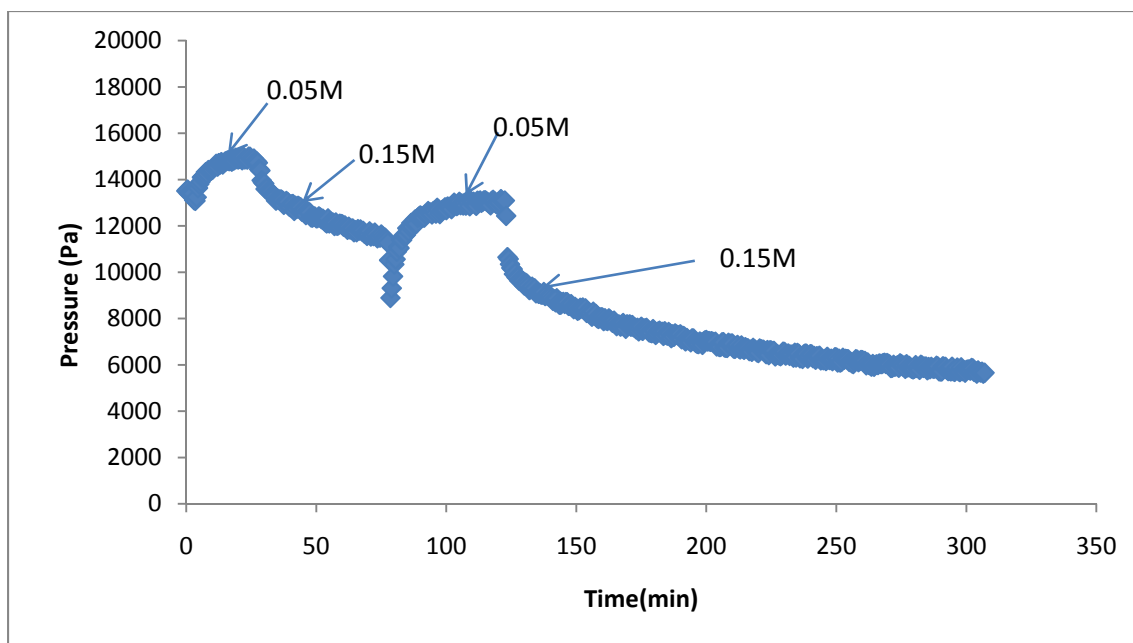


Fig. 5.6. Ionic strength response of macrosize sensor obtained using photopolymerized pH sensitive hydrogel containing HPMA/DMA/TEGDMA (70:30:2) subjected to ionic strength changes between 0.15 M and 0.05 M in PBS buffer at pH 7.4 without hydrogel preconditioning.

This small change of magnitude upon cyclic ionic strength change is most likely due to the lack of preconditioning. After the tests giving the results shown in Fig. 5.6, the hydrogel was kept in PBS for another two days before the testing of Fig. 5.7. Comparing Fig. 5.7 with Fig. 5.6, one observes a sharp contrast in terms of sensor sensitivity in identical ionic strength tests, with a much higher sensitivity observed in Fig. 5.7. This further confirms the impact of hydrogel preconditioning on the ionic strength response of the hydrogels. However, in Fig. 5.7, the ionic strength response is not completely reversible; this behavior might be due to hydrogels that were still not thoroughly preconditioned. In Fig. 5.7, swelling half time for the swelling and deswelling half-cycles is 9 min and 7 min, respectively. This is comparable to the hydrogels synthesized from redox initiator system, at least for the swelling half cycle.

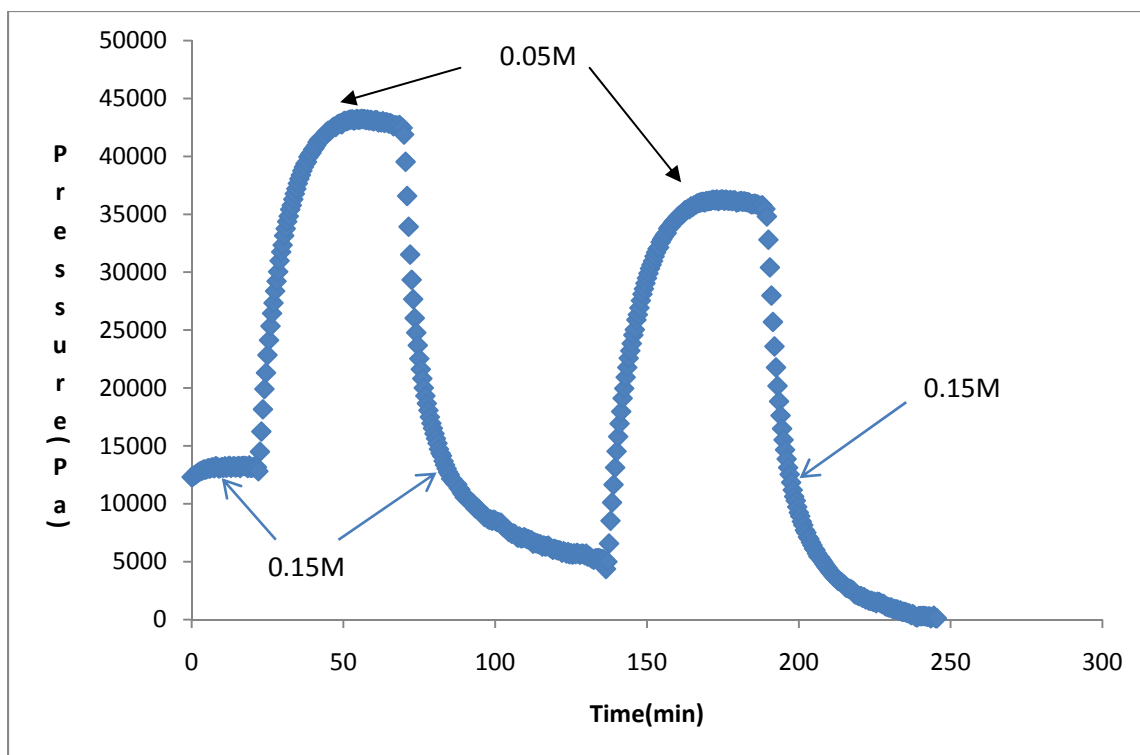


Fig. 5.7. Ionic strength response of macrosize sensor containing photopolymerized pH-sensitive hydrogels having the same composition as in Fig. 5.6 subjected to cyclic ionic strength change between 0.15 M and 0.05 M in PBS buffer after preconditioning with two cycles of ionic strength change between 0.15 M and 0.05 M in PBS buffer and 2 days immersion in PBS 0.15 M.

5.4.3 Conclusions

The results indicate that pH-sensitive hydrogels were successfully synthesized in situ in the microfabricated sensor array via photopolymerization using UV 365 nm for 5 min. Meanwhile, after certain period of preconditioning, UV photopolymerized hydrogels in the macrosize sensor exhibit comparable ionic strength response as hydrogels synthesized via the redox initiator system, namely APS plus TEMED. As seen in Fig. 5.6 and Fig. 5.7, preconditioning has a significant effect on ionic strength response, indicating preconditioning is necessary before one can obtain a stable response. Cyclic ionic strength changes might help to accelerate the cleaning process and shorten

preconditioning time. These results suggest that one should not be surprised if during the first several cycles, the gels were not that responsive to ionic strength changes for an assembled sensor chip containing in situ photopolymerized hydrogels.

5.5 Photopolymerization of glucose sensitive hydrogel

5.5.1 Synthesis

600 mg 2,2-Dimethoxy-2-phenylacetophenone were dissolved in 1 ml of 1-Vinyl-2-pyrrolidinone to obtain the photoinitiator system (600 mg/ml). Glucose sensitive hydrogels containing 3-APB/DMAPAA/AAM/BIS at a nominal mole ratio of 8:10:80:2, with pregel monomer concentration of 12.7 wt%, were synthesized via free radical solution photopolymerization induced by exposure to UV light (365 nm) for 5 min in the presence of the photoinitiator system (40 μ L/ml). In brief, after mixing the photoinitiator into the pregel solution, the mixture was purged with nitrogen gas for about 8 min. A micropipette was used to transfer appropriate amounts of pregel mixture solution to unassembled sensor cavities. Soon after, UV light (365 nm) was applied for 5 min to the sensor cavities containing pregel solution. It was observed that hydrogels were formed inside the cavities after 5 min exposure to UV light at ambient conditions. Unfortunately, evaporation of the pregel solution was also significant and the hydrogel did not completely fill the cavities, even though the reaction time was only 5 min, presumably because UV irradiation increased the temperature and hence the rate of water evaporation. In order to reduce pregel solution evaporation during polymerization, it was decided to further reduce the reaction time. This reduction in reaction time can be achieved by performing the photopolymerization inside a glove box purged with nitrogen. Indeed, 1 min was found to be enough for hydrogel polymerization within the sensor

cavities inside a glove box. More importantly, no significant evaporation was observed and the sensor cavities appeared to be fully filled with hydrogel. In order to further reduce the effects of evaporation, a higher monomer concentration in the pregel solution (20 wt%) with the same mole ratio of 3-APB/DMAPAA/AAM/BIS was employed for the synthesis of glucose sensitive hydrogels. Hydrogels synthesized from a higher pregel monomer concentration are expected to be less affected by evaporation during polymerization with enhanced mechanical properties.

As a check on the properties of the glucose-sensitive hydrogels (GSHs) synthesized in situ on the microfabricated sensor chips, glucose sensitive hydrogels containing 3-APB/DMAPAA/AAM/BIS at a nominal mole ratio of 8:10:80:2, with monomer pregel solution concentration of either 12.7 wt% or 20 wt% were also photopolymerized for 10 min in the macroscopic cavity (thickness 400 μ m) between two plates (polycarbonate and glass) at ambient conditions. The GSHs were detached from the two plates, washed with DI water for one day and then stored in 0.15 M PBS buffer for one day. Subsequently, the gels were subjected to two cycles of ionic strength changes between 0.15 M and 0.05 M PBS in order to further clean the hydrogels. Thereafter the hydrogels were stored in 0.15 M PBS until testing.

5.5.2 Results and discussion

Glucose sensitive hydrogels (GSHs) synthesized between two macroscopic plates were incorporated into the macrosized sensor and subjected to glucose concentration variations between 0 to 5 mM in 0.15 M PBS buffer. The results obtained are shown in Fig. 5.8, where a reversible glucose response between concentration of 0 and 5 mM is observed. The magnitude of hydrogel swelling pressure response induced by 5 mM

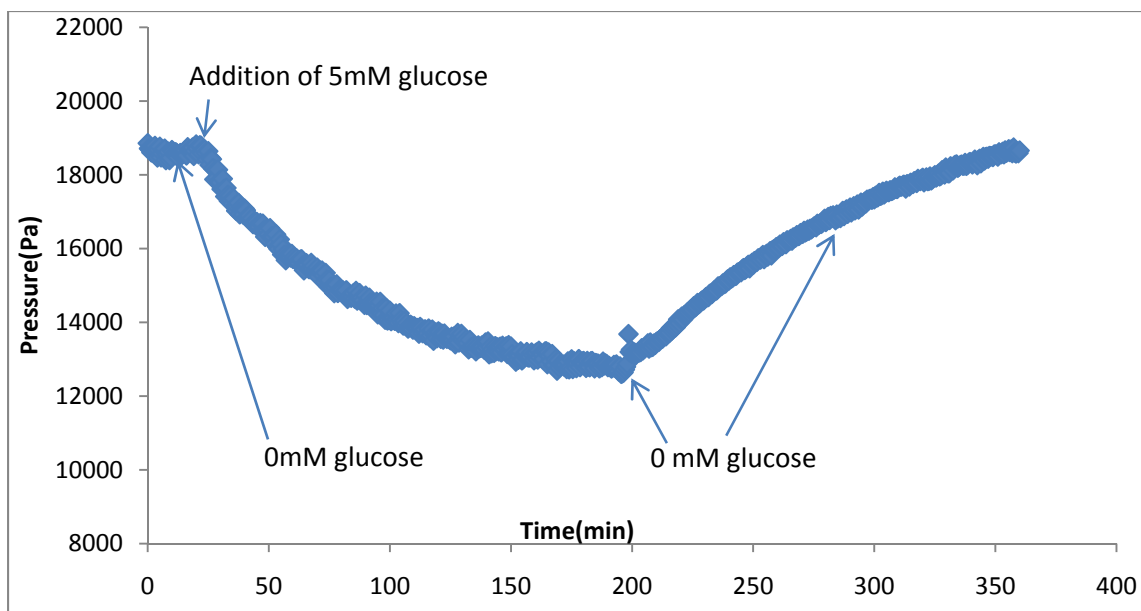


Fig. 5.8. Response of macrosize sensor containing photopolymerized GSH (8:10:80:2) with 12.7 wt% monomer pregel concentration subjected to 5mM glucose reversibility test (first cycle of Fig. 5.9) in 0.15 M PBS at pH 7.4.

glucose increase is about 5.7 kPa as compared to 9 kPa (see chapter 3 Fig. 3.2) obtained from similar GSH with the same mole ratio and pregel monomer concentration synthesized by redox initiator systems (APS plus TEMED). It should be noted that Fig. 5.8 represents the first cycle of Fig. 5.9. However, as shown in Fig. 5.9, subsequent cycles showed an improved sensitivity. For instance, the deswelling magnitude values for the second and third cycle are 8.8 kPa and 7.7 kPa, respectively, which are comparable to the 9 kPa reported earlier in chapter 3. In addition, the average deswelling first-order-time constants in Fig. 5.9 is about 58 ± 14 min, also comparable to 60 ± 15 min reported in chapter 3. One also observes in Fig. 5.9 that the baseline drifts over time, which may affect sensor sensitivity as well. Generally speaking, glucose sensitive hydrogels synthesized by either photoinitiator system or redox initiator system exhibit comparable 5 mM glucose responses.

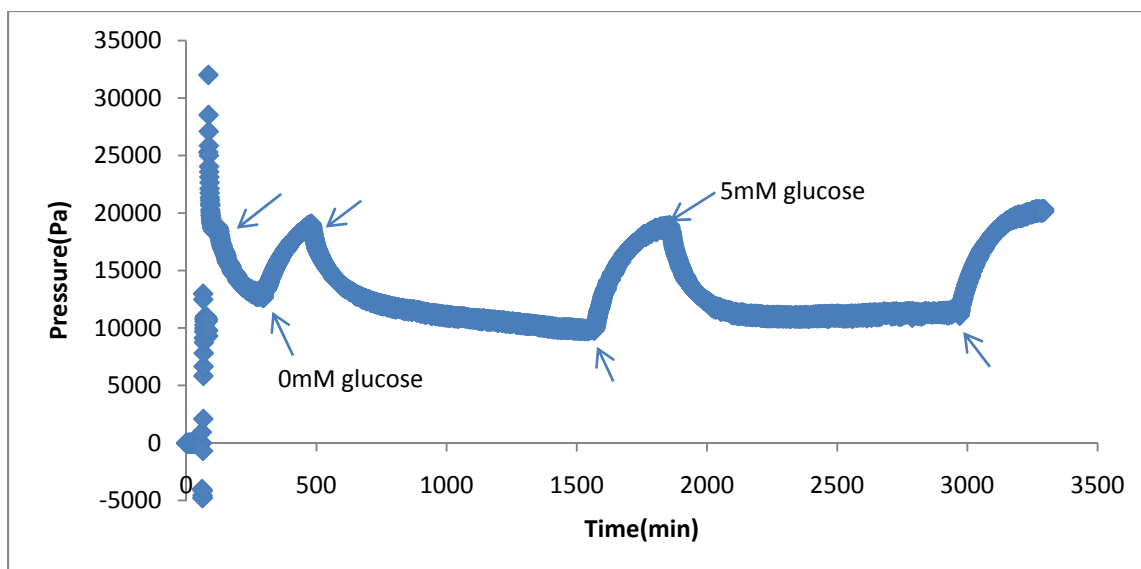


Fig. 5.9. Response of macrosize sensor containing photopolymerized GSH (8:10:80:2) with 12.7 wt% monomer pregel concentration subjected to three cycles of 5 mM glucose concentration change in 0.15 M PBS at pH 7.4. The upper arrows indicate the time when 5 mM glucose was applied, and the lower arrows indicate the time glucose concentrations were switched to 0 mM.

Hydrogels of the same nominal monomer mole ratio but with 20 wt% monomer pregel concentration were also photopolymerized in the macroscopic mold and subjected to 5 mM glucose reversibility tests. The results obtained are shown in Fig. 5.10. As seen in Fig. 5.10, the response is not that stable, with a sudden pressure drop observed in the second cycle due to switching in which the sensor has to be pulled out of the bath containing 5 mM glucose and inserted into another bath containing 0 mM glucose. However, the comparison of the sensitivity between the last deswelling cycle in Fig. 5.10 and the third deswelling cycle in Fig. 5.9 (both in response to increase from zero to 5mM glucose) indicates that both hydrogels synthesized using monomer pregel concentration of 20.0 wt% and 12.7 wt% exhibit comparable sensitivity, with sensitivities of 8.4 kPa and 7.7 kPa, respectively; but exhibit different response kinetics, with first-order-time constants of 139 min and 72 min, respectively.

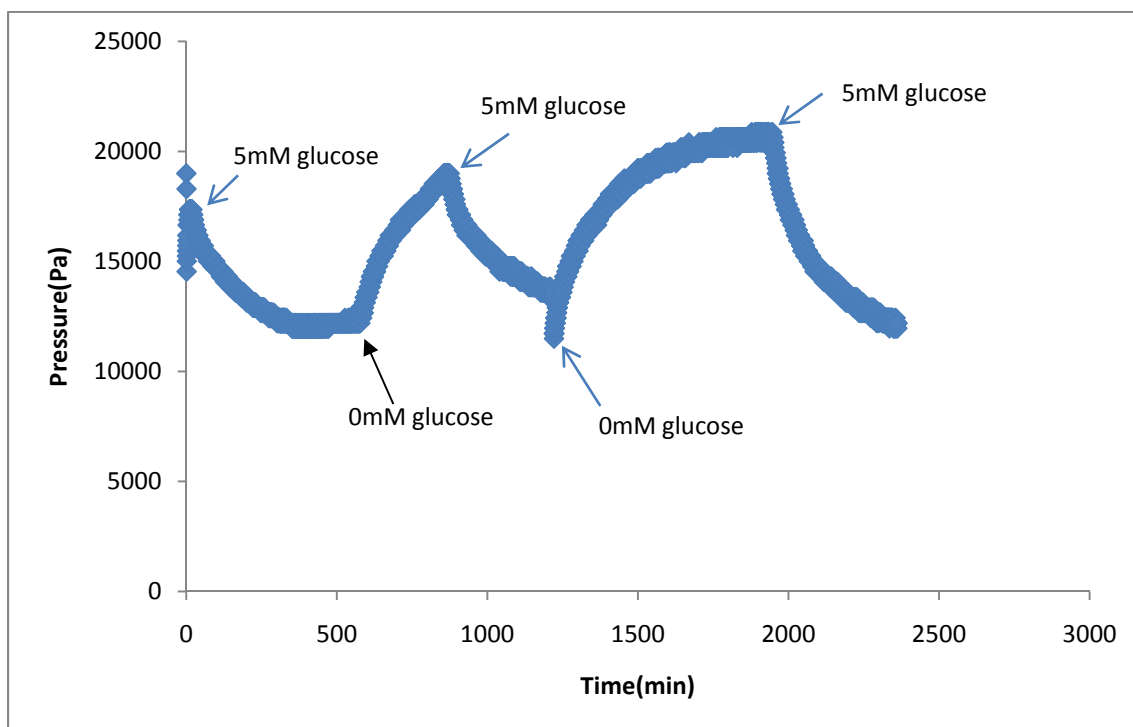


Fig. 5.10. Response of macrosized sensor containing photopolymerized GSH (8:10:80:2) with 20 wt% monomer pregel concentration subjected to 5 mM glucose concentration changes in 0.15 M PBS at pH 7.4. The arrows indicate the time when 5 mM or 0 mM was applied.

Since the glucose sensitive hydrogels synthesized from 20 wt% monomer concentration exhibit comparable sensitivity as that of 12.7 wt%, and yet should have better mechanical strength, this 20 wt% composition was used for the in situ synthesis of glucose-sensitive hydrogels in the four cavities of an assembled microfabricated sensor array. The array pressure sensors had a solid diaphragm and a perforated backing plate with a pore size of $175\ \mu\text{m}$, an open area of 60%, and a thickness of $400\ \mu\text{m}$. After in situ hydrogel synthesis within the sensor array chip in the glove box, glucose response tests for the integrated sensor array were performed in 0.15 M PBS buffer at physiological pH 7.4. The results obtained are shown in Fig. 5.11 and Fig. 5.12.

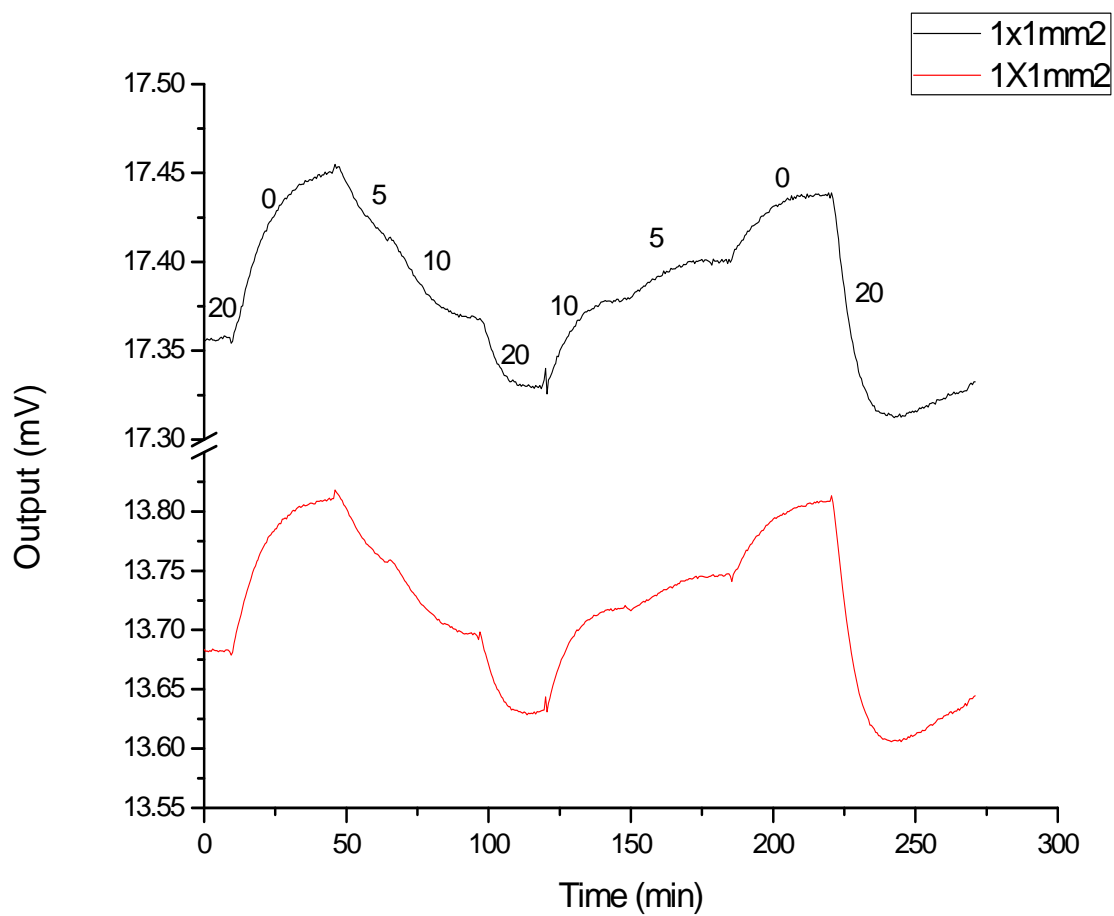


Fig. 5.11 Time dependent glucose response for the integrated sensor array (two sensors with diaphragms size of $1 \times 1 \text{ mm}^2$) containing in situ photopolymerized glucose sensitive hydrogels. The numbers in the plot represent the glucose concentrations (mM) in 0.15M PBS buffer at pH 7.4.

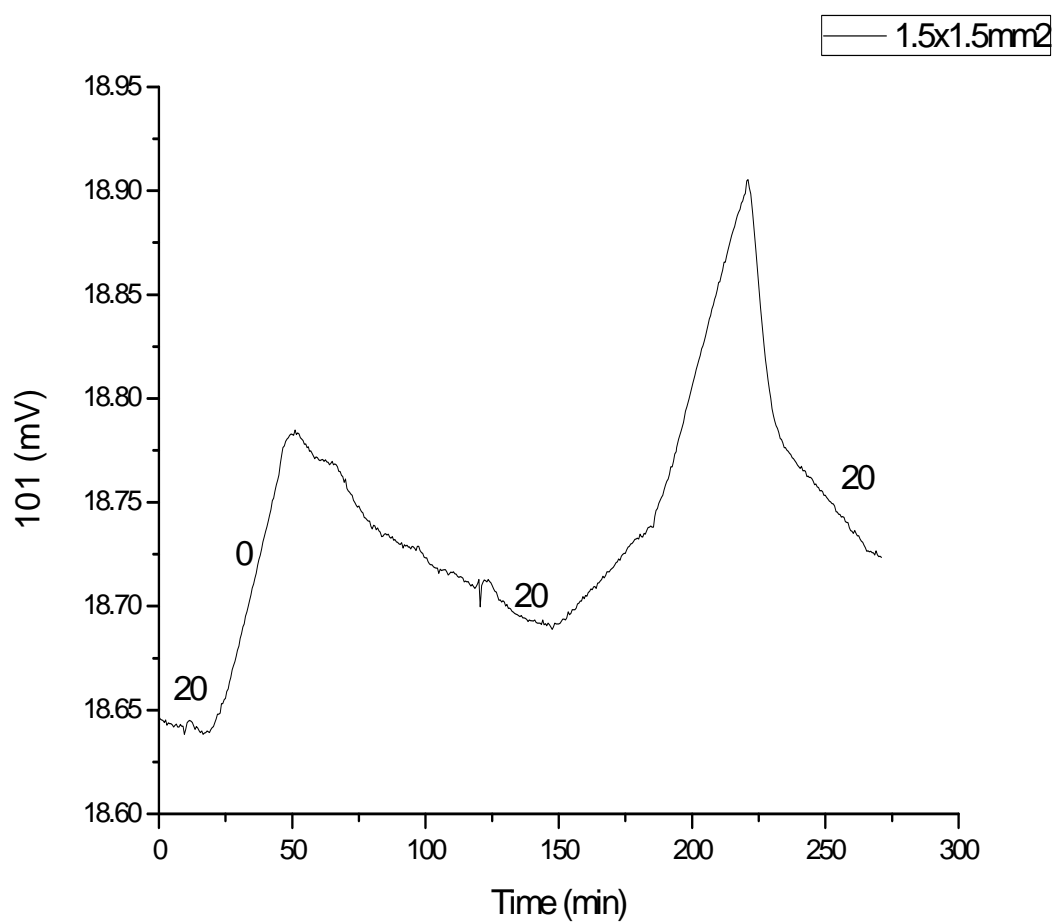


Fig. 5.12 Time dependent glucose response for the integrated sensor array (sensor with diaphragm size of $1.5 \times 1.5 \text{ mm}^2$) containing in situ photopolymerized glucose sensitive hydrogel. Data were taken simultaneously with the data of Fig. 5.11 under the same conditions.

In this sensor array, three out of four sensors were working. Fig. 5.11 contains the results from the two smallest sensors of the sensor array with widths of $1 \times 1 \text{ mm}^2$. As seen in Fig. 5.11, the tests started out with 20 mM glucose, then the glucose concentration was changed to 0 mM and an increase in output signal voltage (mV) was observed. After equilibrium was reached in 0 mM glucose at time around 45 min, glucose concentrations were step-wise increased to 5 mM, 10 mM and 20 mM. Subsequently the glucose concentration was step-wise decreased to 10, 5, and 0 mM, and the sequence concluded with glucose concentration change from 0 mM to 20 mM. One notices that the output signal increases with decreasing glucose concentration, indicating that the hydrogel swells due to the breaking of the reversible glucose crosslinks. Fig. 5.12 contains the glucose response data recorded simultaneously as the data of Fig. 5.11 but obtained from the largest sensor with a diaphragm of $1.5 \times 1.5 \text{ mm}^2$. One observes that this larger sensor exhibit slower kinetics than the sensors noted in Fig. 5.11. This discrepancy in response time occurs presumably because the diaphragm of the larger sensor deflects more at a given swelling pressure. The larger extra space available in the larger diaphragm of the sensor due to more deflection of diaphragm results in longer response time as hydrogels have to expand and fill the extra space before the equilibrium is reached.

One might argue that response observed in Fig. 5.11 and Fig. 5.12 is caused by the osmotic effect of the glucose on the water surrounding the sensor, rather than from glucose-mediated hydrogen crosslinking. If so, any analyte would give a decreasing output signal with increasing analyte concentration due to the osmotic effect. To disprove this argument, 5 mM fructose tests were performed and the data are shown in Fig. 5.13. As observed in Fig. 5.13, the sensor output signal increases with increasing fructose

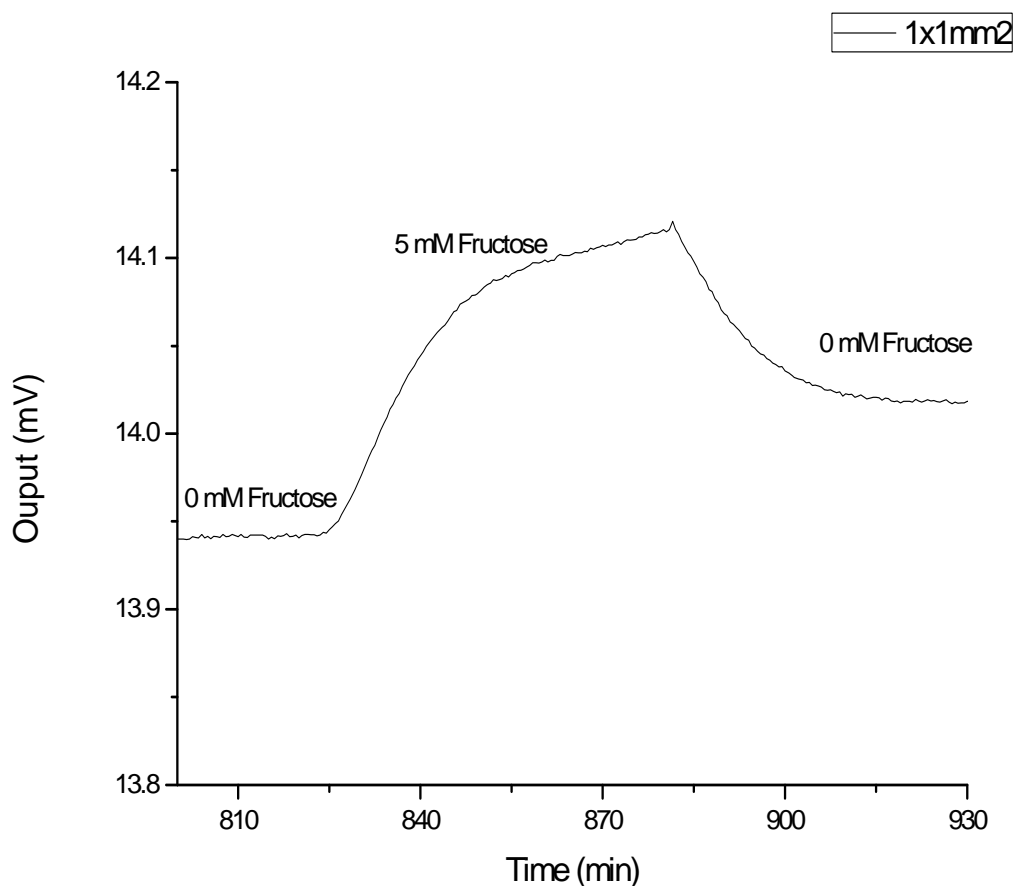


Fig. 5.13. Time dependent fructose response test results for the integrated sensor array (sensor diaphragm size 1x1 mm²) containing in situ photopolymerized glucose sensitive hydrogels.

concentration from 0 to 5 mM in PBS buffer at physiological pH 7.4 and ionic strength 0.15 M. This observed result is consistent with the results reported in chapter 4 where a similar glucose sensitive hydrogel (same mole ratio but with 12.7 wt% pregel monomer concentration) also swells with increasing fructose concentration from 0 to 5 mM. Therefore, glucose-mediated hydrogel crosslinking must be responsible for the decreased signal with increasing glucose concentration observed in Fig. 5.11, Fig. 5.12, and in chapter 4.

5.6 Conclusions

Glucose sensitive hydrogels (GSHs) were successfully synthesized by free radical photopolymerization both in situ within the microfabricated sensor array cavities and in between two macroscopic plates separated by a spacer. The GSH obtained shrinks with increasing glucose concentration as indicated by a decrease in hydrogel swelling pressure and exhibits a reversible glucose response. For the GSH in the macrosized sensor the sensitivity appears to be increasing with cycle number, perhaps because more preconditioning time and cycles of ionic strength change are necessary for photopolymerized GSH. In addition, GSH tests using the macrosized sensor indicate that a comparable glucose response magnitude and response kinetic are observed for GSHs synthesized by either photoinitiator or redox initiator. Therefore, photopolymerization is a better approach for synthesizing GSHs in situ since polymerization time is smaller and manipulation of the pregel solution into the sensor cavities is easier. Significantly, a microfabricated sensor array containing in situ photopolymerized glucose sensitive hydrogels (GSHs) exhibits a reversible response to glucose concentration changes. However, the integrated microfabricated sensor array suffers from a baseline drift over the course of testing, which would compromise the sensor performance. This baseline drift can probably be rectified by improving the encapsulation of the sensor array, because breaks in the encapsulation may lead to current leakage and result in baseline drift [15]. The preliminary data presented herein demonstrated the successful in situ synthesis of pH sensitive hydrogels and glucose sensitive hydrogels. This in situ photopolymerization procedure will be employed in future studies to assess the performance of the integrated sensor array in serum/plasma and in vivo.

5.7 References

1. M.P. Orthner, G. Lin, M. Avula, S. Buetefisch, J. Magda, L.W. Rieth, F. Solzbacher, Hydrogel based sensor arrays (2x2) with perforated piezoresistive diaphragms for metabolic monitoring (in vitro), *Sensors and Actuators B: Chemical*. 145 (2010) 807-816.
2. S. Herber, J. Bomer, W. Olthuis, P. Bergveld, and A. v. d. Berg, A Miniaturized Carbon Dioxide Gas Sensor Based on Sensing of pH-Sensitive Hydrogel Swelling with a Pressure Sensor, *Biomedical Microdevices*. 7 (2005) 197-204.
3. S. Herber, W. Olthuis, P. Bergveld, and A. van den Berg, Exploitation of a pH-sensitive hydrogel disk for CO₂ detection, *Sensors & Actuators: B. Chemical*. 103 (2004) 284-289.
4. S. Herber, W. Olthuis, and P. Bergveld, A swelling hydrogel-based PCO₂ sensor, *Sensors and Actuators B: Chemical*. 91 (2003) 378-382.
5. R. ter Steege, S. Herber, W. Olthuis, P. Bergveld, A. van den Berg, and J. Kolkman, Assessment of a new prototype hydrogel CO₂ sensor; comparison with air tonometry, *Journal of Clinical Monitoring and Computing*. 21 (2007) 83-90.
6. G. Gerlach, M. Guenther, J. Sorber, G. Suchaneck, K. F. Arndt, and A. Richter, Chemical and pH sensors based on the swelling behavior of hydrogels, *Sensors & Actuators: B. Chemical*. 111 (2005) 555-561.
7. Q. Thong Trinh, G. Gerlach, J. Sorber, and K. F. Arndt, Hydrogel-based piezoresistive pH sensors: Design, simulation and output characteristics, *Sensors and Actuators B: Chemical*. 117 (2006) 17-26.
8. J. Sorber, G. Steiner, V. Schulz, M. Guenther, G. Gerlach, R. Salzer, and K.-F. Arndt, Hydrogel-Based Piezoresistive pH Sensors; Investigations Using FT-IR Attenuated Total Reflection Spectroscopic Imaging, *Analytical Chemistry*. 80 (2008) 2957-2962.
9. A. Richter, G. Paschew, S. Klatt, J. Lienig, K. F. Arndt, and H. J. P. Adler, Review on Hydrogel-based pH Sensors and Microsensors, *Sensors*. 8 (2008) 561-581.
10. M. Orthner, L. Rieth, S. Buetefisch, F. Solzbacher, Design, simulation and optimization of a novel piezoresistive pressure sensor with stress sensitive perforated diaphragm for wet sensing and hydrogel applications, *IEEE Sensors* (submitted).
11. N. Orakdogan, O. Okay, Influence of the initiator system on the spatial inhomogeneity in acrylamide-based hydrogels, *Journal of Applied Polymer Science* 103 (2007) 3228-3237.

12. G. Odian, Principles of Polymerization, fourth ed., John Wiley & Sons, Inc. New Jersey, 2004.
13. K. Matyjaszewski, S. Coca, S.G. Gaynor, M. Wei, B.E. Woodworth, Controlled radical polymerization in the presence of oxygen”, *Macromolecules* 31 (1998) 5967-5969.
14. B.K. Mann, A.S. Gobin, A.T. Tsai, R.H. Schmedlen, J.L. West, Smooth muscle cell growth in photopolymerized hydrogels with cell adhesive and proteolytically degradable domains: synthetic ECM analogs for tissue engineering, *Biomaterials* 22 (2001) 3045-3051.
15. M. Orthner, Ph.D Thesis, University of Utah, 2010.

CHAPTER 6

CONCLUSIONS AND FUTURE DIRECTIONS

6.1 Conclusions

Motivated by the limitations of current glucose sensing technology, the long term goal of this thesis research was the development of a chemomechanical sensor array based on smart hydrogels that is suitable for subcutaneous implantation and is able to measure the values of pH and glucose on a long-term basis for diabetic patients. Based on data presented in this thesis, the following conclusions were obtained:

1. Using commercially-available monomers, polyampholytic glucose-sensitive hydrogels (GSHs) can be synthesized that can be combined with piezoresistive pressure sensors to give chemomechanical sensors with equilibrium swelling pressure response that are large enough for diabetes control applications and that are selective for glucose over fructose at typical physiological concentrations.
2. For acrylamide based GSHs, the best composition studied was 3-APB:DMAPAA:AAM:BIS = 8:10:80:2. For this composition, the osmotic swelling pressure response to a glucose change from 0 to 5 mM is a decrease in pressure of 9 kPa, with a sensing range of 0-20 mM glucose. A macrosized chemomechanical sensor containing this GSH (hydrogel thickness 400 μm) obeys first order kinetics with a time constant of 75 ± 15 min for swelling and 60 ± 15 min for deswelling.

3. The polyampholytic GSHs exhibit an isoelectric point (IEP) at which the effect of pH on the glucose-dependent swelling pressure response is minimized, and at which anti-polyelectrolyte behavior is observed. However, gel response kinetics is slower at the IEP. The IEP can be manipulated by varying the monomer ratio of 3-APB to DMAPAA.
4. GSHs of the same type can be UV-polymerized in situ on custom-designed pressure sensor chips to obtain microchip glucose sensors of sensing area 1 mm by 1 mm. The best microchip glucose sensor so obtained had a response time of about 20 min and covered a sensing range of at least 0-20 mM glucose. Photopolymerization using photoinitiator is more advantageous over thermal polymerization using redox initiator for the hydrogel in situ synthesis in the microfabricated sensor array cavities.
5. Comparing the response behavior of thermally and UV cured GSHs, one finds that the response kinetics and sensitivities are comparable.
6. GSH can also be synthesized with replacement of potentially toxic acrylamide (AAM) monomers with more benign methacrylate (HEMA) monomers. Comparing the properties of AAM-based and HEMA-based GSHs, one finds that HEMA-based GSHs are more responsive to glucose at high glucose concentration, with much slower response kinetics than AAM based GSHs. The equilibrium water content is higher for AAM-based GSHs than HEMA-based GSHs. In addition, both types of GSHs fit first order model kinetics at low glucose concentration. At high glucose concentration, however, only AAM based GSHs follow first order model kinetics.
7. For GSH containing lower equilibrium water content subjected to large increases in environmental glucose concentration, highly unusual response kinetics are observed,

in which the swelling pressure decreases in a two-step process. The two-step process is probably caused by the formation of a low permeability skin layer due to a large glucose-mediated crosslinking density gradient along the surface of the hydrogel.

6.2 Future directions

Glucose and ionic strength response tests in this thesis were primarily performed for proof-of-concept, and are not representative of the benchmarks that should be satisfied by a successful implantable glucose sensor. According to a well-known expert in the field of glucose sensing [1], a successful implantable glucose sensor should: (1) have a glucose sensing range of 0 to 20 mM; (2) have a glucose sensitivity of ± 0.5 mM or better; (3) have a response time of 5 min or less; (4) have an oxygen-independent signal, (5) have a glucose signal that is only slightly altered (no more than 0.5 mM) by physiological amounts of endogenous interferants such as ascorbate, fructose, etc. In addition, when Clarke error grid analysis is applied to in vivo tests, at least 98% of the sensor measurements should fall in zone A and B [1]. For a chronic sensor, we have to add the requirement that the sensor is stable for at least 30 days. Also, variations of ionic strength and pH in the typical physiological range, 145-155 mM and 7.2-7.4, respectively, should change the apparent glucose signal by 0.5 mM or less. Therefore, in order to meet these benchmarks, the following future tests on the GSH are recommended:

1. Glucose variation tests - A more representative glucose variation test would start out with the normal glucose level (5 mM) and then subject the sensor to stepwise glucose changes of 10% or 20% of the normal value. This should be performed in the range of at least 0 to 20 mM. Extra attention should be paid to the sensor's performance at the hypoglycemic range (below 5 mM), as hypoglycemia can occur abruptly and can be

associated with fatal consequences [2].

2. Testing solutions and interfering substances - Phosphate buffer saline (PBS) was employed in this thesis to evaluate the sensor performance. In the future study, more aggressive solutions such as serum and plasma should be used to evaluate the sensor performance, as significant difference in sensitivity and baseline current have been reported between PBS buffer and plasma or serum for enzymatic glucose sensors [3-4], which may be also true for our chemomechanical glucose sensors. The glucose-sensitive hydrogels employed in the thesis are based on the functional moiety boronic acid which can react with cis-diols in general. Hence, potential interferences from other components in the blood such as glycoproteins, glycerol, and lactate should be taken into account and assessed [5]. Although glycoproteins concentration is low in blood serum or blood plasma, one glycoprotein has many sugar groups which may simultaneously react with multiple boronic acid moieties [5], and thus may induce non-negligible interference. For the sensor tests in blood plasma, one should also be aware of the potential interference from the commonly used anticoagulants heparin and citrate, which can combine to form crosslinks with boronic acids [6], as reported for a sensor containing similar glucose-sensitive hydrogels as in this thesis [5]. The use of ethylenediaminetetraacetic acid (EDTA) was suggested as the best anticoagulant candidate for blood plasma tests because the four hydroxyl groups in the EDTA are perhaps too far apart as compared to that in citrate and heparin, hence cannot form the EDTA-mediated crosslinks and result in minimal interference [5]. To evaluate the interferences from interfering substances, sensor performance upon a typical glucose concentration change (say, from 5 mM to

10 mM) should be compared in PBS buffer or serum containing physiological values of interfering substances and with sensor performance in control PBS buffer or serum. A less than 10% difference in output signal, in terms of sensor sensitivity and response time, is acceptable.

3. pH and ionic strength effect - To assess the extent of interferences from the typical slight physiological changes in pH and ionic strength, sensor performance should be checked in solutions with slight change in pH and ionic strength. Sensor testing should start out with physiological glucose concentration 5 mM, pH 7.4 and ionic strength 0.15 M in PBS or serum. Subsequently, the sensor should be subjected to a typical glucose concentration change (say, 5 mM to 10 mM). Meanwhile, pH value of the testing solutions should be adjusted to value of 7.2 and then subject the sensor to glucose concentration change same as that in pH 7.4. Same glucose concentration change should also be performed in a similar fashion in the testing solutions with differing ionic strength of 150 mM, 140 mM, and 160 mM. The glucose-dependent signal should over this pH and ionic strength range should vary by less than 10% from the signal observed at physiological pH 7.4 and ionic strength 0.15 M.
4. Temperature - To mimic the situation in vivo, the temperature should be adjusted to 37 °C for the sensor tests, as opposed to room temperature used in this thesis. In addition, the polyampholytic glucose sensitive hydrogel response kinetics and sensitivity have been reported elsewhere as being temperature dependent [5].
5. Stability - The stability of the sensor should be assessed in PBS buffer and blood plasma containing 5 mM glucose concentration with the baseline drift monitored over the course of several days. Subsequently, representative glucose variation tests as

discussed in step 1 should be performed for over 30 days.

In addition to the sensor in vitro testing protocols mentioned above, other aspects of the sensor design should also be improved or developed. In the future, the pore size of the porous membrane that holds the hydrogel in place and allows analyte diffusion should be further optimized. Ideally, the porous membrane should provide adequate mechanical strength to hold the hydrogel in place and prevent the hydrogel from exuding through the pores. In addition, the ideal pore size should allow small molecules such as glucose diffuse through while excluding other big molecules like proteins. Hydrogel response time should be substantially reduced to about 5 min or less. This reduction in response time may be achieved by further decreasing the hydrogel thickness or introducing an interconnected porous network into the hydrogel. Investigations should be performed to address the baseline drift problem of the microfabricated piezoresistive sensor (see Fig. 5.11), so that a stable response can be obtained. The sensor baseline should not deviate more than 10% from the initial stable baseline over the course of testing. This drift may be rectified by improving the circuitry encapsulation or passivation process. Furthermore, a surface coating with excellent biocompatibility should be developed to prevent aggressive foreign body reaction. Ideally, the surface coating should be nontoxic and will be able to actively mediate and promote angiogenesis around the sensor so that the sensor has continuous and stable access to the analyte of interest like glucose. One may design an active hydrogel coating that can gradually and continuously release nitric oxide to stimulate angiogenesis surrounding the sensor [7,8]. Lastly, if all aforementioned requirements are met, toxicity evaluation should be performed on the integrated sensor array before a legitimate effort can be made to test the sensors in animal models.

6.3 References

1. G.S. Wilson, Y. Zhang, Introduction to the glucose sensing problem, in: D.D. Cunningham, J.A. Stenken, *In vivo glucose sensing*, John Wiley & Sons, Inc., New Jersey, 2010, pp. 1-28.
2. H.E. Koschwanetz, W.M. Reichert, In vitro, in vivo and post explantation testing of glucose-detecting biosensors: Current methods and recommendations, *Biomaterials* 28 (2007) 97-106.
3. W. Kerner, M. Kiwit, B. Linke, F.S. Keck, H. Zier, E.F. Pfeiffer, The function of a hydrogen peroxide-detecting electroenzymatic glucose electrode is markedly impaired in human sub-cutaneous tissue and plasma, *Biosensors and Bioelectronics* 8 (1993) 473-482.
4. D.S. Bindra, Y.N. Zhang, G.S. Wilson, R. Sternberg, D.R. Thevenot, D. Moatti, Design and in vitro studies of a needle-type glucose sensor for subcutaneous monitoring, *Anal. Chem.* 63 (1991) 1692-1696.
5. S. Tierney, B.M.H. Falch, D.R. Hjelm, B.J. Stokke, Determination of glucose levels using a functionalized hydrogel - Optical fiber biosensor: Toward continuous monitoring of blood glucose in vivo, *Anal. Chem.* 81 (2009) 3630-3636.
6. L.I. Bosch, T.M. Fyles, T.D. James, Binary and ternary phenylboronic acid complexes with saccharides and Lewis bases, *Tetrahedron* 60 (2004) 11175-11190.
7. Y. Wu, and M.E. Meyerhoff, Nitric oxide-releasing/generating polymers for the development of implantable chemical sensors with enhanced biocompatibility, *Talanta* 75 (2008) 642-650.
8. H.S. Paul, M.H. Schoenfisch, Nitric oxide-releasing subcutaneous glucose sensors, in: D.D. Cunningham, J.A. Stenken, *In vivo glucose sensing*, John Wiley & Sons, Inc., New Jersey, 2010, pp. 243--267.